UNIVERSIDAD AUTÓNOMA DE BAJA CALIFORNIA

INSTITUTO DE INGENIERíA

Maestría y Doctorado en Ciencias e Ingeniería

"Determinación de Trazas de Impurezas Aplicando Voltametría Diferencial de Pulsos"

TESIS

Que para obtener el grado de

Doctor en Ingeniería

Presenta

José Adolfo Valera González

Director de tesis

Dr. Roumen Koytchev Zlatev

Mexicali B.C. **Abril 2012**

AGRADECIMIENTOS

A

Dios

Mi admiración, reconocimiento y respeto para ustedes sinodales:

Dr. Roumen Koytchev Zlatev	*por su alegría constante*
Dr. Benjamin Valdez Salas	*por su exigencia continúa*
Dra. Margarita Stilanova Stoycheva	*por su entrega en la docencia*
Dra. Mónica Carrillo Beltrán	*por su amable paciencia*
Dra. Lidia Esther Vargas Osuna	*por su cordial atención*

A todos mis maestros y compañeros de estudio del Instituto de Ingeniería

A CONACYT y UABC

A ustedes maestros por su valiosa aportación en mi formación profesional

Prof. Rafael Hernández Pulido (CBTIS 63)
Mtra. Nidia Josefina Ríos Vázquez (ITSON)
Dr. Víctor Manuel Sánchez Corrales (UNISON)
Dr. Nicola Radnev Nedev (UABC)

A mis compañeros y amigos:

Jesús Salas, Daniela Valenzuela, Hortencia Gracia, Ana Laura Holguín Edna Moreno, Jorge Ramírez, Leonel Ibarra, Fernando Gómez de Silva, Leticia Vizcarra, Elba Villaseñor, Adrián Carrazcosa, Eunice Fuentes, Irma López, Francisco Toledo, Ysabel Márquez, Sandra Manríquez, Mariana Briceño, Alejandra Pérez Cano, Connie Payán, Sonia Martínez, Ignacio Santos, Carlos Pérez Tello, Miguel y Rossy, Claudia y René, Karla y Juan, Claudia y Oscar, MariJose y Heriberto, Marisela y Rafael.

Por su apoyo incondicional a las familias:

Valera Valdez, Valenzuela Valera, Sánchez Valera, Valera Noriega, Valera Rosas, Jiménez Quintero, Martínez Loya, Salas Sotres, Toledo De La Torre, Ibarra Márquez, Corral Manríquez, Osuna Lau, Soto Ruiz, Montijo Corrales, Martínez Valenzuela, Villalobos González, Villafaña Pérez, Gutierrez Verdugo, Mendívil Soto,

DEDICATORIA

A

Mi esposa

BALVANEDA BELTRÁN MORALES

"Nely: tu Amor nos permite que seamos esto y más"

Nuestros Hijos

"Por su alegría infinita"

Jesús Adolfo **Luz Carolina** **José Daniel**
Maria Luisa **Fernanda Edith**

Nuestros Padres

José Porfirio (†) y Esthela **Sergio y Luz**

Nuestros Hermanos

Valera González	Beltrán Morales
Abraham	**Sergio**
Marisela	**Martha**
Rosa Esthela	**Jesús**
José Porfirio	
Salvador	
Maribel	
Liliana	

ÍNDICE DE CONTENIDO

Lista de Abreviaturas

A	Amper
AAS	Espectroscopia de Absorción Atómica
AOAC	Asociación de Químicos Analíticos Oficiales
APHA	American Public Health Association
BDD	Diamante Dopado de Boro
D.E	Diámetro exterior
D.I	Ddiámetro interior
DAPV	Voltametría Diferencial de Pulsos Alternativos
DDPP	Polarografía Diferencial de Doble Pulso
DFRP	Polarografía Diferencial con Rectificación Farádica
DME	Electrodo de Gota de Mercurio
DPP	Polarografía Diferencial de Pulsos
DPV	Voltametría Diferencial de Pulsos
e^-	Electrón
$E_{1/2}$	Potencial de media onda
ECS	Electrodo de calomelanos saturado
E_{dep}	Potencial de deposición
Ep	Potencial de pico
EPA	Agencia de Protección Ambiental
ERP	Error relativo preestablecido
ETAAS	Espectroscopia de Absorción Atómica Acoplado a Horno de grafito
ETV	Vaporización Electrotérmica
g	Gramo
g/cm^3	Gramos por centímetro cúbico
GFAAS	Espectroscopia de Absorción Atómica en conjunto con atomización Electrotérmica
HG	Generación de Hidruros
HPLC-ICP-MS	Comatografía Líquida de Alta Resolución-Plasma-Masas
I	Corriente
ICP	Plasma Acoplado Inductivamente
ICP-MS	Plasma Acoplado Inductivamente a Masas
ICP-OES	Espectrometría de Emisión Óptica con Plasma Inductivo acoplado
I-E	Corriente-potencial
L	Litro
LOD	Límite de detección
M	Molaridad (moles por litro)
mg/L	Mili-gramo por litro
mL	Mili-litro
mm	mili-metro
mm^2	mili-metro cuadrado

Lista de Abreviaturas
(continuación)

mV	Mili-volts
mV/s	Mili-volts por seg
NIOSH	Instituto Nacional de Salud y Seguridad Ocupacional
OMS	Organización Mundial de la Salud
p.p.	Pico a pico
PBS	Solución Buffer de Fosfatos
PCB	Printed Circuit Boar
pH	Potencial de hidrógeno
ppb	Partes por billón
ppm	Partes por millón
PTFE	Teflón (politetraflruroetileno)
r^2	Coeficiente de correlación
RFP	Polarografía de Radiofrecuencia
RSD	Desviación Estándar Relativa
s	Segundo
SEM	Microscopia Electrónica de Barrido
SHACP	Polarografía AC de Segunda Armónica
SHACV	Volatmetría CA de Segunda Armónica
SMMDE	Formador de Gota de Mercurio
STD	Estándar
SWASV	Voltametría de Onda Cuadrada de Disolución Anódica
SWCSV	Voltametría de Onda Cuadrada de Disolución Catódica
SWV	Voltametría de Onda Cuadrada
t_{dep}	Tiempo de deposición
V	Volts
vs	Versus
ηg/L	Nanogramo por litro
ηg/ml	Nanogramo por mililitro
>	Mayor de o mayor que
ΔI	Diferencia de corriente
µA	Micro-amper
µg	Micro-gramo
µg/L	Micro-gramo por litro
µL	Micro-litro
µM	Micro-molar (micromoles por litro)
µm	Micro-metro
µs	Micro-segundo
1N-2Nf	1 Nitroso - 2 Naftol
2N-1Nf	2 Nitroso - 1 Naftol

LISTA DE FIGURAS

Figura Página

LISTA DE TABLAS

Resumen

Al aplicar los métodos analíticos tales como: Espectroscopia de Absorción Atómica (AAS, por sus siglas en inglés) y Plasma Acoplado Inductivamente (ICP, por sus siglas en inglés) en la medición simultánea de diferentes contaminantes en: soluciones industriales, aguas naturales y aguas negras, es necesario un tratamiento preliminar de las muestras para separar cada una de las especies. Además, cuando se utilizan los métodos AAS o ICP para analizar una solución que contiene un componente en alta concentración junto con las especies a determinar, que están en muy baja concentración, dicho componente tiende a cristalizarse en el momento en que las altas temperaturas provocan la evaporación de la solución, dañando así el nebulizador del equipo medidor.

Estos problemas se pueden evitar de dos formas: i) diluyendo la muestra, que a su vez disminuye considerablemente la concentración de las especies presentes, con el riesgo incluso, de que sea por debajo del límite de detección (LOD, por sus siglas en inglés) y ii) separar cada uno de los componentes aplicando diferentes métodos químicos como: precipitación, extracción, complejación, etc., lo cual incrementa considerablemente los costos para la determinación de cada una de las especies.

Los métodos voltamétricos se pueden aplicar para la determinación de componentes en soluciones en las que las diferentes especies pueden estar tanto en altas como en bajas concentraciones. También pueden ser aplicados in situ, tal

como se requiere para el análisis de aguas naturales, donde algunos iones, que son medidos fuera de lugar, se oxidan (por ejemplo arsénico que pasa de As^{+3} a As^{+5}), alterando la concentración original del contaminante en la muestra.

Los métodos v oltamétricos, además de poder realizar la medición in situ o sobre la línea del proceso de producción en tiempo real, nos permiten medir en forma simultánea diferentes especies presentes en soluciones reales evitando en lo posible, los tratamientos previos de la muestra.

En este trabajo están aplicados varios métodos voltamétricos: Voltametría Diferencial de Pulsos Alternativos (DAPV, por sus siglas en inglés), Voltametría de Diferencial de Pulsos (DPV o DPP, por sus siglas en inglés) y Voltametría de Onda Cuadrada (SWV, por sus siglas en inglés) para la determinación simultánea de iones en muestras de aguas naturales y soluciones industriales, utilizando electrodos convencionales, así como electrodos innovados y avanzados.

I.- INTRODUCCIÓN.

1.1 Antecedentes

Existe una gran necesidad de medir las impurezas (metales y no metales), en soluciones industriales y sobre todo, en aguas naturales las cuales son de interés particular para el consumo humano. Las industrias generadoras de soluciones residuales que contienen impurezas metálicas requieren, para el control de sus procesos de purificación, de métodos: simples, rápidos y en línea, para la determinación de la concentración de cada una de las especies.

Por su parte las plantas de electro-extracción de Zn, trabajan con soluciones electrolíticas que contienen alrededor de 150 g/L de Zn^{+2} y una gran variedad de impurezas, tales como: Cd^{+2}, Cu^{+2}, Pb^{+2}, Sb^{+3}, Co^{+2}, Fe^{+2}, Ni^{+2}, Ge^{+4}; la mayoría de ellos en niveles de partes por billón (ppb) [1, 2]. La producción de un metal de alta pureza y el logro de una alta eficiencia de corriente de la electrólisis requiere la eliminación de estas impurezas para evitar que se co-depositen junto con el Zn^{+2}, que favorece la evolución H_2 debido a la disminución del potencial del hidrógeno en las áreas del cátodo que contienen cobalto. [2-12].

Algunos investigadores sugieren aplicar voltametría utilizando varios tipos de electrolitos soporte [1,13]. Bond [1] manifiesta que la alta concentración de Zn^{+2} no interfiere en la determinación voltamétrica de los iones: Sb^{+3}, Cd^{+2}, Ni^{+2}, Ge^{+4} y Cu^{+2}. Pilkington [2] recomienda usar métodos espectrales para determinar el Co^{+2} debido al traslape de los picos del Zn^{+2} sobre los de cobalto. Meites [14] utiliza DPP y la formación de quelatos lo que requiere altas concentraciones del

reactivo quelatante siendo insatisfactorio el bajo LOD. Así mismo, varios autores mencionan diferentes métodos para atacar este problema, incluyendo el uso de compuestos orgánicos al utilizar voltametría diferencial de pulsos con disolución absortiva (SWASV, por sus siglas en inglés) [15-18] logrando buenos resultados. También, se sugiere un filtrado posterior (matriz de intercambio) [19] o utilizar como quelatante el 1-nitroso-2-naftol [20-26].

Similar a lo que sucede con el Zn, en las plantas productoras de Cu se disuelve un ánodo, producto de la fundición, en ácido sulfúrico donde se genera un lodo anódico con impurezas como: Pb, As, Sb, Bi, Se, Te, incluyendo Au y Ag, que deben ser identificadas y cuantificadas para lograr una producción eficiente del cátodo de cobre por electro-refinación.

Por otra parte, es de vital importancia el realizar monitoreos continuos de las aguas que son para el uso diario y el consumo humano, ya que puede haber en ellas, determinadas especies metálicas y/o no metálicas como: Pb, Cr, Fe, As, Se, entre otras, que al sobrepasar los rangos permitidos de concentración pueden, por contacto o ingestión de las mismas, causar graves daños biológicos y fisiológicos tanto en el hombre como en los animales.

Por ello es importante analizar los resultados de los métodos voltamétricos: DPV y DAPV para cuantificar las impurezas: in situ, en tiempo real y sin el complicado y costoso tratamiento previo de la muestra. El DAPV combina la alta sensibilidad del DPV con la alta resolución de las técnicas de segundo orden, lo que permite su aplicación en la determinación simultánea de especies.

1.2 Planteamiento del problema

La actividad minero-metalúrgica requiere, además de evitar la contaminación de aguas y ríos con sus desechos, el poder detectar y eliminar las impurezas dentro sus mismos procesos de purificación como sucede en las producciones electroquímicas de: Zn y Cu. Estas industrias metalúrgicas se ven involucradas en la problemática de tener que monitorear y cuantificar, en forma continua, in situ y en tiempo real, las impurezas metálicas que acompañan al metal de interés dentro de su respectiva solución analítica, para:

a) Controlar la purificación del metal de interés y
b) Vigilar los desechos industriales que se puedan estar generando hacia el medio ambiente.

Así mismo, las instituciones y agencias encargadas de la protección del medio ambiente, tienen la necesidad y obligación de monitorear constantemente los contenidos de arsénico (As^{+3}, As^{+5} y As^{0}) que existen tanto en las aguas subterráneas como superficiales.

Los métodos espectrales (absorción y emisión) más aplicados tanto en la industria como en el monitoreo de las aguas son: AAS, (ICP-MS) y la cromatografía líquida de alta resolución (HPLC-ICP-MS). Al usar estos mismos métodos en las plantas electrolíticas, con altas concentraciones de la sal matriz, como son: $ZnSO_4$ para Zn^{0} y $CuSO_4$ para Cu^{0}; durante las mediciones se produce la cristalización del nebulizador a altas temperaturas y se dificulta la automatización del proceso de medición in situ.

1.3 Justificación

Los métodos analíticos espectrométricos actuales como AAS e ICP son costosos, algunos tienen baja resolución y miden la concentración total de una especie sin distinguir sus estados de oxidación. Al utilizarlos para la determinación de diferentes especies en una misma solución, requieren del uso adicional de un equipo sofisticado y costoso que permita la separación previa de cada especie, haciendo con ello, más difícil la automatización in situ.

La métodos voltamétricos nos permiten realizar mediciones in situ en menor tiempo y a un costo mucho más bajo. Así también es necesario desarrollar y mejorar estos métodos con el propósito de que podamos distinguir, tanto los estados de oxidación de una misma especie, así como la determinación simultánea de especies in situ, en tiempo real.

1.4 Objetivos

1.4.1 Objetivo General

Desarrollar métodos voltamétricos, aplicando las técnicas: Voltametría Diferencial de Pulsos (DPV), Voltametría de Onda Cuadrada (SWV) y Voltametría Diferencial de Pulsos Alternativos (DAPV) para la determinación de contaminantes en bajas concentraciones (trazas) en aguas naturales y en soluciones industriales.

1.4.2 Objetivos Específicos:

1. Desarrollar un método voltamétrico aplicando Voltametría de Onda Cuadrada de Disolución anódica (SWASV) para la determinación de As^{+3} en aguas naturales con un electrodo de diamante dopado con boro (BDD) modificado con TiO_2.

2. Desarrollar un método voltamétrico aplicando DPV para la determinación de trazas de Co^{+2} en un electrolito industrial de Zn^{+2}, para el proceso de electrowinning de Zn.

3. Desarrollar un método voltamétrico aplicando DPV y DAPV para la determinación simultánea de As^{+3}, Pb^{+2} y Tl^{+1} en aguas naturales y verificar los resultados con métodos espectrométricos.

II.- Marco Teórico.

2.1 Impurezas industriales

En este trabajo se denomina “impurezas industriales” a los elementos metálicos y no metálicos que están presentes en forma de trazas (ppm o ppb) como:

i) Contaminantes ambientales, donde el ser humano está en contacto directo o indirecto con ellos en el medio ambiente, el agua (mares, ríos, aguas subterráneas, etc.), en las plantas y en los organismos vivos.

ii) Contaminantes industriales, elementos que dificultan la extracción de productos metálicos en forma pura y su posterior transformación industrial, por lo que deben ser cuantificados y separados del producto de interés. Estas complejas operaciones metalúrgicas pueden convertir, tanto al contaminante industrial como al nuevo producto, en posibles contaminantes ambientales si no se les trata o almacena adecuadamente antes de ser expuesto o vertidos al ambiente.

2.1.1 Elementos Metálicos

El 80% de los elementos conocidos por el hombre son metales, los cuales han desempeñado un papel fundamental en el desarrollo de las civilizaciones, tales como: Pb, Hg, Be, Cd, Cu, Mn, Ni, Sn, V, Zn y Fe. Aun cuando algunos metales se presentan en forma escasa o indisoluble, surge un grave problema cuando el crecimiento demográfico y la rápida industrialización obligan al hombre a que se exceda en la producción y/o uso de estos metales, lo que provoca graves daños por contaminación que deteriora el medio ambiente.

Dentro de estos contaminantes se pueden citar a los ***metales pesados*** los cuales constituyen un grupo aproximado de 40 elementos de la tabla periódica que tienen una densidad mayor o igual a 5 g/cm^3. Estos metales fueron introducidos al ambiente como resultados de: erupciones volcánicas, lixiviados de suelos y rocas, además de actividades antropogénicas como la agricultura, desechos industriales, mineros, metalúrgicos y domésticos. Una vez emitidos, pueden permanecer en el ambiente durante cientos de años, al no ser química ni biológicamente degradables; pudiendo ser detectados ya sea en su estado elemental (sin modificaciones), o enlazados en varios complejos con sales.

El rasgo distintivo de la ***fisiología de los metales pesados***, es que aún cuando muchos de ellos son esenciales para el crecimiento como: Na, K, Mg, Ca, V, Mn, Fe, Co, Ni, Cu, Zn y Mo; existen algunos iones metálicos que pueden alterar las enzimas, por su facilidad de formar enlaces coordinados, por ejemplo: Fe^{+3} (inhibidor) y Mn^{+2} (activador) [27]. Debido a su movilidad en los ecosistemas acuáticos naturales, los ***iones de metales pesados*** presentes en los abastecimientos de aguas superficiales y subterráneos, se les ha dado prioridad como los ***contaminantes inorgánicos más importantes*** en el ambiente convirtiéndolos, según Bautista y Zúñiga (1999) no sólo en un *problema ambiental sino también de salud pública* [28]. Aún en concentraciones del orden de ppb, la persistencia de metales pesados en cuerpos de agua, implica que a través de procesos naturales como la bio-acumulación, pueden incrementar su concentración, al grado de que empiece a ser tóxica [29]. Ver Tabla 1.

Tabla 1. Límites de la dosis máxima de metales pesados en la ingesta humana según la EPA de Estados Unidos.

Hg	144	ng/L	(*)
Cu	1	µg/L	(#)
Zn	5	µg/L	(*)
Cd	10	µg/L	(*)
Cr	50	µg/L	(+)
Pb	50	µg/L	(*,p)
Ni	632	µg/L	(*)
As	50	µg/L	(+)
Se	50	µg/L	(@)
Al	50	µg/L	
Be	1	µg/L	(a)

*: criterios para el agua; +: máximo nivel de contaminación; p: en adultos;
#: nivel que jamás debe ser superado; @: en agua; a: aire

Los metales pesados tóxicos más conocidos son: Hg, Pb, Cd y Tl; grupo al que se suele incluir a un *semi-metal como es el As* y, en raras ocasiones, *algún no metal como el Se*. A veces se incluyen en este grupo a otros elementos tóxicos más ligeros como: Al y Be.

2.1.2 Elementos no metálicos

El *selenio* es un no metal necesario en pequeñas cantidades para los seres humanos y ciertos animales, pero en exceso puede provocar fatiga, irritabilidad, caída del cabello y las uñas y daño hepático, renal y daño severo del sistema nervioso; se acumula en los tejidos vivos, especialmente en los peces. Tiene un LOD de 0.5 µg/L mediante AAS con HG.

El ***arsénico*** puede encontrarse en ambientes naturales bajo diferentes estados de oxidación y, la movilidad y toxicidad dependen en gran medida de la forma en que se encuentra. Por ejemplo, en aguas subterráneas está predominantemente como As^{+3} y As^{+5}, y solo hay cantidades menores de metil y dimetil arsénico.

Los organismos vivos están expuestos a especies tóxicas de arsénico provenientes de alimentos y aguas, por lo que también puede entrar en la cadena alimentaria humana a través de plantas y animales causando serios problemas en la salud; sin embargo: peces, frutas y vegetales contienen, en principio mayormente arsénico orgánico (menos tóxico) y solo un 10 % de arsénico inorgánico (de mayor toxicidad). Aunque otros alimentos como la leche, cereales y carne de cerdo presentan una situación invertida en cuanto a concentración de arsénico orgánico e inorgánico. La OMS (Organización Mundial de la Salud) ha fijado un límite máximo 10 µg/L en la concentración de arsénico, en aguas para consumo humano. [28,30,31]. Por otra parte, el ***arsénico,*** *junto con los compuestos de* ***cobre*** *y* ***cromo***, es un ingrediente muy común en los conservantes de la madera. El aumento en el uso del carbón incrementará la exposición a los metales, porque las cenizas que contienen muchos metales tóxicos, pueden ser aspiradas hasta el interior de los pulmones.

Por todo lo anterior, la exposición a arsénico puede causar una gran variedad de padecimientos en la salud de las personas, tales como problemas: cardiovasculares, respiratorios, gastrointestinales y efectos carcinogénicos.

2.2 Técnicas analíticas.

Los métodos más comunes para la determinación de especies: inorgánicas y metales, en muestras ambientales, incluyen varios técnicas instrumentales de laboratorio, las cuales son aprobadas por la Agencia de Protección Ambiental (EPA), el Instituto Nacional de Salud y Seguridad Ocupacional (NIOSH), la Asociación de Químicos Analíticos Oficiales (AOAC) y la American Public Health Association (APHA). [28,30,31].

Algunas de estas técnicas no electroanalíticas proporcionan datos sobre la cantidad total del metal, pero no permiten distinguir entre los diferentes estados de oxidación del mismo. La especiación de los estados de oxidación requiere de un pretratamiento complejo de las muestras tales como: quelación, precipitación, extracción o cromatografía. [28,30]

2.2.1 Generación de Hidruros (HG)

La técnica HG, es la más comúnmente utilizada para la detección de especies inorgánicas de arsénico y puede ser aplicada para metodologías en línea permitiendo eliminar interferencias y aumentar la sensibilidad, logrando la determinación diferencial de As^{+3} y As^{+5} , aunque existen algunas interferencias provocadas por la presencia de metales de transición [31].

La técnica HG combinada con espectrometría de absorción atómica y fluorescencia atómica, ambas acopladas a diferentes técnicas de separación como extracción líquido-líquido, resinas de intercambio, entrampado en frío, etc.

ha generado metodologías de un alto nivel de sensibilidad para producir la tan importante especiación del arsénico [31,32].

La espectroscopia de absorción atómica en conjunto con la atomización electrotérmica (ETAAS) o con horno de grafito (GFAAS), son técnicas analíticas que también pueden ser acoplados con HG. La técnica ETAAS es una de las más aceptadas para la determinación de trazas de arsénico en sistemas acuosos.

2.2.2 Espectrometría

Estas técnicas incluyen: Espectrometría de Emisión Óptica con Plasma Inductivo Acoplado (ICP-OES) y Espectrometría de Masas con Plasma Inductivamente Acoplado (ICP-MS).

La técnica de ICP utiliza el plasma para atomizar, ionizar y excitar todas las formas del arsénico que son enviadas hacia el plasma para su detección/determinación.

El acoplamiento de: cromatografía líquida, HG e ICP-OES, permite la determinación de arsenito, arseniato, y especies órgano-arsenicales. La gran ventaja es, los bajos límites de detección alcanzados sin necesidad de preconcentración (ηg/ml).

Los posibles problemas del empleo de esta técnica radican en la formación de especies moleculares argón-cloruro en el plasma, cuya masa atómica es la misma que la de 75 As. La vaporización electrotérmica (ETV) soluciona este problema ya que la muestra se introduce directamente en el plasma en forma de un vapor atómico. [31].

2.2.3 Fluorescencia de rayos X

El fundamento de la flourescencia de rayos X, radica en la existencia de un sistema atómico con distintos niveles de energía y las posibles transiciones electrónicas entre ellos.

Esta técnica es muy efectiva para la detección/determinación de arsénico en el terreno, siendo particularmente útil cuando se trata de muestras sólidas (suelos y sedimentos sobre sustrato sólido, cinta de celofán).

El futuro de esta técnica y con referencia a la determinación de arsénico en aguas y en el nivel de vestigios, pasa fundamentalmente por el desarrollo de metodologías de preconcentración adaptables tanto a los equipos de laboratorio como para aquellos que permiten la determinación “in situ”. [31]

2.3 Técnicas electroanalíticas.

Las técnicas electroanalíticas son capaces de proporcionar límites de detección bajos y una abundante información sobre las características que describen los sistemas susceptibles de ser tratados con la electroquímica como: la estequiometría y la velocidad de transferencia de carga interfacial, la velocidad de transferencia de masa, la extensión de la adsorción o quimiosorción y las constantes de velocidad y de equilibrio de reacciones químicas. [33]

Las técnicas electroanalíticas se basan en la medida de una magnitud eléctrica básica como lo son: la intensidad de corriente, el potencial, la resistencia (o conductancia) y la carga; estas técnicas se pueden clasificar según la Figura 1.

2.3.1 Técnicas electródicas: interfase electrodo-solución.

Se encargan de medir magnitudes asociadas a procesos de electrodo tales como: potenciales, corrientes de celda, cargas eléctricas y resistencias. Estas técnicas se pueden subdividir en dos grupos:

a) Técnicas electródicas estáticas: sucede cuando el potencial es medido en el equilibrio sin *electrólisis*, tal es el caso de las mediciones *potenciométricas*.

La *potenciometría* mide el potencial de un sistema electroquímico en equilibrio para determinar la actividad de algunas sustancias de la disolución, sin paso de corriente apreciable.

b) Técnicas electródicas dinámicas: se lleva acabo cuando sí existe una electrólisis. Cuando se trabaja a un *potencial constante* se usan las técnicas de: electrogravimetría, ***voltamperometría*** y colombimetría. A su vez, si la *intensidad es constante* se utilizan las técnicas de: colombimetría, y electrogravimetría.

Por su parte la *electrogravimetría* determina la cantidad de analito presente mediante su conversión electrolítica en un producto que se deposita y se pesa en uno de los electrodos. La *colombimetría* determina la cantidad de analito midiendo la cantidad de carga eléctrica necesaria para convertir totalmente el producto.

2.3.2 Técnicas iónicas: seno de la solución

Estas técnicas miden las propiedades electroquímicas en la disolución iónica, donde la electroforesis y conductimetría son los métodos comunes aplicados. La *conductimetría* mide la conductividad de una disolución iónica o salina de gran movilidad entre dos puntos de diferente potencial.

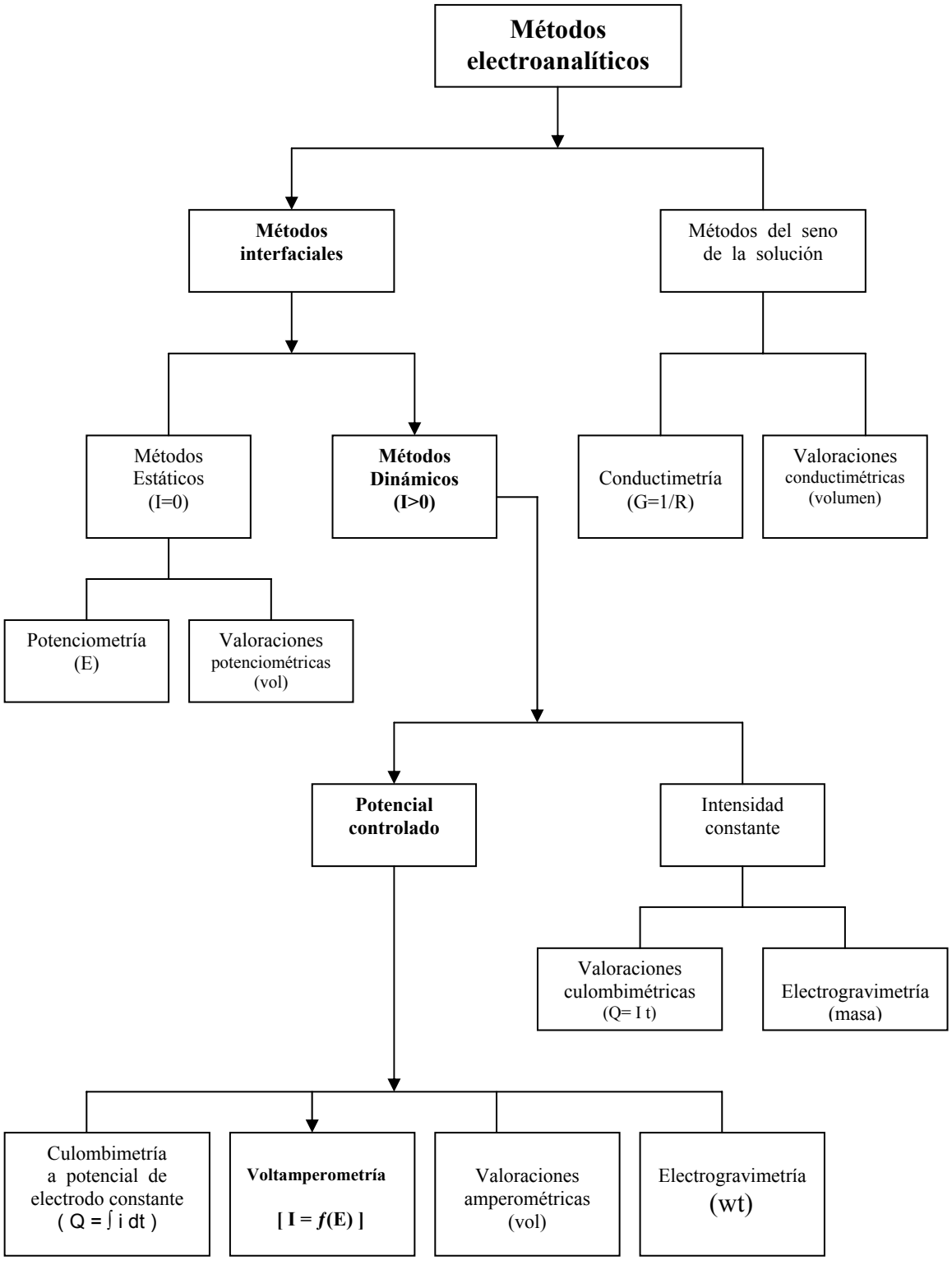

Figura 1. Resumen de los métodos electroanalíticos comunes. [33]

2.4 Técnicas voltamétricas.

La ***voltametría*** es una técnica que se basa en la medida de la corriente en función del potencial aplicado a un electrodo pequeño, indicador, sumergido en disolución, con una especie electroactiva en condiciones de polarización con un consumo mínimo de analito, que en otras técnicas, casi todo se convierte en producto. [33,34].

La voltametría se desarrolló del descubrimiento de la polarografía (electrodo de Hg) por el químico checoslovaco Jaroslav Heyrovsky en 1922, haciéndolo acreedor del Premio Nobel. Matherson y Nichols desarrollaron los métodos de barrido de potencial rápido, (lineal y cíclico) que fueron descritas por Randles y Sevcik.- Véase Figura 2.

En la voltametría, se estudian los cambios de corriente, como una función del potencial aplicado a través de la celda electrolítica. El proceso involucra la electrólisis de una o más especies electroactivas, el cual comprende: reacción de la especie electroactiva en el electrodo y mecanismo de transferencia de masa, lo cual puede ser por: migración (movimiento de especies por diferencia de carga), convección (movimiento de la materia por cambios físicos) y difusión (movimiento de las especies por gradiente de concentración). En la mayoría de los casos, la electrólisis se efectúa bajo condiciones tales, que la difusión sea el proceso fundamental en el transporte de la especie electroactiva; la migración y la convección se minimizan por la adición de un exceso de electrolito soporte, evitando el movimiento de agitación y gradientes de temperatura.

Nombre	**Forma de Señal**	**Tipo de Voltamperometría**
a) Barrido Lineal	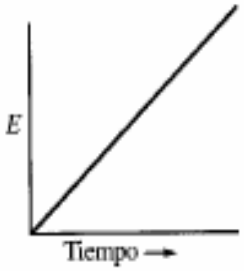	Polarografía Voltametría De barrido lineal
b) Impulso Diferencial	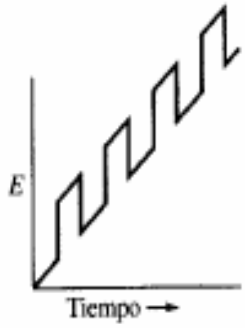	Polarografía Diferencial de Impulsos
c) Onda Cuadrada	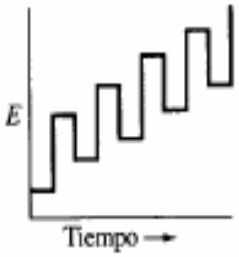	Voltametría De onda cuadrada
d) Triangular		Voltametría cíclica

Figura 2. Señales de potencial versus tiempo para diferentes técnicas voltamétricas. [33]

Considerando que las reacciones electroquímicas reversibles de difusión controlada, obedecen a la siguiente ecuación:

$$E = E_{1/2} + \frac{RT}{nF} \ln \frac{I_l - I_t}{I_t} \qquad (1)$$

Donde:

E: potencial
$E_{1/2}$: potencial de media onda
R: constante de gases
T: temperatura absoluta
n: número de electrones transferidos
F: constante de Faraday
I_l: corriente límite
I_t: corriente instantánea

Esta misma relación no lineal es aplicada para los métodos voltamétricos de primero y segundo orden. [35] Actualmente se han desarrollado numerosas técnicas voltamétricas de alta sensibilidad, que tienen cada día mayor campo de aplicación en las diversas áreas de la ciencia y la tecnología como son en: química orgánica, bioquímica e incluso física, no tanto para analizar una determinada muestra, sino más bien para estudiar procesos de oxidación y reducción, procesos de adsorción, entre otros. [34, 36, 37]. Los métodos voltamétricos y polarográficos tienen un amplio rango de aplicaciones particularmente para el análisis de trazas en soluciones acuosas sobre todo en la determinación de metales tóxicos. [38,39]

2.4.1 Voltametría de barrido lineal.

El voltaje aplicado va aumentando linealmente, hasta un máximo, en un determinado tiempo. Se obtiene una gráfica de la intensidad de corriente medida en función del tiempo. Ver la Figura 3.

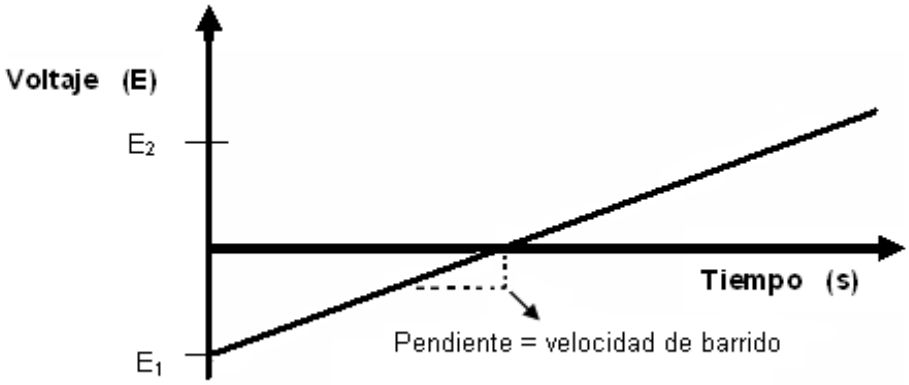

Figura 3. Señal de potencial de excitación en voltametría de barrido lineal.

La velocidad de barrido se calcula de la inclinación de la pendiente. Modificando el tiempo que tarda en barrer el rango de voltajes se puede cambiar la velocidad de barrido [36].

Los voltamogramas de barrido lineal dependen de varios factores:

- La tasa de la reacción de transferencia de electrones.
- La reactividad química de las especies electroactivas.
- La velocidad de barrido de voltaje.

En la Figura 4, por la parte izquierda no hay flujo de corriente. Cuando el voltaje se barre hacia la derecha (a valores más reactivos), la corriente comienza a fluir y eventualmente alcanza un pico antes de que vuelva a caer. Para comprender el comportamiento necesitamos considerar la influencia de un voltaje en equilibrio establecido sobre la superficie del electrodo. La corriente aumenta cuando el voltaje se barre desde su valor inicial mientras que la posición de equilibrio se mueve hacia la parte de la derecha, convirtiendo así más reactantes.

El pico marca el potencial de reacción máximo, llegándose a oxidar o reducir completamente la superficie del electrodo a tratar, y no existe más flujo de electrones. Esto provoca que no se cumpla la ecuación de Nerst, utilizada para calcular el potencial de reducción de un electrodo cuando las condiciones no son las estándar en equilibrio [36].

En la Figura 5, se observa la variación de la intensidad de corriente respecto de la diferencia de potencial aplicada, para una reacción electrolítica de reducción, en la cual un analito A se reduce para formar un producto P, con un micro-electrodo de película de mercurio [33]. Las gráficas de los voltamperogramas de barrido lineal, toman frecuentemente la forma de una curva sigmoidea, conocida como onda voltamperométrica.

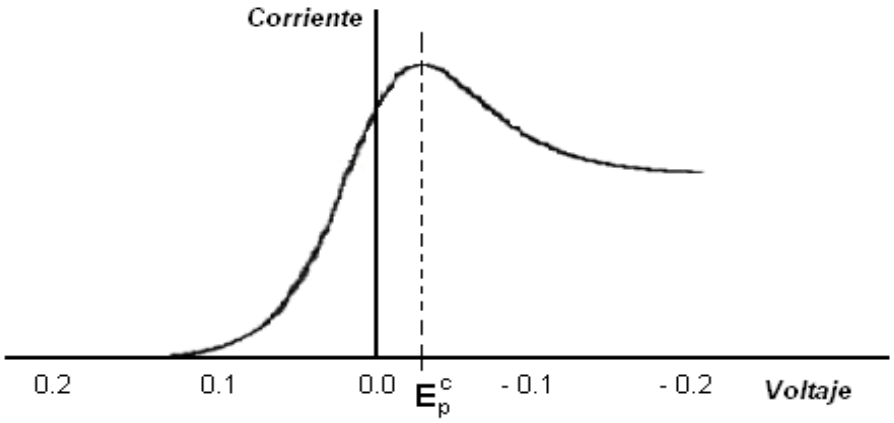

Figura 4. Gráfica de corriente (voltaje lineal)

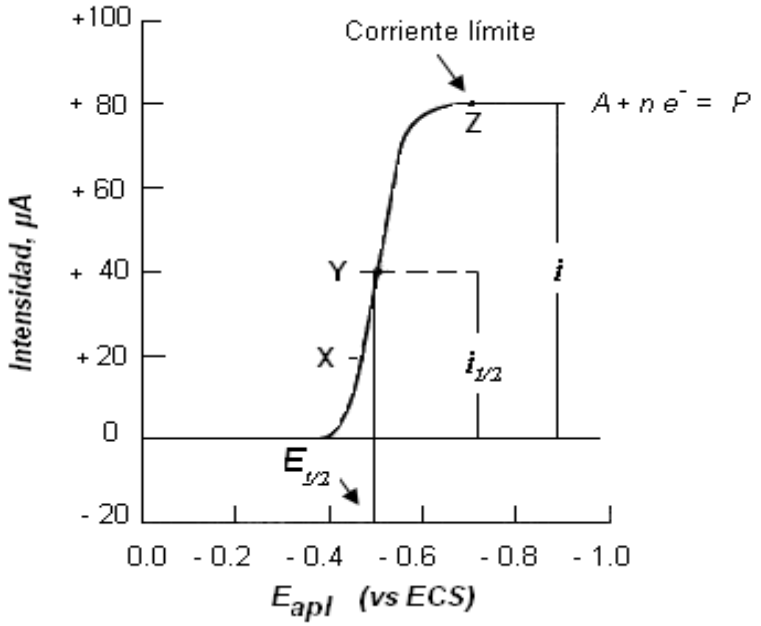

Figura 5. Voltamograma de barrido lineal de reducción de una especie hipotética A para dar un producto P.

2.4.2 Voltametría de primer orden (AC SWV DPV).

Las técnicas voltamétricas de primer orden tales como: DPV, SWV voltametría AC etc. [40-48], se basan en la no linealidad de I-E que es característico en sistemas electroquímicos. Estas técnicas son: económicas y automatizables; sus lecturas pueden ser in situ y en tiempo real.

La altura de picos registrada como una respuesta de corriente (causada por una pequeña superposición de la amplitud rectangular del pulso sobre el potencial de electrodo), es proporcional a la concentración de la especies presente en la reacción electroquímica. La mitad del ancho de pico que depende principalmente de la reversibilidad de la reacción electroquímica, determina la potencia de resolución: una mayor nitidez en la altura de pico. [38,39,41,42].

2.4.3 Voltametría de segundo orden

Estas técnicas basadas en el efecto de rectificación de Faraday [40-49] incluyen: RFP: Polarografía de radiofrecuencia, DFRP: Polarografía diferencial con rectificación farádica, DDPP: Polarografía diferencial de doble pulso y SHACP: Polarografía AC de Segunda Armónica [50,55]. La forma de las curvas registradas, de la primera derivada, (que contienen la parte anódica y catódica), permiten distinguir las especies con los picos situados a ambos lados de la línea cero. Algunos de estos métodos tienen gran resolución y alta sensibilidad*; su desventaja es el complejo y caro equipo (RFP y DFRP*), insuficiente sensibilidad (SHACP) o en los problemas generados en su aplicación a alta frecuencia.

2.5 Voltametría de onda cuadrada (SWV).

Esta técnica de impulsos posee una gran velocidad y elevada sensibilidad, por lo que un voltamograma completo se obtiene en 10 ms. Al utilizar el electrodo de gotas de Hg, se logra un barrido en los últimos milisegundos de vida de una única gota, exactamente cuando la intensidad de corriente es constante. SWV se usa también con electrodos de Hg de gota colgante y con detectores cromatográficos. [33]. Las Figuras 6 y 7 muestran una señal de excitación de SWV.

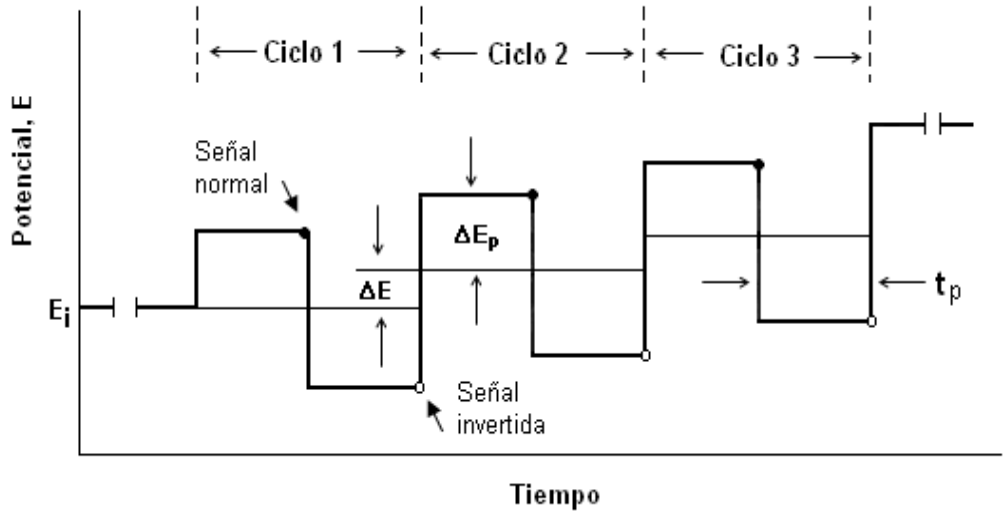

Figura 6. Superposición de un tren de impulsos de la señal escalonada.

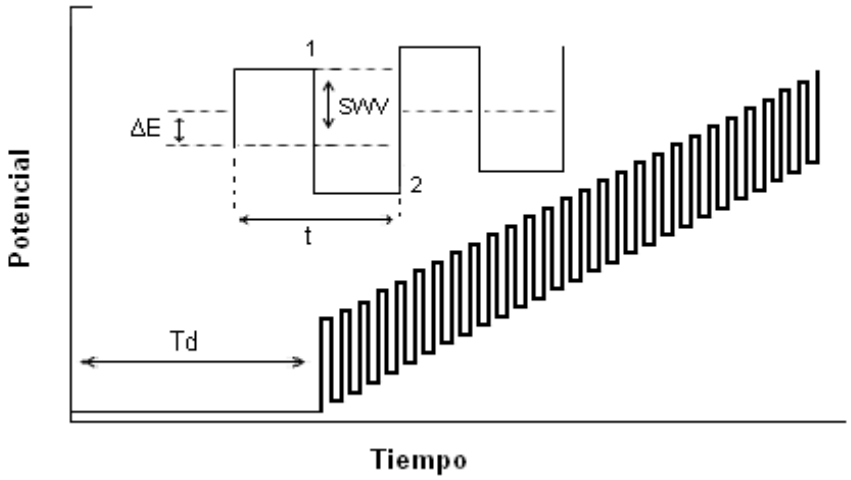

Figura 7. Señal de excitación escalonada de SWV.

Así mismo en la Figura 8, se observa una respuesta de corriente para una reacción reversible en función de la señal de excitación. El impulso directo produce una corriente catódica (A), mientras que el impulso inverso dá una corriente anódica (B). Los voltamogramas son producto de la diferencia de estas dos corrientes (C), la cual es directamente proporcional a la concentración y el potencial del pico corresponde al potencial de semi-onda polarográfico. En la actualidad los métodos de impulsos han sustituido casi en su totalidad al barrido lineal, logrando desarrollar la voltametría de onda cuadrada de disolución anódica (SWASV) y catódica (SWCSV), con mayor sensibilidad, adecuación y selectividad. Se han hecho publicaciones con límites de detección de 10^{-7} a 10^{-8} M, usando SWV. [33].

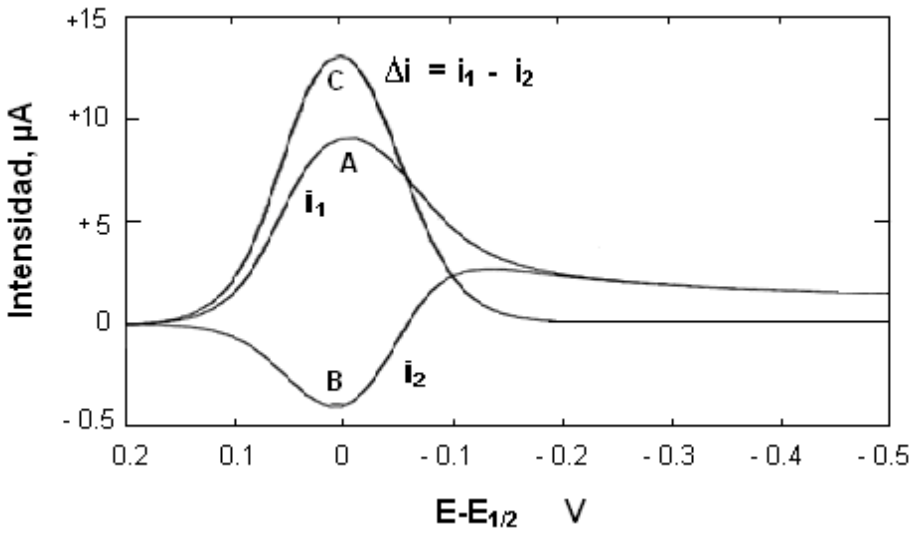

Figura 8. Respuesta de corriente para una reacción reversible a la señal escalonada en voltamograma SWV.

2.6 Voltametría diferencial de pulsos (DPV)

En esta técnica se designan a las corrientes originadas por la electrólisis como *corrientes farádicas*, sin embargo siempre que un electrodo tiene un potencial aplicado que cambia, hay otra contribución no farádica, es el resultado de tener que cargar el electrodo a medida que cambia el potencial a un nuevo valor; donde la corriente total es la suma de los dos tipos de corriente. Para la determinación cuantitativa de analitos por voltametría dentro de un intervalo comprendido entre 10^{-4} M y 10^{-5} M no tenemos que preocuparnos de la corriente de condensador no farádica, las corrientes farádicas de la electrolisis del analito son más grandes y duran más tiempo.

Sin embargo, para determinar la concentración de la disolución más diluida (del orden de 10^{-6} M o inferiores) hay que poner especial cuidado para separar las corrientes farádicas de las no farádicas y de las corrientes residuales.

Para lograr lo anterior, se usan dos métodos diferentes de voltametría de pulsos (polarografía y voltametría diferencial de impulsos). Ver Figuras 9 y 10.

El objetivo de su utilización es disminuir la influencia de corrientes no farádicas durante las mediciones.

Las corrientes farádicas tienen dos propiedades:

i) Cuanto más rápido es el cambio de potencial, mayores son las corrientes no farádicas.

ii) Después de un cambio de potencial, las corrientes no farádicas disminuyen muy rápido en relación con las corrientes farádicas.

Para minimizar las corrientes de condensador, la corriente total se mide justo antes del impulso y de nuevo hacia el final del mismo (después de cientos de μs).

La primera medida proporciona la línea base, y las siguientes ocurren cuando las corrientes no farádicas disminuyen significativamente. Esta manipulación del potencial en el electrodo de trabajo y la toma de la muestra se realiza electrónicamente.

La mejora en la sensibilidad se logra midiendo con cuidado las corrientes farádicas analíticamente útiles. Sin embargo las corrientes farádicas residuales de las disoluciones, aun permanecen.

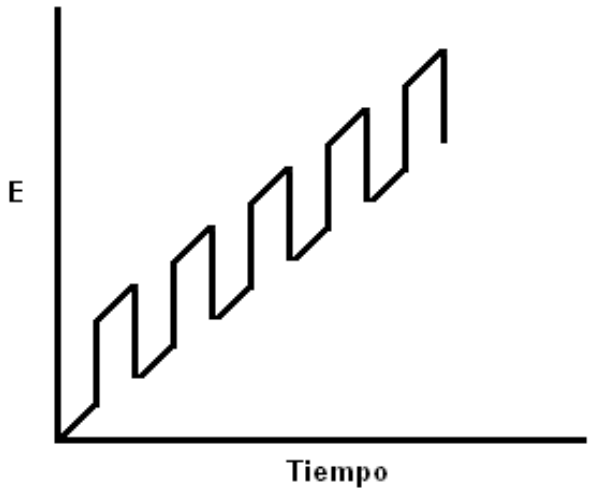

Figura 9. Señal de un impulso diferencial.

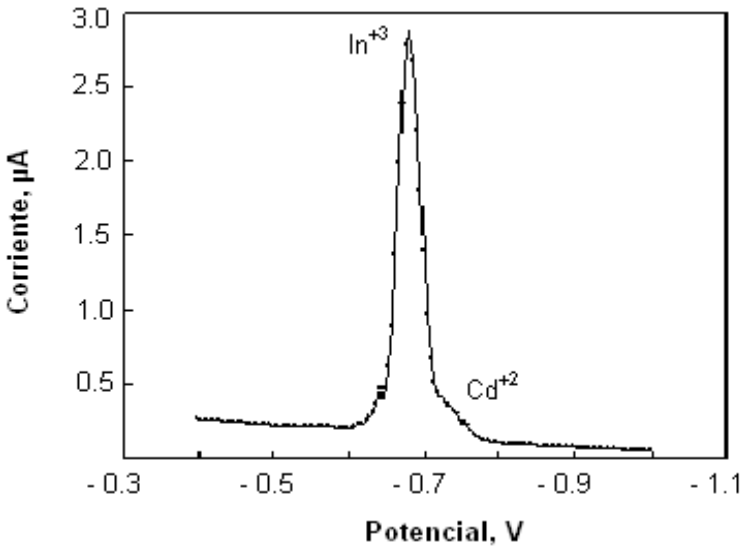

Figura 10. Ejemplo de un voltamograma real utilizando DPV.

La voltametría diferencial de pulsos es un sistema experimental diseñado para minimizar los efectos de las corrientes farádicas residuales, midiendo éstas corrientes y restándolas del total de corrientes farádicas (suma de corrientes farádicas del analito y la residual). El registro de las corrientes en el voltamograma se presenta como la diferencia entre estas dos intensidades de corriente, $I_2 – I_1$, en función del potencial, dando origen a los picos DPV.

El aumento de sensibilidad, se debe a la disminución de la contribución de la componente de intensidad capacitiva, una vez que se procede a la sustracción de dos valores relativamente próximos, permitiendo alcanzar los límites de detección, para la generalidad de especies, del orden que va de 10^{-7} M hasta 10^{-8} M. [33,56,57].

2.6 Voltametría diferencial de pulsos alternativos (DAPV)

El método DAPV desarrollado por autores recientes [35] es una técnica voltamétrica simple de segundo orden, que proporciona la ***misma sensibilidad*** del método DPV ***combinado*** con la ***alta resolución*** de métodos de segundo orden. Dos pulsos rectangulares con polaridades opuestas se superponen paso a paso, en el potencial de electrodo. Lo cual se debe a la característica de no linealidad en la relación I-E y el promedio de las corrientes farádicas ocasionada por cada par de pulsos de polaridad opuesta (superpuesto al mismo potencial) desviados de la corriente.- Ver Figura 11.

Los pulsos de corriente –dIp y +dIp son generados por la superposición de pulsos rectangulares –dE y + dE sobre el potencial de electrodo [58-60], los cuales son descritos por las siguientes ecuaciones:

$$dIp_{-} = \frac{n^2F^2}{RT} AC(-dE)\sqrt{\frac{D}{\pi t}}\frac{P_{-}}{(1+P_{-})^2} \qquad (2)$$

$$dIp_{+} = \frac{n^2F^2}{RT} ACdE\ \sqrt{\frac{D}{\pi t}}\frac{P_{+}}{(1+P_{+})^2} \qquad (3)$$

donde:

$$P_{-} = \exp[(\ E - E_{1/2} - \frac{dE}{2})\frac{nF}{RT}\ ]$$

$$P_{+} = \exp[(\ E - E_{1/2} + \frac{dE}{2})\frac{nF}{RT}\ ]$$

La Figura 11A muestra la superposición de los pares de pulsos rectangulares de polaridades opuestas, con un tiempo de retardo entre ellos. Esto, combinado con un procesamiento de señal como lo indica la ecuación 4, permite un método voltamétrico de alta resolución y alta sensibilidad así como una simplicidad de los instrumentos.

$$dIp = \frac{n^2F^2}{RT} ACdE\sqrt{\frac{D}{\pi t}}[\frac{P_{+}}{(1+P_{+})^2} - \frac{P_{-}}{(1+P_{-})^2}] \qquad (4)$$

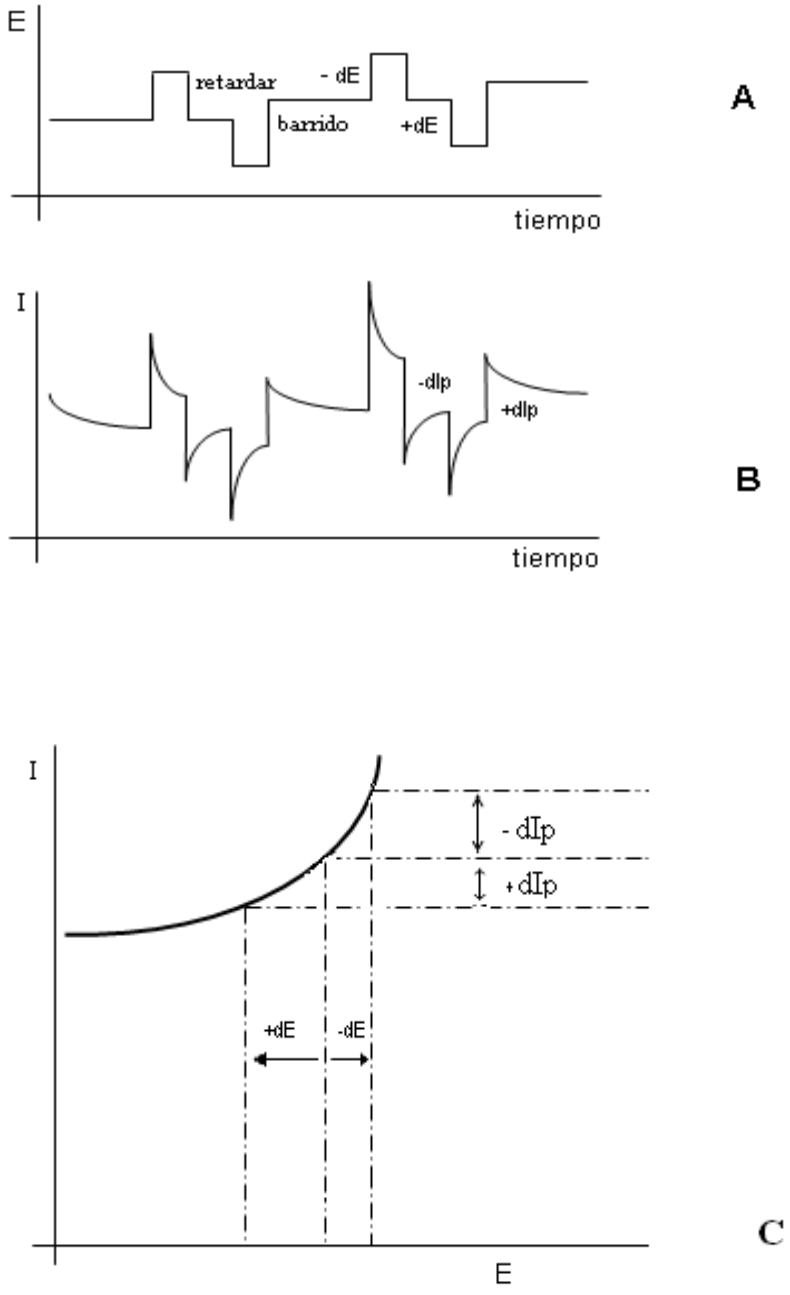

Figura 11. Voltametría diferencial de pulsos alternativos DAPV.

La Figura 11B, presenta la corriente como función del tiempo; mientras que la Figura 11C nos muestra que debido a la no linealidad de la I-E, los valores absolutos de las respuestas farádicas: catódica y anódica no son iguales, propiedad peculiar de un sistema electroquímico.

Considerando la ecuación 4, las curvas 1 y 2 para dI_p/E de la Figura 12 representan las respuestas anódica y catódica según las ecuaciones 2 y 3, mientras que la curva 3 representa la suma de ambas, dando la curva DAPV.

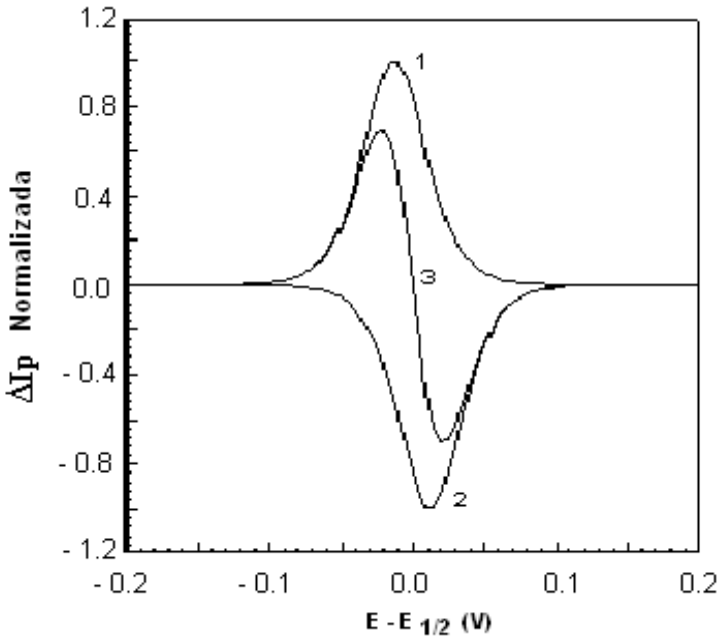

Figura 12. Respuesta de la corriente provocada por pulsos anódicos y catódicos curvas (1 y2). La curva 3 representa la suma de 1 y 2, produciendo la curva DAPV.

III.- Materiales y Métodos.

3.1 Técnica voltamétrica SWASV para determinación de As^{+3} utilizando electrodos BDD.

3.1.1 Reactivos

Los reactivos utilizados son de pureza de grado analítico. Una solución estándar de As^{+3} (1000 mg/L) se utilizó para la preparación diaria de la solución madre. El agua des-ionizada producida por ósmosis inversa en instalaciones Milli Q (Millipore, USA), se usó para la preparación de todas las soluciones. El electrolito soporte fue 0.1 M PBS (pH=5). Las soluciones con baja concentración de As^{+3} se preparon directamente en la celda electroquímica en rangos de µL, de la solución madre diluida, con pipetas automáticas.

3.1.2 Instrumentación y electrodos de trabajo

Preparación del electrodo BDD y su modificación con nanopartículas de Au

Se mezclaron piezas de obleas de silicio "Si" (100) de 5 x 5 mm cubiertas con diamante dopado con boro (BDD) de una muy buena conductividad eléctrica, con un soporte acrílico. El contacto eléctrico se hizo en la cara lateral para evitar la resistencia de la oblea. Una pequeña gota de pasta conductora de Ag curada a temperatura ambiente fue puesta en contacto con: una parte muy pequeña de la superficie del BDD y alambre de Sn, la otra terminal se conectó al electrodo. El área de contacto BDD fue aislada por una gota de resina acrílica de curado rápido a temperatura ambiente, adecuado para la determinación de arsénico [61-63].

La superficie BDD se utilizó verticalmente para evitar la acumulación de burbujas de gas producidas sobre su área durante el proceso. La activación del electrodo BDD por deposición de nanopartículas de Au se llevó acabo como se describe, sin ninguna modificación, según en el procedimiento aplicado por Yamada [62] con una muy baja concentración de sales de Au en H_2SO_4 (50 μM).

Electrodo BDD modificado con TiO_2

En este trabajo se aplicó el procedimiento propuesto por Kavan y otros [64] para deposición de óxido de estaño sobre indio, mejorado por Manivanaan y otros [65] y adaptado para la modificación de BDD con TiO_2, que fue depositado electrolíticamente a potencial constante a partir de una solución acuosa diluida de $TiCl_3$ a pH=2 siguiendo el procedimiento de los autores [65]. Se determinó que el máximo porcentaje de recubrimiento de la superficie BDD por TiO_2 fue cercano al 73%, usando micrografías SEM (microscopia electrónica de barrido) Ver anexo C.

3.1.3 Procedimiento analítico

La cuantificación de As^{+3} se hizo con voltametría de onda cuadrada de disolución anódica (SWASV). A -400 mV, ocurre una reducción:

$$As^{+3} + 3\ e^- = As^0$$

produciendo una monocapa sobre el electrodo; después, en la disolución cerca de los 0.00 V, el arsénico se oxida:

$$As^0 - 3\ e^- = As^{+3}$$

Es muy importante regular el tiempo de deposición como una función de la concentración de As^{+3}, debido a la baja conductividad de los depósitos de As^0.

3.2 Técnica voltamétrica DPV para determinación de Co^{+2} y Co^{+3}, en electrolito de Zn^{+2}, para electrowinning.

3.2.1 Reactivos

Todos los reactivos son de pureza de grado analítico (Merck y Sigma) y el agua des-ionizada se produjo en un sistema de Millipore, MilliQ. La solución madre del electrolito soporte de amonio fue preliminarmente preparada con una mezcla de NH_4OH con HCl concentrado, con una relación volumétrica de 8 a 1; seguido de un enfriamiento mediante una corriente de agua. El exceso de NH_4OH permitió la formación del quelato soluble de amonio-Zn^{+2}, evitando la formación de un precipitado. La solución 1nitroso 2naftol (1N-2Nf) se preparó preliminarmente con 50 mg de 1N-2Nf en 50 ml de etanol y 1 ml de HCl.

3.2.2 Instrumentación y electrodos de trabajo

Instrumentación

Las determinaciones polarográficas en el laboratorio, fueron hechas mediante un analizador polarográfico Modelo 264A modificado, acoplado con un equipo Modelo 303A SMDE/HMDE de (EG& PAR, USA con su respectivo electrodo auxiliar y de referencia), controlado por una PC mediante la ejecución de un software diseñado especialmente para esto. Un módulo de medición de conductividad controlada fue incorporado para la aplicación del analizador polarográfico el cual, determina el coeficiente de corrección de reproducibilidad superficial. Algunas de las curvas fueron registradas sobre papel, para después escanear y digitalizar.

Determinación industrial en línea

Se utilizó un tipo de celda polarográfica de flujo con un titulador especial para la aplicación de los electrodos desechables, usados como electrodos de trabajo. También se usó un equipo que consta de un electrodo Z59 (ZENIT Lab.) acoplado con un potenciostato Z58 controlado por un software de potenciostato Z54. El electrodo de referencia es Ag/AgCl/3M KCl y alambre de platino de 1 mm de diámetro como electrodo auxiliar. En la preparación del análisis de la muestra, se usó un una jeringa como dispensador/diluyente tipo Hamilton A ML-501A.

Electrodo de Trabajo

Los electrodos de trabajo desechables, introducidos recientemente por los autores [24] y producidos, a muy bajo costo, con la aplicación de la tecnología Printed Circuit Boar (PCB), se recubrieron, in situ, con una película de Hg, pocos segundos antes de la aplicación, aprovechando la superficie del electrodo de Hg sin ningún riesgo de derrame. El electrodo soporte es una placa de resina epóxica (0.5 mm de espesor) reforzada con fibra de vidrio y cubierta con 17μm de Cu; no se utilizó Ag debido a que en presencia de H_2S, se forma Ag_2S sobre su superficie afectando la formación de la amalgama [66].

Los electrodos de trabajo en forma de un disco, con diámetro 0.5 mm están recubiertos con 0.5 μm de Ni y 1 μm de Au. Estos electrodos pueden ser almacenados por tiempo indefinido y después de su aplicación serán fácilmente reciclables. Una banda de plástico conteniendo cerca de 1000 electrodos, fue cargada con un rollo controlado por computadora para cambiar los electrodos.

3.2.3 Procedimiento analítico.

Los experimentos polarográficos de laboratorio fueron realizados con la celda polarográfica PAR303A empleando el modo DME (Electrodo de gota de mercurio).

El electrolito de Zn industrial (con impurezas de Co^{+2}) y el electrolito soporte conteniendo una solución con 600 ppb de 1N-2Nf (2N-1Nf o una Sal-Nitroso-R para alguno de los experimentos) se adicionaron dentro de la celda polarográfica en relación 5 a 5 ml, con un dispensador-diluyente tipo Hamilton A ML-501A.

Los polarogramas DPP se registraron de un potencial inicial de -200 mV hasta -800 mV con una velocidad de barrido de 10 mV/s con una amplitud de pulso de -50 mV.

Las determinaciones en línea de las soluciones industriales reales se llevaron acabo en una celda voltamétrica especial de flujo; antes de la medición se depositó una película de Hg sobre el electrodo auxiliar (de Cu-Au), mediante electrolisis en la misma celda. Para ello se adicionó una solución de $HgCl_2$ en 0.1M HCl con una bomba peristáltica, donde la electrólisis se llevó acabo durante 30 segundos. Después se lava la celda con la bomba y se agregan: 5 ml del electrolito de Zn industrial, seguido de 5 ml de electrolito soporte, conteniendo 1N-2Nf, colocando después el electrodo desechable.

Los polarogramas fueron registrados de la misma forma que en las condiciones de laboratorio arriba mencionadas, para luego calcular la concentración de las impurezas de Co^{+2} mediante una PC.

3.3 Técnicas voltamétricas: DAPV y DPV, para determinación simultánea de As^{+3}, Pb^{+2} y Tl^{+1}.

3.3.1 Reactivos

Todos los reactivos incluyendo las soluciones patrón de Pb^{+2} y As^{+3} (1000 mg/L) son de pureza de grado analítico. Las soluciones en rangos de ppb y ppm utilizadas para la construcción de curvas de calibración o adiciones estándar, fueron preparadas, directamente en la celda electroquímica, usando pipetas automáticas BIOHIT (µL). Las soluciones experimentales fueron hechas con agua des-ionizada producida por ósmosis inversa en equipo MilliQ (Millipore, USA). El electrolito soporte para todas las determinaciones fue HCl 1M. Se utilizó gas nitrógeno para desoxigenar la solución.

3.3.2 Instrumentación y electrodos de trabajo

Un analizador de trazas polarográfico POL 150 controlado por software TM5 conectado a un electrodo (EG & G PAR modelo 303A SMDE/HMDE) como interfase fue utilizado en el laboratorio para la determinación polarográfica (DPP).

Una celda electroquímicas de vidrio de 10 mL, un electrodo de referencia (Ag/AgCl/3M KCl) y un electrodo de alambre de Pt, todos estas partes del Modelo 303A se utilizaron en todos los experimentos de laboratorio.

Un potenciostato portátil Z58, controlado por el software Z54 (ZENIT Lab), fue empleado para la determinación DAPV in situ con la aplicación del electrodo soporte Z59 (ZENIT Lab), una versión mejorada del SMMDE (electrodo de gota de mercurio múltiple) desarrollado y descrito por R. Zlatev et al. (2009) [24].

Como depósito para el Hg, se utilizó un tubo de ultra-micro-calibre de PTFE (Cole Parmer, EE.UU.), con 30 mm de largo, 0.1 mm de diámetro interno y 0.4 mm de diámetro exterior. La parte inferior desempeñó el papel de capilar, mientras que la parte superior (20 mm de largo) contenía cerca de 5 µL de Hg, equivalente a 6 gotas. Se utilizó un tubo capilar de acero inoxidable (0,1 mm D.I. x 0.3 mm D.E.; GL Ciencia, Tokio, Japón) como contacto eléctrico con la columna de mercurio. Antes de usar el depósito de SMMDE, el Hg permanece en la parte superior del tubo de PTFE sin estar en contacto con el metal. Para asegurar una estabilidad mecánica al final del capilar, el tubo de PTFE se colocó a 3 mm del diámetro exterior del de cuerpo de polietileno, que es la mitad de la parte superior abierta y accesible para un rollo, siendo una parte de la base del electrodo.

En la Figura 13 se muestra la construcción del SMMDE y la formación de la gota, basada en el funcionamiento de la bomba peristáltica: se cierra la tapa *(6)* y las juntas *(5)* para evitar que se derrame mercurio. El rodillo de plástico *(1)*, como parte del electrodo, empuja al mercurio hacia afuera formado así la gota de mercurio. Luego se abre la tapa *(6)* para que la solución entre en contacto con la gota de mercurio a través del orificio de la parte superior de la tapa. Después de la determinación, la tapa *(6)* se presiona hacia arriba y se cierra. Así las gotas desalojadas de Hg se mantienen en el volumen pequeño en la parte pseudo-cónica de la tapa *(6)*. La solución en exceso es expulsada a través de los orificios de las tapas durante el movimiento. El tamaño de la gota formada de Hg es controlado por el desplazamiento del rodillo *(1)*.

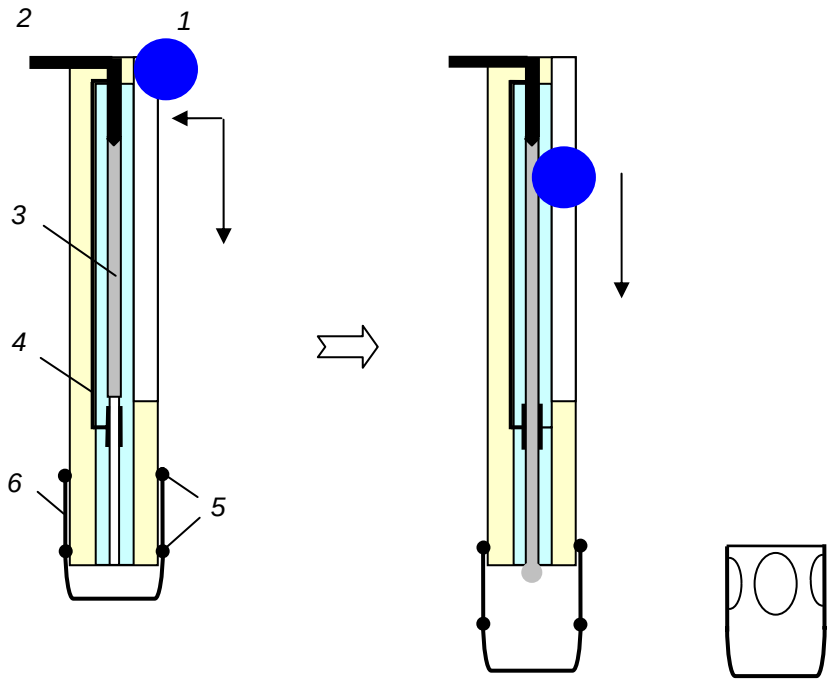

Figura 13. Representación esquemática del nuevo formador de gota de mercurio (SMMDE). *1*: Rodillo de plástico, *2*: Contacto, *3*: Hg, *4*: Alambre, *5* "O ring" y *6*: Tapa

Se aplicaron dos métodos para la formación de gota de mercurio: *i)* "fijo" y *ii)* "crecimiento controlado". En el primero, el rodillo *(1)* pasa siempre a la misma distancia, empujando hacia fuera el Hg, formando la gota. La influencia de las irregularidades del tubo flexible no se pueden evitar, por lo que la reproducibilidad de la superficie de Hg fue menos precisa comparada con el segundo método que se basa en la medición de conductividad. Para lo anterior se aplicó un voltaje AC de 10 mV p.p de amplitud en la formación de la gota. El rodillo *(1)* se detuvo en el

instante en cual el flujo de corriente fluye a través del electrolito soporte alcanzando el valor obtenido por la gota utilizada para la construcción de la curva de calibración de acuerdo al procedimiento descrito por R. Zlatev et al. (2009) [24].

Los resultados del DAPV fueron comparados con análisis de referencia hechos en el laboratorio utilizando un Espectrofotómetro Gillford (Stasar III) y un Analizador Modelo Perkin Elmer 200.

3.3.3 Procedimiento Analítico

Las soluciones modelo conteniendo: As^{+3}, Pb^{+2} y Tl^{+1} fueron preparadas adicionando µL de soluciones madre sobre 10 mL de HCl 1M en la celda polarográfica, que fueron desoxigenadas durante 4 minutos con nitrógeno antes de la determinación. Soluciones madre frescas de As^{+3} fueron preparadas diariamente.

Las muestras reales fueron tratadas de la misma forma, después de la adición de 1 mL de HCl concentrado en 9 mL de agua de la muestra. Los experimentos se realizaron a temperatura ambiente considerando dos diferentes tipos de condiciones de barrido para el análisis de muestras:

Condiciones de escaneo (1): para As^{+3}, Pb^{+2} y Tl^{+1} con una velocidad de barrido de 5 mV/s, y una amplitud de los pulsos de ± 25 mV para DAPV y de -25 mV para DPP.

Condiciones de escaneo (2): para As^{+3} y Pb^{+2}, con una velocidad de barrido de -5 mV/s y de -10 mV/s y una amplitud de los pulsos de ± 50 mV para DAPV y de -50 mV para DPP.

IV.- Resultados y Discusiones.

4.1 Técnica voltamétrica SWASV para determinación de As^{+3}

4.1.1 Electrodos BDD

Para la determinación de la concentración de As^{+3} se utilizaron dos tipos de electrodos BDD:

a) Activado sólo por nanopartículas de ***Au*** (BDD-Au).- Las nanopartículas de Au depositadas en la superficie BDD juegan un papel muy importante en la formación de compuestos inter-metálicos con el As^0 durante la etapa de deposición.

b) Activado por nanopartículas de ***Au*** y modificado con ***TiO_2*** (BDD-Au-TiO_2).

Por su parte, el TiO_2 aumenta la concentración local del As^{+3} sobre la superficie del electrodo.

4.1.2 Mediciones voltamétricas

Las propiedades semiconductoras que tienen los depósitos de As^0 provocan que, durante disolución anódica, sólo se forme una monocapa sobre la superficie del electrodo BDD y aun cuando se incrementa el tiempo de deposición no se logra una mejora considerable ya que: *i)* la monocapa se comporta como aislante haciendo imposible la deposición electroquímica, *ii)* no se ve reflejado en el aumento de la altura de pico registrado durante la disolución y *iii)* se limita el rango de determinación de respuesta lineal. Esto hace complicado la aplicación de cualquier tipo de electrodo sólido en la determinación por disolución de As^{+3}.

4.1.3 Efecto de los electrodos: BDD-Au vs BDD-Au-TiO_2

Las propiedades adsortivas del TiO_2 sobre As^{+3} provocan un incremento en la concentración local del As^{+3} sobre la superficie del electrodo BDD, durante la determinación por disolución, afectando la etapa de deposición. En la primera etapa del análisis de disolución, las nanopartículas de Au son consideradas como zonas activas para deposición de As^0, por lo que las nanopartículas de TiO_2 pueden ser localizadas muy cercanas a las de Au; donde se ve el efecto de la adsorción de As^{+3} por TiO_2. El gran recubrimiento de TiO_2 sobre el BDD, incrementa la probabilidad de la deposición de nanopartículas de TiO_2 cercanas a las de Au, provocando el aumento de adsorción de TiO_2 sobre As^{+3}. Esto hace que la cantidad de As^0 depositada sea mayor, al utilizar el electrodo BDD-Au-TiO_2, que también registra una mayor altura de picos.

En la Figura 14 se ven las curvas SWASV para As^{+3}, obtenidas con los siguientes parámetros de disolución: área= 25 mm^2, E_{dep} = -0.4 V y t_{dep} = 60 s; en la Tabla 2, se observa que el aumento del porcentaje de cobertura de superficie del BDD por TiO_2, en función del tiempo, provoca un incremento en la altura de pico SWASV de As^{+3}; siendo esto mejor para porcentajes de cobertura superiores a 45%. Esto puede ser provocado por el comportamiento caótico de las nanopartículas de TiO_2 y Au sobre el BDD.

Para mantener el rango de linealidad es necesario evitar la saturación de la superficie del electrodo con As^0, por lo que el tiempo de deposición debe ser menor al usar el electrodo BDD-Au-TiO_2 comparado con el BDD-Au.

Tabla 2. Altura de pico en función del porcentaje de cobertura de TiO_2 en BDD

Electrodo	% Incremento altura de pico	% cobertura TiO_2
1	0	0
2	22	0
3	31	0
4	45	3.4
5	58	22.1
6	73	49.4

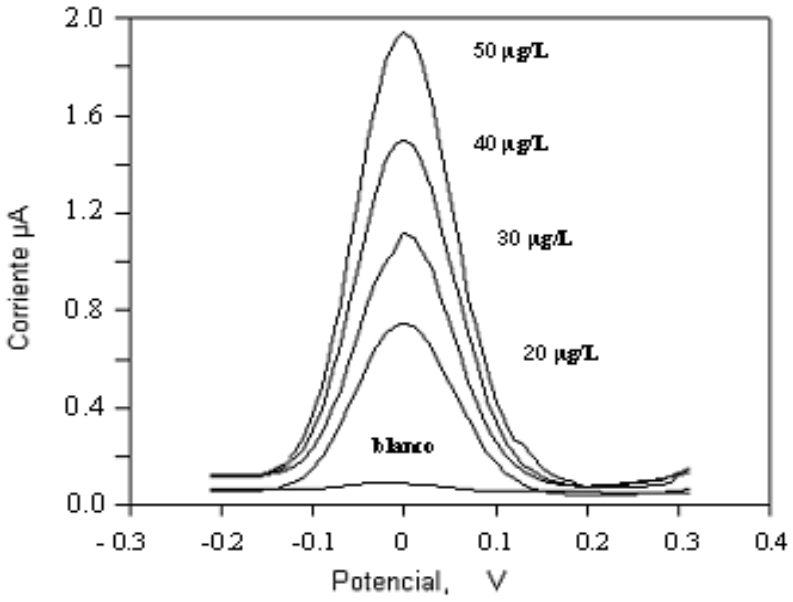

Figura 14. Grupo de curvas SWASV para As^{+3} en el rango de concentración de 0 a 50 ppb en PBS (pH=5) con un electrodo BDD-Au-TiO_2 con 73% de cobertura.

La Figura 15 nos muestra las curvas de calibración obtenidas a partir de los picos SWASV parcialmente mostrados en la figura 14; curvas que fueron hechas utilizando los dos tipos de electrodos. BDD-Au y BDD-Au-TiO_2.

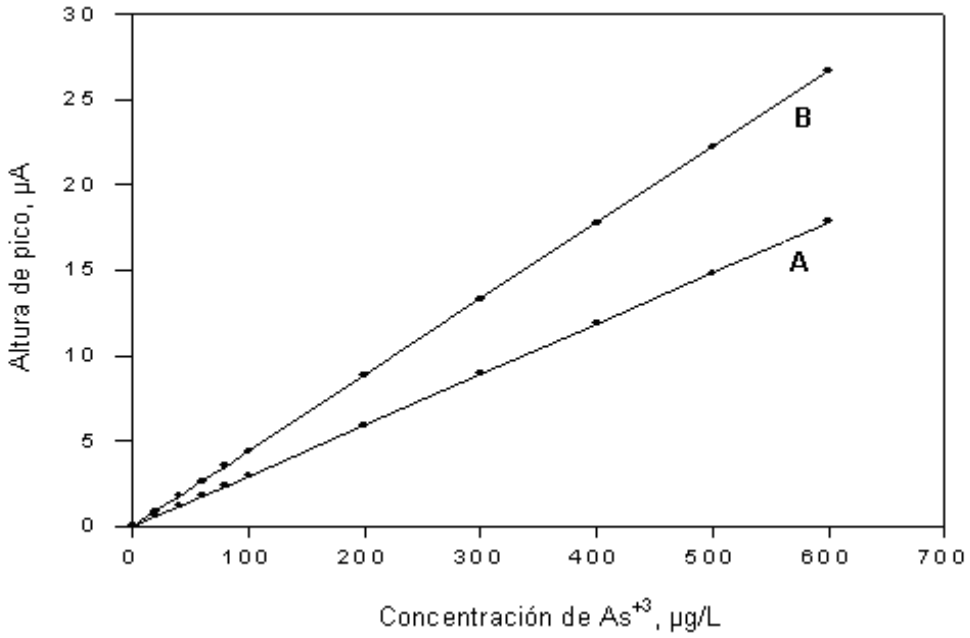

Figura 15 Curvas de calibración para concentraciones de As^{+3} de 0 a 500 ppb: curva A para electrodo BDD-Au y curva b para electrodo BDD-Au-TiO_2 con 75% de cobertura.

Las propiedades de adsorción del TiO_2 depositado sobre el BDD, resultaron en un incremento en la sensibilidad en las determinaciones SWASV de As^{+3} al utilizar el electrodo BDD-Au-TiO_2 con 73% de cobertura, en comparación con el electrodo BDD-Au.

4.2 Técnica voltamétrica DPV para determinación de Co^{+2} y Co^{+3}, en electrolito de Zn^{+2}, para electrowining.

4.2.1 Reproducibilidad de superficie del electrodo de trabajo.

El área del electrodo de trabajo fue un disco de Au (0.5 mm de diámetro) ubicado por en la parte de abajo de una barra de plástico de 5 x 30 mm. Se determinó la reproducibilidad superficial del disco de Au, antes de recubrirlo con Hg, el cual tuvo un valor de 4.3% de desviación estándar relativa (RSD) de electro-conductividad, tal como lo describen R. Zlatev et al. (2009) [24].

La conductividad del Hg^{+2} en solución, utilizado para deposición de Hg, se midió usando el módulo de conductividad incorporado en el analizador polarográfico Modelo 264A.

Estas mediciones se realizaron inmediatamente después de la deposición de la película de Hg sobre el Au, vía electrólisis. Así, se pudo mantener constante la concentración de Hg^{+2} en solución, siendo la conductividad medida, proporcional sólo a la superficie del electrodo a una temperatura constante.

El coeficiente de corrección se calculó contra el electrodo empleado para realizar la curva de calibración como lo manifiestan por R. Zlatev et al. (2009). [24].

La determinación de reproducibilidad de 10^{-6} M de Co^{+2} tuvo, según el procedimiento ya descrito, una RSD de ±3.6%; mientras que la reproducibilidad determinada aplicando DME tuvo una RSD de 1.4% para la misma concentración. Se aplicaron también la superficie de electrodos de Hg desechables, tal como se indica en el procedimiento de corrección descrito por R. Zlatev et al. (2009) [24].

4.2.2 Formación del quelato 1N-2Nf-Co y su aplicación para DPP.

El 1N-2Nf es uno de los primeros reactivos orgánicos aplicados en química analítica, utilizado durante mucho tiempo para la medición gravimétrica de Co^{+2} [21-23] debido a su gran facilidad de oxidarse de Co^{+2} a Co^{+3} y formar un quelato poco soluble [67].

El reactivo 1N-2Nf, proporciona una buena solubilidad en muchos solventes orgánicos como: acetona, etanol, benceno, etc. Siendo también soluble en solución acuosa, así como el ácido acético, el NaOH, tartrato, etc. [67, 68, 69]. La solubilidad de (1N-2Naftalato) Co^{+3} en agua es de 1.5 mg/L como lo reporta Piatnikyi [67]. Una coloración rojo-café de la solución aparece sólo en presencia de Co^{+2} en niveles de ppb, debido a que probablemente no ocurre la precipitación de quelatos. Esto permite, las determinaciones polarográficas directas de bajas concentraciones de Co^{+2} que se llevan acabo fuera aplicando DME sin preconcentración del quelato sobre la superficie del electrodo.

La adición de 1N-2Nf sobre la solución con Co^{+2} da como resultado la aparición y el incremento de un pico DPP bien definido a -550 mV el cual corresponde a la reducción electroquímica de Co^{+3}, producido por la oxidación del Co^{+2} al añadir el reactivo orgánico, mientras que al mismo tiempo la altura del pico de Co^{+2} situado a -1335 mV disminuye respectivamente. Así, el Co^{+2} es oxidado, sólo parcialmente, por el reactivo orgánico y por la concentración de Co^{+3} formado, y por lo tanto la sensibilidad de las lecturas depende de la concentración del 1N-2Nf. Véase Figura 16.

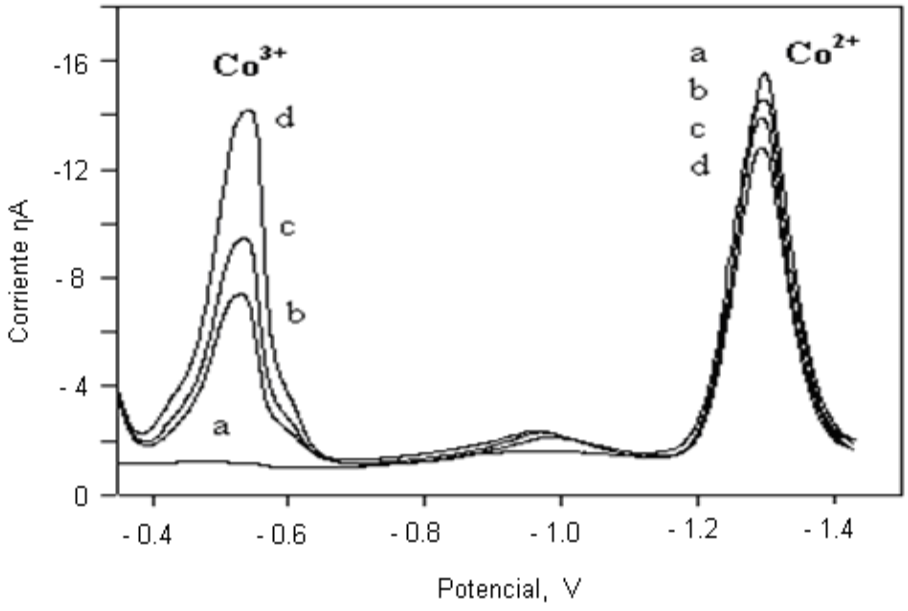

Figura 16. Polarogramas DPP de Co^{+2} después de adicionar 1N-2Nf. Curva a: sólo 100 ppb de Co^{+2} en solución buffer de amonio; Las curvas b, c y d: en presencia de 1N-2Nf con 400, 500 y 800 ppb respectivamente.

Como lo muestran Kolthoff y otros autores [21-24,59,60,67] la composición del quelato formado puede describirse como $Co(R)_3$, determinando la relación de concentración óptima: 1N-2Nf/Co que deberá ser de 3 a 1. Se puede esperar que la altura del pico de Co^{+3} se incremente por esta relación y que de esta forma alcance una concentración de 600 ppb, que fue escogida como una adición óptima para el 1N-2Nf, 3 veces más alta que el límite superior del rango de concentración del Co existente en la planta electrolítica industrial de Zn (que es de 20 a 200 ppb).

La concentración seleccionada de 1N-2Nf, se probó haciendo la curva de calibración en coordenadas: altura de pico de Co^{+3} vs concentración de Co^{+2}, siendo lineal en la presencia de 600 ppb de 1N-2Nf en el rango de concentración de Co^{+2} de 20 a 500 ppb con una pendiente: 0.084 ηA/ppb.

Se obtuvo un coeficiente de correlación, para altas concentraciones de Co^{+2} (>200 ppb), cuyo valor es r^2 = 0.946, mientras que para concentraciones bajas, de 20 a 200 ppb, (típico en impurezas de Co^{+2} en soluciones electrolíticas de plantas industriales de Zn) el coeficiente de correlación de la curva de calibración es r^2 = 0.987. Experimentalmente se encontró que la altura del pico de Co^{+2} alcanzó un máximo con el incremento de la concentración de 1N-2Nf y probablemente la parte decreciente de la curva después del máximo se debe a que el valor del producto de solubilidad del 1N-2naftalato de Co^{+2} provoca la precipitación del quelato disminuyendo así la lectura de la concentración de Co^{+3}.

El 1N-2Nf es una sustancia electroquímicamente activa, que produce un pico DPP a -250 mV vs Ag/AgCl/3M KCl, en el mencionado electrolito soporte de amonio, lo que permite ver la oxidación y formación del quelato de Co^{+2}.

En la Tabla 3 se muestran los resultados que reflejan la influencia de la concentración de Zn^{+2} sobre Co^{+2}. Se realizaron determinaciones, incrementando la concentración (en un rango de 20 a 200 ppb) en una solución modelo conteniendo 150 g/L de Zn^{+2}. En la Figura 17 se observa el consumo de 1N-2Nf al incrementarse la concentración de Co^{+2}, donde el pico inicial de 1N-2Nf disminuye con la sucesiva adición de Co^{+2}.

Tabla 3. Precisión de la determinación de Co^{+2} en la presencia de 150 μg/L de Zn^{+2} aplicando la técnica DAPV en soluciones modelo.

Concentración STD ppb	Determinación de concentraciones ppb	Determinación de concentraciones ppb	Error relativo ppb	Error relativo %
20	21.80	21.80	-1.8	-9.0
50	53.20	53.20	-3.2	-6.4
100	9.71	9.71	2.9	-2.9
150	148.20	148.20	-1.8	1.2
200	197.60	197.60	2.4	1.4

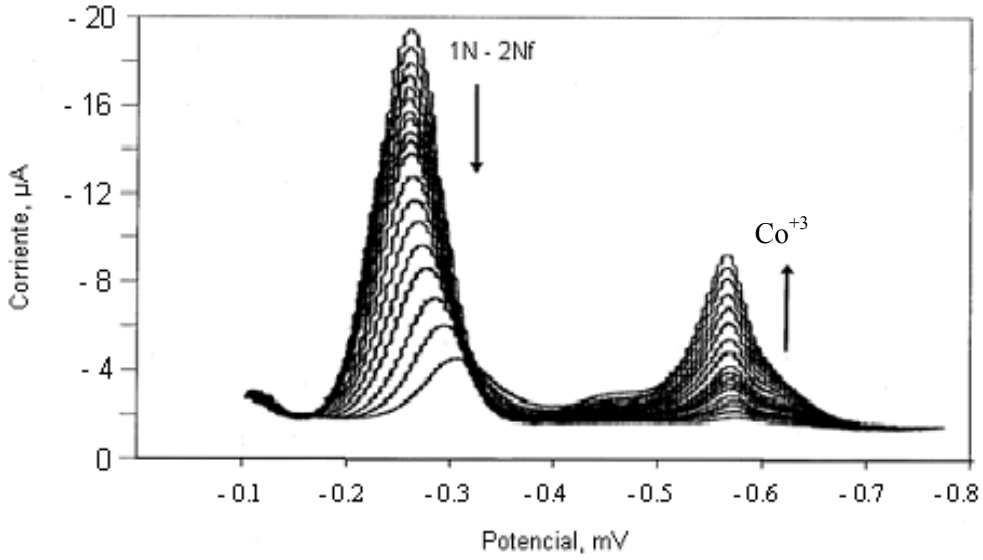

Figura 17. El decremento del pico DPP de 1N-2Nf (600 ppm de concentración inicial) situado a -250 mV, ocasionado por la sucesiva adición e Co^{+2} en el rango de 0 a 800 ppb.

La importancia analítica del pico de Co^{+3}, es que aparece a -550 mV (Ag/AgCl 3M KCl). El pico Zn^{+2} corresponde a una baja concentración con el fin de marcar sólo el potencial de pico. Véase Figura 18.

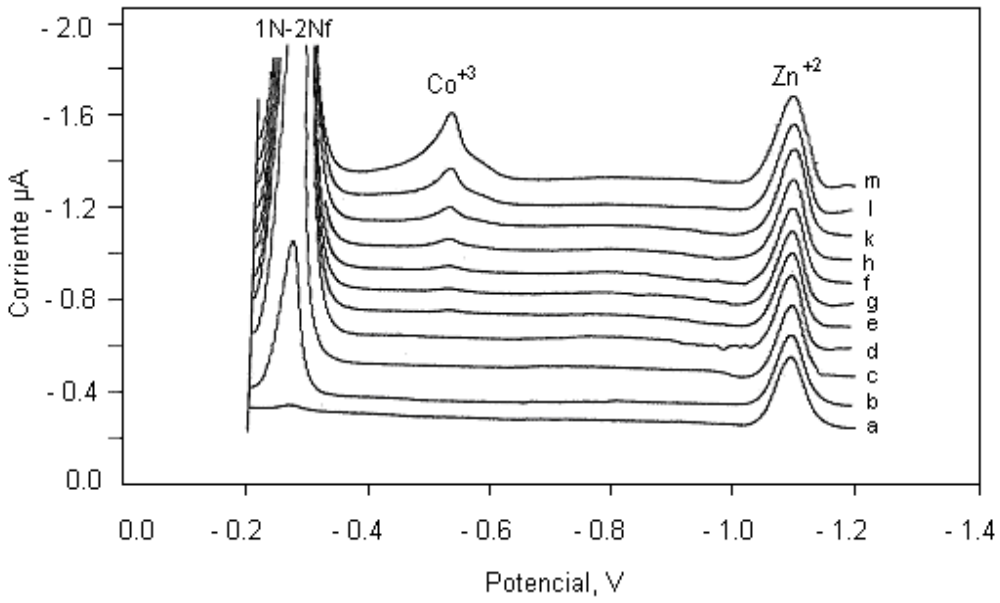

Figura 18. El pico DPP de Co^{+3} (*E*p = -550 mV) resultado de la oxidación del Co^{+2} (*E*p = -1335 mV) por los picos DPP de: 1N-2Nf y Zn^{+2} (*E*p = -1350 mV). La curva a: es Zn^{+2} puro; las curvas b, c y d: se deben a la adición posterior de 1N-2Nf; las curvas de e hasta m: son debido a la adición sucesiva de Co^{+2}.

A pesar de la alta sensibilidad en la determinación espectrofotométrica de Co^{+2} con aplicación de 2N-1Nf comparado con 1N-2Nf, su comportamiento polarográfico resultó ser inferior.

La altura de pico DPP de Co^{+3} en el electrolito soporte de amonio, aplicado en el presente trabajo, es mucho más bajo y aparece para potenciales mucho más negativos, aún alejado del potencial de pico de Zn^{+2} como se ve en la Figura. 19.

Los tres reactivos orgánicos del grupo nitroso-naftol aplicados en la química analítica, la sal nitroso-R dio un amplio pico de Co^{+3} a una sensibilidad inferior de las lecturas comparada con la aplicación de 1N-2Nf.

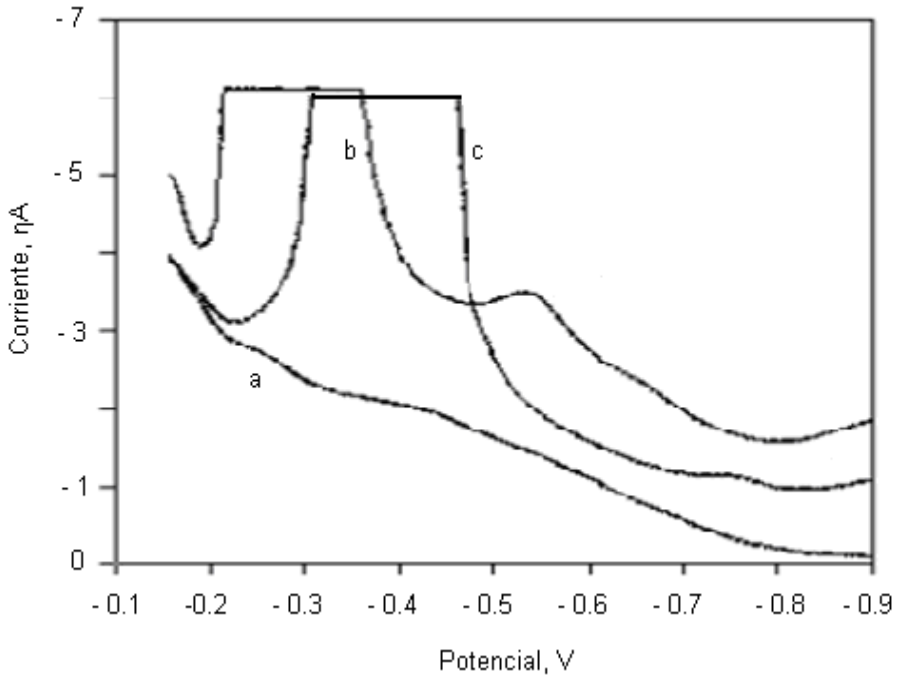

Figura 19. Picos DPP.- Curva b: Co^{+3} y 1N-2Nf.- Curva c: 2N-1Nf y Co^{+3} y Curva a: el blanco.

4.2.3 Determinaciones aplicadas a muestras reales

En la Figura 20 se muestran las curvas típicas de electrolito de Zn industrial conteniendo Co^{+2}. El pico 1N-2Nf con 600 ppm aparece a -250 mV, no interfiere con el pico de Co^{+3}, sin embargo aparece el traslape del pico de Ni^{+2} a -430 mV al utilizar electrolito soporte. Dado que las concentraciones de Co^{+2} y Ni^{+2} son del mismo orden, el pico de Ni^{+2} no interfiere con las lecturas de Co^{+2}. Los resultados experimentales muestran que la concentración de Zn^{+2} no interfiere, con ninguna de las lecturas de Co^{+2} obtenidas por el método utilizado en este trabajo, en toda la gama de concentraciones de Co^{+2} presente en la solución.

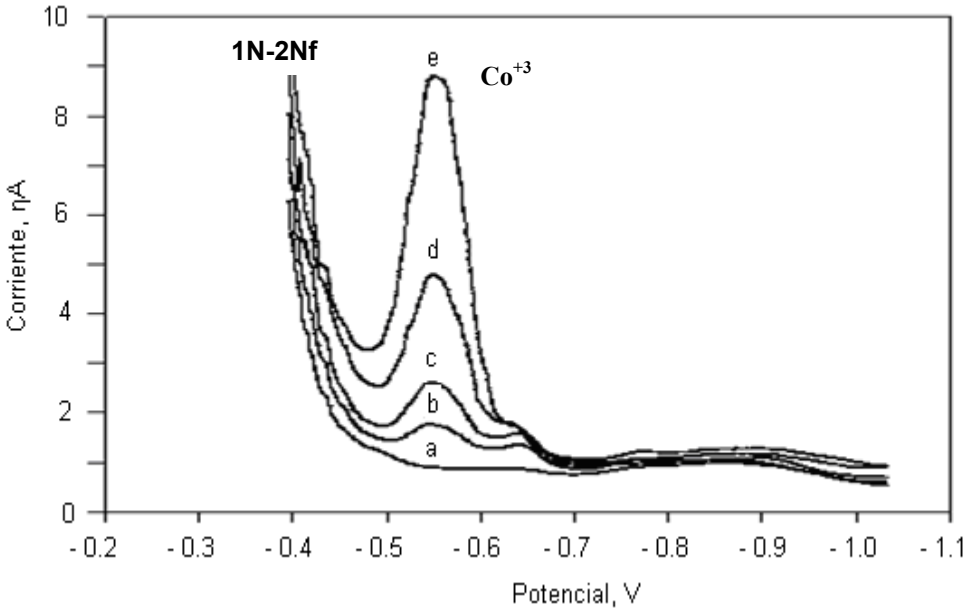

Figura 20. Picos de Co^{+3} a diferentes concentraciones de Co^{+2}: 20 ppb (curva b); 40 ppb (curva c); 80 ppb (curva d) y 160 ppb (curva e) en solución electrolítica industrial de Zn; blanco (curva a).

4.3 Técnicas voltamétrica: DAPV vs DPV para As, Pb y Tl

4.3.1 Determinación de potenciales de pico aplicando DPP.

Es muy común que las aguas contaminadas con As^{+3}, contengan Pb^{+2} y otros metales pesados, sobre todo las aguas residuales de las industrias. En la Figura 21 se ve el voltamograma DPP de una muestra de agua residual industrial conteniendo: As^{+3}, Pb^{+2} y Cd^{+2}. Los primeros picos de As^{+3} y Pb^{+2} tiene una diferencia de $E_{1/2}$ de unos 50 mV haciendo que el As^{+3} aparezca como un traslape sobre el pico Pb^{+2}. Aun cuando variamos las relaciones de concentración entre As^{+3} y Pb^{+2}; esa pequeña diferencia de $E_{1/2}$, dificulta poder distinguir cada pico DPP de ambas especies, obligando a una separación preliminar de las mismas.

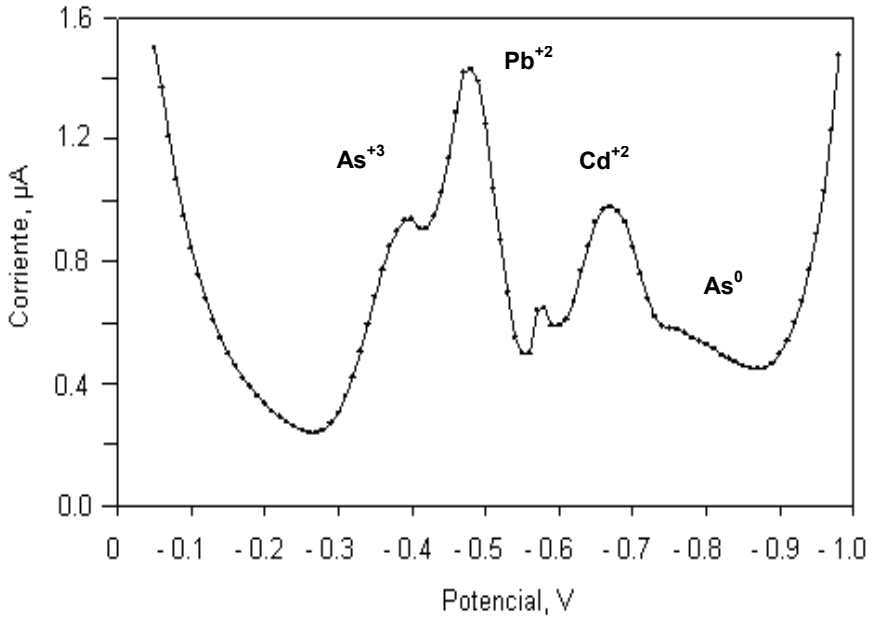

Figura 21 Voltamograma DPP de aguas residuales conteniendo: As^{+3}, Pb^{+2} y Cd^{+2}. Condiciones de escaneo (tipo 2).

Por otra parte, en la Figura 22, el Pb^{+2} se sitúa en -0.48 V, mientras que el Tl^{+1} aparece a un potencial más negativo de -0.52 V. La diferencia entre sus potenciales también es muy pequeña lo que hace que también ocurra la superposición para cualquier relación de concentración entre ambas especies.

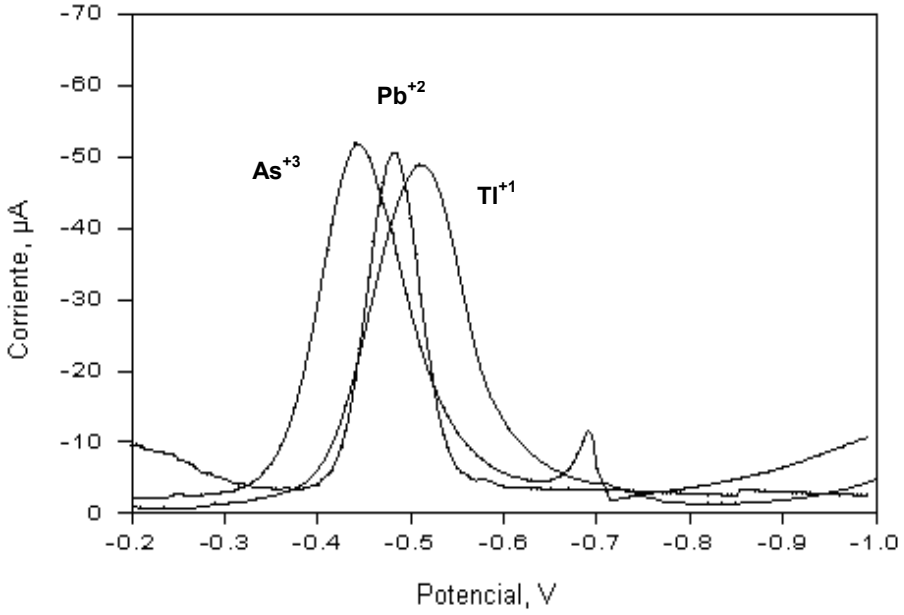

Figura 22 Picos DPP de As^{+3} Pb^{+2} Tl^{+1}. Condiciones de escaneo (tipo 1).

En la Figura 23, del voltamograma DPP (electrolito soporte HCl 1M), se ven dos picos de As^{+3}. El primer pico situado a -0.43 V corresponde a la reducción de 3 electrones de As^{+3} a As^{0}. Segundo pico a -0,78 V producto de la reducción posterior de: As^{0} a As^{-3} al formarse AsH_3. Un tercer pico muy estrecho (un máximo polarográfico) surge en -0.7V cuando la concentración de As^{+3} es mayor de 300 mg/L [70].

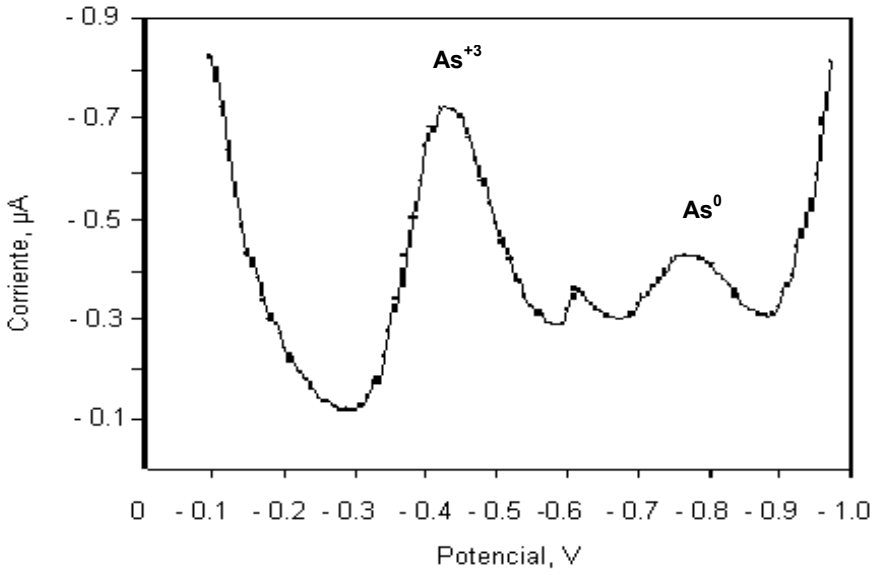

Figura 23 Voltamograma DPP, 300 ppb de As^{+3} sólo, en HCl 1M. Condiciones de escaneo (tipo 2).

Lo que sí podemos verificar es la relación directa entre el aumento de corriente debido al incremento en la concentración. La *curva c* de la Figura 24, (relación 1:5) presenta una menor respuesta de corriente en comparación con la *curva c* de la Figura 25, con una relación de concentración entre As^{+3} y Pb^{+2} de 1:10; esto nos muestra el claro incremento en la respuesta de corriente.

Por lo anterior podemos decir que las determinaciones simultáneas de las especies contaminantes mediante la técnica DPP, son muy difíciles debido a la superposición de picos, ya que una gran cantidad de especies tienen muy pequeñas diferencias entres sus $E_{1/2}$. El problema se puede resolver sólo con dos criterios: la separación preliminar de especies o la aplicación de una técnica voltamétrica con mayor potencia de resolución.

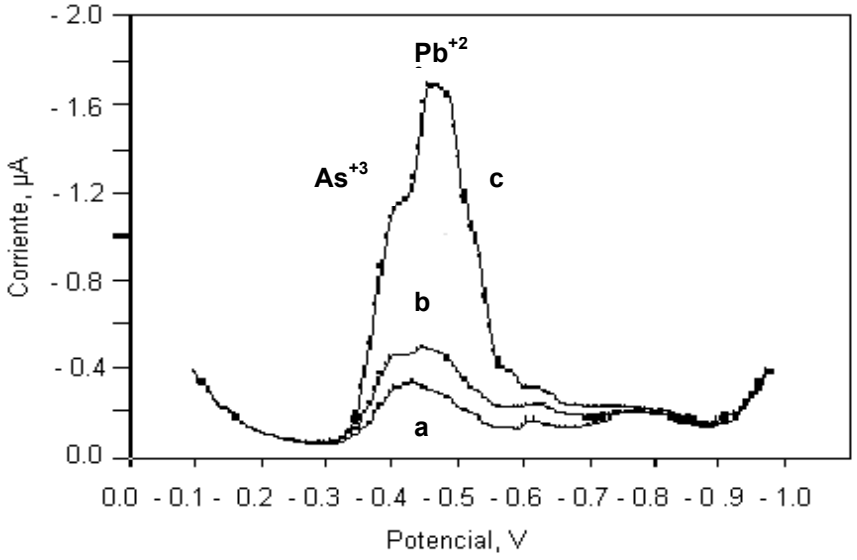

Figura 24 **Voltamograma DPP para 300 ppb de As^{+3} en HCl 1M, con la adición de Pb^{+2}, a diferentes relaciones de concentración: curva a = 1:0; curva b = 1:1 y curva c = 1:5 . Condiciones de escaneo (tipo 2).**

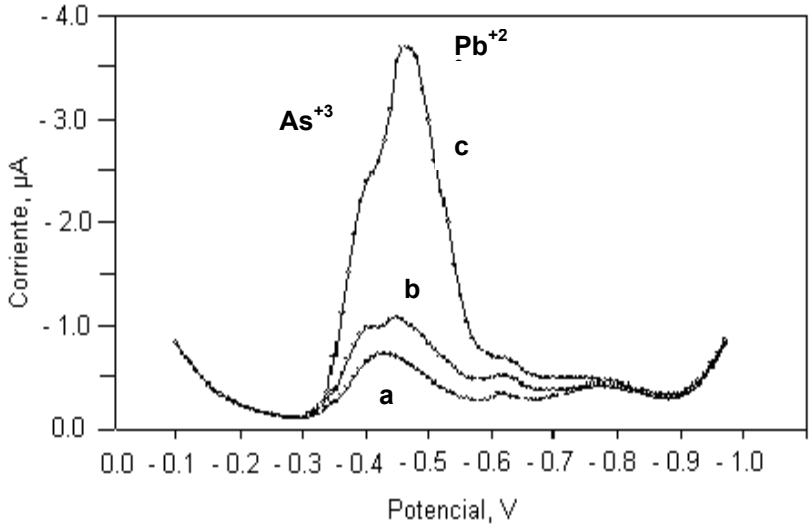

Figura 25 **Voltamograma DPP de 300 ppb de As^{+3} y 300 ppb de Pb^{+2} en HCl 1M para diferentes relaciones de concentración curva a = 1:0; curva b = 1:1; curva c = 1:10. Condiciones de escaneo (tipo 2).**

4.3.2 DAPV para la determinación simultánea de especies.

4.3.2.1 Principios de DAPV.

La superposición de pulsos rectangulares con polaridad opuesta sobre el potencial del electrodo de trabajo, es resultado de los pares de pulsos con corrientes farádicas de polaridad opuesta.

Al graficar el incremento de la corriente contra la diferencia de potencial, se produce el voltamograma DAPV que tiene la forma de la segunda derivada de una onda polarográfica (no linealidad de I vs E), como se ve en la Figura 26.

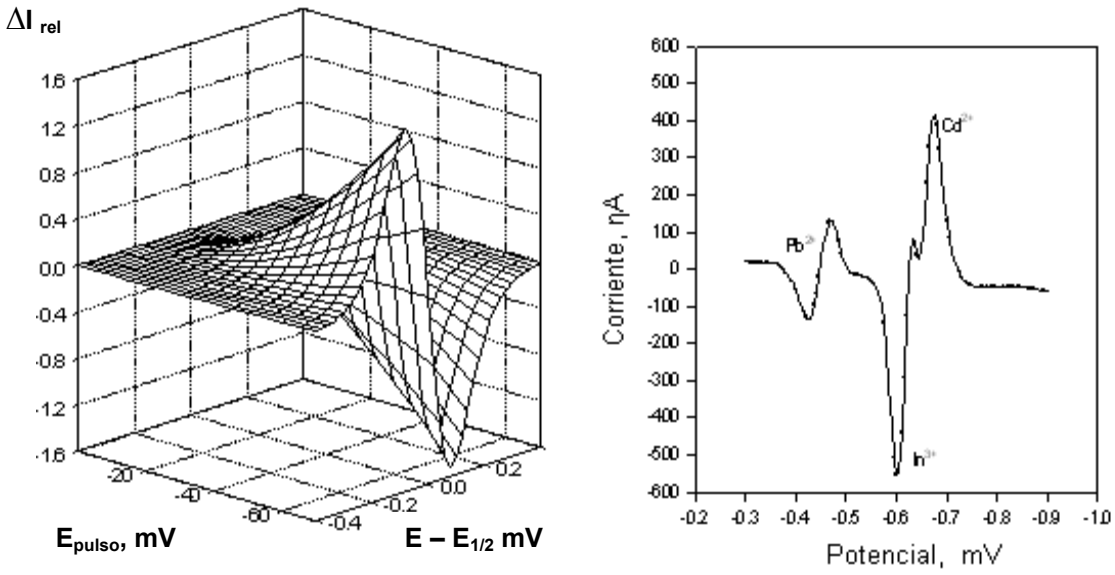

Figura. 26 Voltamogramas DAPV: Teórico (izquierda) y Real (derecha).

En estos voltamogramas DAPV, los picos se sitúan en ambos lados de la línea de cero, donde: las alturas son proporcionales a la concentración y el potencial de pico (potencial máximo) caracteriza la naturaleza del analito [35].

La mitad del ancho de los picos definen el poder de resolución de cada método analítico: a mayor nitidez de los picos, mayor es la resolución. La mitad del ancho de los picos DAPV es de aproximadamente el 70% de la obtenida por el método convencional de voltametría DPV [35]. Este pequeño valor permite la distinción simultanea de especies (sin su separación analítica preliminar) cuyas diferencias entre sus potenciales de pico son pequeñas, por ejemplo: As^{+3} y Pb^{+2}, Pb^{+2} y Tl^{+1}; As^{+3} y Cd^{+2}, Co^{+2} y Ni^{+2}, etc.

La alta sensibilidad de DAPV, como la de DPP, [35] permite realizar la determinaciones en matrices con alta concentración, no siendo necesario la separación de especies o el pretratamiento preliminar sobre la muestra.

4.3.2.2 Aplicación de DAPV.

La ventaja principal de DAPV es el uso de los picos anódicos y catódicos, los cuales se utilizaron para las evaluaciones de concentraciones de cada especie en caso de traslape. La precisión de las lecturas tiene como parámetro base, la relación de concentración entre las especies. Para un control interno de los procesos de purificación en planta, se consideró un error relativo preestablecido (ERP=10%) para obtener la relación máxima de concentración, posible, para cada par de especies: Pb^{+2}, As^{+3} y Pb^{+2}, Tl^{+1}, de manera que se pudieran realizar las lecturas de cada especie, sin la interferencia de una sobre la otras.

4.3.2.3 Determinación simultánea de Pb^{+2} y Tl^{+1}.

Se obtuvo la relación de concentración máxima entre Tl^{+1} y Pb^{+2}, en exceso de Tl^{+1}, registrando los incrementos en la concentración de Tl^{+1} en voltamogramas DAPV, mantenimiento constante la concentración de Pb^{+2}.

El DAPV de la Figura 27 muestra, bien definidos y separados, dos picos: el anódico de Tl^{+1} y el catódico de Pb^{+2}, para relaciones de concentración tan altas como 6 a 1. Para relaciones más elevadas, el pico catódico de Tl^{+1} incrementa su interferencia sobre el pico de Pb^{+2}.

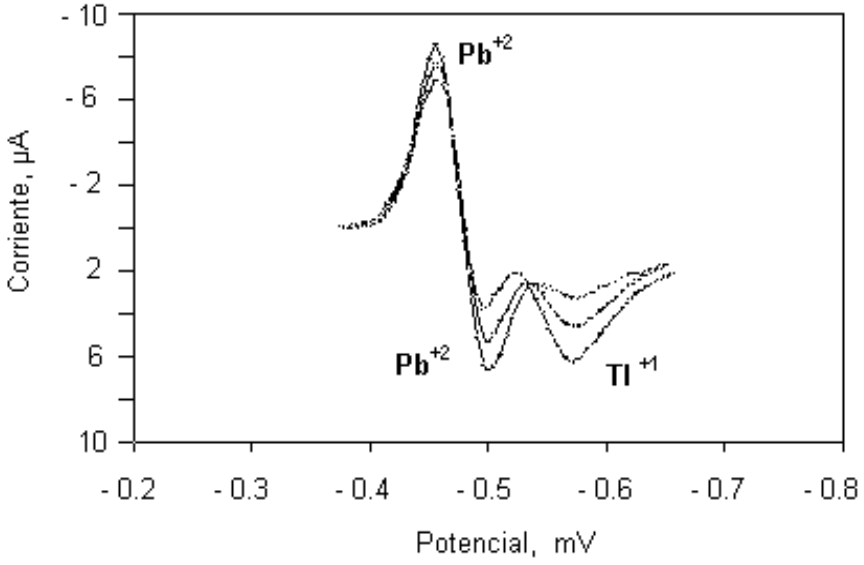

Figura 27. DAPV de Pb^{+2} y Tl^{+1} en HCl 1M para diferentes relaciones de concentración 4:1 (pico superior de Tl^{+1}), 2:1 (de en medio) y 1:1 (pico inferior de Tl^{+1}).

Se determinó que es posible medir la altura del pico catódico de Pb^{+2} situado sobre el pico de Tl^{+1}, para relaciones de concentración tan altas como 16 a 1.

Sin embargo, varios picos de Pb^{+2} se registraron para relaciones de concentración tan altas como 20 a 1, pero su uso analítico requiere el aplicar complicados procedimientos matemáticos, no garantizando la precisión preestablecida de la determinación.

Para el caso de exceso de Pb^{+2} es más complicado debido a que: la mitad del ancho de pico de Tl^{+1} es más grande y la técnica voltamétrica tiene mayor sensibilidad hacia el Pb^{+2}.

En estas condiciones de exceso de Pb^{+2}, el Tl^{+1} puede ser determinado, aplicando DAPV, para relaciones respectivas de concentración menores de 5 a 1; mientras que un traslape completo de los dos picos aparece para relaciones tan pequeñas como 1 a 1 como se ilustra en las Figuras 28 y 29.

Los resultados obtenidos, aplicando DAPV para Pb^{+2} y Tl^{+1} con exceso de Pb^{+2}, fueron también comparados con los resultados logrados con la técnica de voltamétrica CA de segunda armónica (SHACV), de la cuál se registraron diferentes picos, con importancia analítica, para relaciones de concentración de Pb^{+2} a Tl^{+1} hasta de 4 a 1.

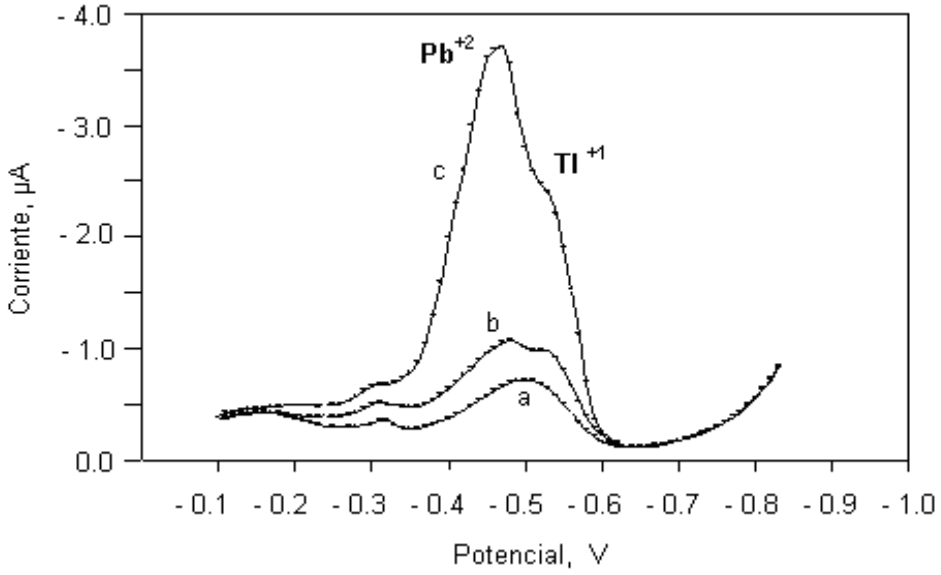

Figura 28. DPP de Pb^{+2} y Tl^{+1} en HCl 1M con exceso de Pb^{+2}. Para diferentes relaciones de concentración: Curva a: 0:1, Curva b: 1:1 y Curva c: 4:1.

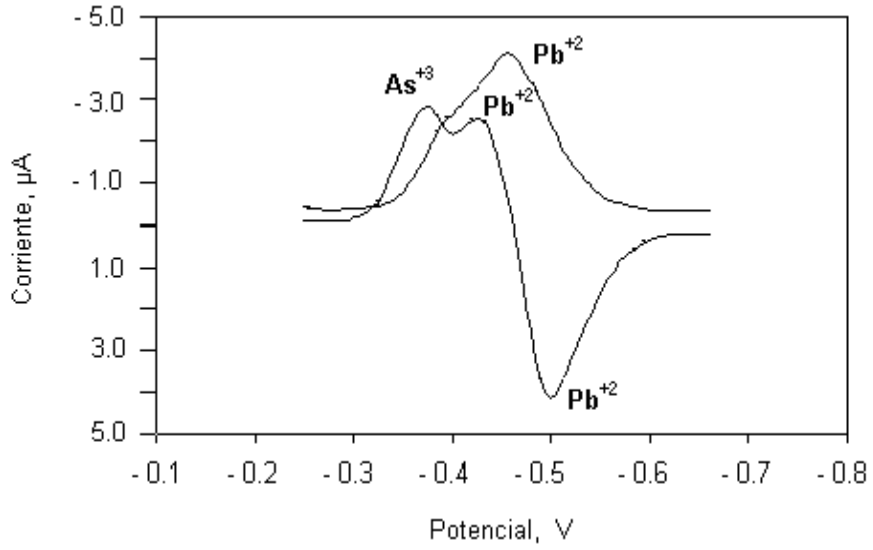

Figura 29. Picos DAPV de As^{+3} y Pb^{+2} en HCl 1M con relación de concentración 1:5.

4.3.2.4 Determinación simultánea de As^{+3} y Pb^{+2}.

Este caso es similar al anterior de Pb^{+2} y Tl^{+1}, debido a lo grande de la mitad de ancho de pico del As^{+3}, producto de la reducción irreversible de esta especie y la alta sensibilidad de la técnica voltamétrica hacia el Pb^{+2}.

Una curva DAPV con 60 ppb de concentración de As^{+3} y Pb^{+2} con relación 1:5 (con exceso de Pb^{+2}), se muestra en la Figura 29; donde se compara con una curva DPP en HCl 1M con las mismas condiciones experimentales.

Para la curva DPP los dos picos son nada distinguibles, mientras que la curva DAVP contiene, bien definidos y separados, un par de picos: anódicos de Pb^{+2} y catódico de As^{+3}.

Los picos de As^{+3} y Pb^{+2} colocados en ambos lados de la línea cero, están completamente separadas al tener 6 veces en exceso el Pb^{+2}, lo que permite determinarlos en forma directa, simultánea y sin previo tratamiento de la muestra.

Para el As^{+3} se encontró un comportamiento lineal de su curva de calibración, en un rango de concentración de 8 a 2000 µg/L.

La desviación estándar relativa, que caracteriza la reproducibilidad, fue menor al 3% en la parte superior del rango de concentración lineal y cercana al 10% para la parte inferior del mismo rango.

El límite de detección de DAPV para determinar As^{+3} es de 6.7 µg/L, con un intervalo de confianza de 95%.

En la Figura 30, se muestra una pendiente de calibración para As^{+3} para una relación de concentración de As^{+3} a Pb^{+2} de 1/1 a 20/1 (con exceso de As^{+3}). Los resultados sobre la determinación de Pb^{+2}, se muestran en la Tabla 4.

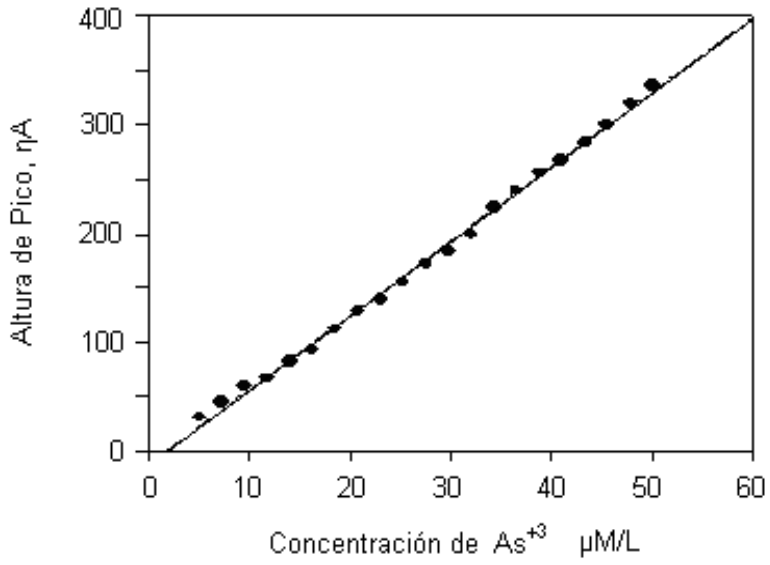

Figura 30. Curva de calibración para As^{+3} (de 5 µM a 50 µM) en HCl 1M en presencia de 5 µM de Pb^{+2}.

Los resultados obtenidos al aplicar la técnica DAPV fueron comparados con los obtenidos por métodos espectrales como son la espectrofotometría (con di-etil-di-tiocarbamato de plata después de la dilución de la muestra) y AAS en un laboratorio de referencia. Se utilizó una muestra real de agua residual conteniendo: As^{+3} y Pb^{+2} con una relación de concentración de 1:2.

Tabla 4. Determinación de As^{+3} y Pb^{+2} aplicando diferentes métodos analíticos.

[μg/L]	**DAPV**	**AAS**	**Fotometría**	**DAPV**	**AAS**
Número	As^{+3}	As^{+3}	As^{+3}	Pb^{+2}	Pb^{+2}
1	47.2	42.2	49.3	106.3	98.2
2	51.0	47.7	51.4	102.4	100.7
3	49.7	46.1	53.7	98.5	101.1
4	46.3	45.2	47.3	100.7	97.2
5	48.3	50.5	50.2	98.2	99.5
Porcentaje	48.5 ± 3.89	46.3± 6.63	50.4 ± 4.73	101.2 ± 3.28	99.3 ± 1.66

En esta Tabla 4 se observa que los tres métodos coinciden en sus resultados obtenidos. Algunos procedimientos apropiados de pretratamiento de muestra, fueron realizados antes de aplicar los métodos espectrales. Las determinaciones DAPV fueron hechas directamente, después de adicionar HCl. No se presentan datos obtenidos sobre aplicación de DPP, debido al traslape total entre los picos de As^{+3} y Pb^{+2}, incluso para la relación de concentración 1:1.

4.3.2.5 Determinación simultánea de As^{+3}, Pb^{+2} y Tl^{+1}.

Este caso es mucho más complicado, en particular, para la determinación de Pb^{+2} ya que los picos: catódico y anódico de Pb^{+2} se traslapan en ambos lados, en función de la relación de concentración de As^{+3}**:** Pb^{+2}**:** Tl^{+1}. La gran variación de valores de la relación hace impredecible una determinación simultánea de las tres especies cualquier caso en específico debe ser tratado por separado.

V.- Conclusiones

5.1 Determinación de As^{+3} usando SWASV y electrodos BDD.

Se desarrolló un método voltamétrico para la determinación de As^{+3} aplicando la técnica SWASV, en donde además se utilizaron electrodos de diamante altamente dopados con boro (BDD) activados con nanopartículas de Au, que fueron modificados electro-químicamente mediante TiO_2.

Las propiedades de adsorción, de 73% de cobertura de TiO_2 depositado sobre la superficie del electrodo BDD-Au-TiO_2, propició el incremento en un 49.7% sobre la sensibilidad durante las determinaciones SWASV del As^{+3}, comparado con el electrodo no modificado BDD-Au. Cabe señalar que para coberturas menores del 45% no se verifican cambios apreciables en la sensibilidad debido a la distribución caótica de las nanopartículas tanto de Au como de TiO_2.

Se lograron resultados confiables en las determinaciones de As^{+3}, lo cual permite realizar mediciones in situ, no exponiendo las muestras al oxígeno evitando así la oxidación de As^{+3} a As^{+5}.

5.2 Determinación de Co^{+2}, Co^{+3} y Zn^{+2} usando DPV y 1N-2Nf.

Se desarrolló un método voltamétrico DPV para la determinación de cobalto, para lo cual se utilizó 1-nitroso-2-naftol para: la oxidación del Co^{+2} a Co^{+3} y la formación del quelato utilizando un electrolito soporte de NH_4OH/HCl en relación 8 a 1.

La gran diferencia entre los potenciales de pico DPP de Co^{+3} y Zn^{+2}, permitió determinar la concentración de Co^{+2}, eliminando por completo la interferencia del Zn^{+2}; logrando así, resultados confiables para rangos de concentración de Co^{+2} de 20 ppb a 200 ppb en la planta electrolítica de Zn.

Como parte de los objetivos de este trabajo, se utilizaron electrodos de Hg desechables (electrodos de trabajo) para desarrollar y aplicar un simple y rápido método de polarografía diferencial de pulsos (DPP) en línea, para la determinación directa de Co^{+2} en la planta electrolítica de Zn.

5.3 Determinación simultánea de As^{+3}, Pb^{+2} y Tl^{+1} usando DAPV y DPV.

Se desarrolló un método voltamétrico para la determinación simultánea directa de As^{+3}, Pb^{+2} y Tl^{+1}, basado en voltametría diferencial de pulsos alternativos (DAPV). Este método combina la alta sensibilidad del método DPV, con la gran resolución de los métodos voltamétricos de segundo orden.

Se determinaron los límites de las relaciones de concentración entre las especies, para su determinación simultánea utilizando DAPV, con una precisión preestablecida menor del 10% utilizando HCl 1M como electrolito soporte.

Se aplicó DAPV para determinaciones in situ de As^{+3}, Pb^{+2} y Tl^{+1} en muestras industriales, para el control interno del proceso de purificación. Aunque cabe mencionar que debido a la gran variación de valores de la relación, hace impredecible una determinación simultánea de las ***tres*** especies, cualquier caso en específico, se recomienda darle un trato por separado.

VI Bibliografía

1 E. Pilkington, C. Weeks and A. Bond, Anal. Chem., 48, 1665 (1976).

2 D. A. Bond, Anal. Chim. Acta, 400, 333 (1999).

3 G. T. Wever, J. Metals, 11, 130 (1959).

4 G. C. Bratt, Electrochem. Technol., 2, 323 (1964).

5 V. L. Klimenko, Sov. J. Non-Ferrous Metals, 12, 18 (1971).

6 A. R. Ault, J. H. Bain, D. J. Palmer and J. B. Pullen, in South Australia Conference, p. 225, Australian Institute of Mining and Metallurgy, Melbourne, (1975).

7 U. F. Turoshima and V. V. Stender, J. Appl. Chem. USSR, 28, 151 (1955).

8 H. H. Fukabayashi, T. J. O'Keefe and W. C. Clinton, U. S. Bur. Mines Rep. RI 7966, Rolla, Mo., (1974).

9 G. Steinvelt and H. Holtan, Jr., J. Electrochem. Soc., 107, 247 (1960).

10 I. Ivanov, Hydrometallurgy, 72, 73 (2004).

11 C. Bozhkov, M. Petrova and St. Rashkov, J. Appl. Electrochem., 22, 73 (1992).

12 C. L. Mantell, Electrochemival Engineering, p. 210, 4th Ed., McGraw-Hill, N. Y., (1960).

13 J. Wang, Analytical Electrochemistry, 2nd Ed., Willey, N. Y., (2000).

14 L. Meites, Polarographic Techniques, p. 614, 2nd Ed., Willey, N. Y, (1965).

15 E. A. Bobrowski and A. Bond, Electroanalysis, 16, 1536 (2004).

16 G. R. Mrzljak, A. Bond, T. Cardwell, R. W. Cattrall, R. W. Knight, O. M. G. Newman, B. R. Champion and J. Hey, Anal. Chim. Acta, 281, 281 (1993).

17 M. Korolczuk, A. Moroziewicz, M. Grabarczyk and K. Paluszek, Talanta, 65, 1003 (2005).

18 M-H. Zhang and Y-Z. Liang, J. Trace and Microprobe Techniques, 14, 1 (2002).

19 R. Mrzljak, A. Bond, T. Cardwell, R. Cattrall, R. Knight, M. Newman, B. Champoin, J. Hey and A. Bobrowski, Anal. Chim. Acta, 281, 281 (1993).

20 S. E. Lloyd and B. A. Gatehouse, Anal. Chem., 27, 901 (1955).

21 C. I. M. Kolthoff and E. Jacobsen, J. Am. Chem. Soc., 79, 3677 (1957).

22 A. M. Bobtelskya and E. Jungreis, Anal. Chim. Acta, 12, 248 (1955).

23 I. M. Kolthoff and A. Langer, J. Am. Chem. Soc., 62, 3172 (1940).

24 R. Zlatev, M. Stoytcheva, B. Valdez, L. Álvarez and J. M. Cobo, ECS Transactions, 20, 3 (2009).

25 Kh. Brainina, Frez. Z. Anal. Chem., 312, 428 (1982).

26 R. Jugade and A. Joshi, Ind. J. Chem., Section A, 42, 94 (2003).

27 Stoycheva M. (1994): Bioeletrocataytical Determination of some Havy Metals and their influence on tha Catalytic Activity of the Inmobilized Acethylcholinesterase. 0037-9646/94 Bull. Soc. Cim. Belg. Vol. 103/ 4/1994. p147-149

28 Ovalle M. (2009): Caracterización y Aplicación de Biosensores para el Monitoreo de Contaminantes Ambientales. Tesis doctoral, Inst. de Ing. de la UABC. Diciembre 2009

29 Atkinson, B. W., F. Bux y H. C. Kassan (1998): “Considerations for Application of Biosorption Technology to Remediate Metal-Contaminated Industrial Effluents. Water SA. 24:129-135.

30 Argüelles M.M. (2011): Desarrollo de Método Voltamétrico para Medición de As(III) en Aguas Naturales. Tesis maestría, Inst. de Ing. UABC, Junio 2011.

31 Galindo G y Otros: Arsénico en Aguas: Origen, Movilidad y Tratamiento II Seminario Hispano-LatinoAmericano sobre Hidrología Subterránea IV Congreso Hidrogeológico Argentino. Octubre 2005.

32 Hung D.Q., Nekrassova O., Compton R.G. (2004). Analytical Methods for Inorganic Arsenic in Water: A. Review. Talanta, 64, 269–277

33 Skoog, West, Holler, Crouch (2005): “Fundamentos de Química Analítica”. Ed: Thomson p. 700-720

34 Harvey D.(2002): “Química Analítica Moderna”. Ed: McGraw-Hill.

35 R. Zlatev, M. Stoytcheva, B. Salas, J.-P. Magnin and P. Ozil, Electrochem. Commun., 8, 1699 (2006).

36 González A.: Medidor de Voltametría Cíclica para Dispositivos de Transmitancia Controlable Univ. Carlos III de Madrid, Esc. Politécnica Superior.

37 Ortiz R. 2006: Técnicas Electroanalíticas Parte II, Voltamperometría. Depto. De Química Facultad de Ciencias . Univ. de los Andes. Mérida Venezuela.

38 Tacussel, P. Leclerc y J J Fombon. 1986: “Pulse Voltammetry and Polarogrphy Recent Progress in Microprocessor Instrumnetation. J. Electroanal Chem. 214 (1986) 79-84.

39 Stoycheva M./Tzvetkov S. M 2003 Application of differential double pulse polarography for arsenic determination in waste water from copper producing plant. Annual, vol. 46 part II Mining and Mineral Processing, Sofia Bulgaria].

40 K. B. Oldham, D. J. Gavaghan and A. M. Bond, J. Phys. Chem. B, 106, 152 (2002).

41 Barker G. C., 1958. Anal. Chim. Acta, 18, 118 (1958)

42 Barker G.C, Gardner A.W. and Williams M. J., Electroanal. Chem., 42, 21 (1973).

43 T. Kambara and Sh. Watarai, Bull. Chem. Soc. Jpn., 39, 521 (1966).

44 G. Wolff and W. H. Nurnberg, Frezenius Z. Anal. Chem., 224, 332 (1967)

45 V. V. Senkevich, L. P. Chernega, V. I. Bodyu and Yu. S. Lyalikov, Zavod. Lab., 34, 1176 (1968).

46 H. P. Agarwal and M. Saxena, Ind. J. Chem. A, 16, 754 (1978).

47 G. C. Barker, Proc. Anal. Div. Chem. Soc., 12, 179 (1975).

48 D. Saur, Frezenius Z. Anal.Chem., 298, 128 (1979).

49 C. Peker, M. Herlem, J. Badoz-Lambling, Z.1966: Anal. Chem., 224, 284.

50 K. S. G. Doss and H. P. Agarwal, J. Sci. Industr. Res. India B, 9, 280 (1950).

51 K. S. G. Doss and H. P. Agarwal, Proc. India Acad. Sci. A, 34, 263 (1951).

52 K. S. G. Doss and H. P. Agarwal, Proc. India Acad. Sci. A, 35, 45 (1952).

53 K. B. Oldham, Trans. Faraday Soc., 53, 80 (1957).

54 P. Delahay, M. Senda and C. Weis, J. Am. Chem. Soc., 83, 312 (1961).

55 P. Delahay, M. Senda and C. Weis, J. Phys. Chem., 64, 960 (1960).

56 Bard, A.J., Faulkner L.R., Controlled Potential Microelectrode Techniques – Potential Step Methods. In Electrochemical Methods, Fundamentals and Applications; John Willey & Sons, Inc.: New York, EE. UU. 1980.

57 Florence, T.M., Electrochemical Techniques for Trace Element Speciation in Waters. In Trace Element Speciation: Analytical Methods and Problems; G. E. Batley, Ed.; CRC Press, Florida, EE. UU: 1986.

58 R. A. Osteryoung, J. Osteryoung, Phil. Trans. Royal Society of London, Series A: Math., Phys. Eng. Sci. 302 (1981) 315.

59 J. Tacussel, P. Leclerc, J. J. Fombon, J. Electroanal. Chem. 214 (1986) 79.

60 B. B. Damaskin, Principles of the modern methods for investigation of the electrochemical reactions, MGU, Moscow, 1965, pp. 11 – 25.

61 Y. Song and G. M. Swain, Anal. Chem., 79, 2412 (2007).

62 D. Yamada, T. A. Ivandini, M. Komatsu, A. Fujishima and Y. Einada, J. Elecroanal. Chem., 615, 145 (2008).

63 D. Gandini, P.A. Michaud, I. Duo, E. Mahé, W. Hänni and A. Perret, New Diamond and Frontier Carbon Technology, Ed. MYU, Tokyo, JP, 9/5 303 (1999).

64 L. Kavan, B. O'Regan, A. Kay and M. Grätzel, J. Electroanal. Chem., 346, 291 (1993).

65 A. Manivannan, N. Spataru, K. Arihara and A. Fujishima, Electrochem. Solid-State Lett., 8, C138 (2005).

66 L. Vargas, B. Valdez, L. Veleva, R. Zlatev, M. Schorr and J. Terrazas, Anti-Cor. Methods and Materials, 56, 218 (2009).

67 I. Pjatnickyi, Analytical Chemistry of Cobalt, p. 54-55, Nauka Press, Moscow, (1965).

68 T. Uchida, M. Sugawara and T. Kambara, Fres. J. Anal. Chem., **315**, 487 (1983).

69 T.Uchida and M.Sugawara, Fres. J. Anal. Chem, **322**, 470 (1985).

70 Myers D., Osteryoung J., 1983. Anal. Chem., Vol. 45, 2, 267-271.

VII Anexos

Anexo A

J. A. Valera, R. K. Zlatev, M. S. Stoytcheva, and B. Valdez
Determination of Trace Concentrations of Co (II) in Electrolyte for Electrowinning of Zn by Differential Pulse Voltammetry
ECS Transactions, 29 (1) 409-419 (2010) 10.1149/1.3532337
© The Electrochemical Society.
USA Dec 2010

Anexo B

J. A. Valera, R. Zlatev, M. Stoytcheva, B. Valdez, M. Carrillo
Simultaneous Species Determination in Industrial Solutions by Differential Alternative Pulse Voltammetry (DAPV)
ECS Transactions, 28 (18) 99-108 (2010) 10.1149/1.3491282
© The Electrochemical Society.
USA Dec 2010

Anexo C

R. Zlatev, M. Stoytcheva, J-P Magnin, B. Valdez, M. Argüelles and J. A. Valera
Application of TiO_2 Modified Boron Doped Diamond (BDD) Electrode for As(III) Determination in Natural Waters,
ECS Transactions, 19 (32) 87-93 (2009)10.1149/1.3268165
© The Electrochemical Society.
USA Dec 2009

Anexo D

J. Adolfo Valera, R. Zlatev*, M. Stoytcheva, B. Valdez
Determination of Trace Concentrations of Cobalt (II) in Electrolyte for Electrowinning of Zn by Differential Pulse Voltammetry
XXV Congreso de la Sociedad Mexicana de Electroquímica.
3er Meeting of the Mexican Section ECS.
Zac. Mex. Mayo 3-Jun 4 2010

Anexo E

J. Adolfo Valera, R. Zlatev, M. Stoytcheva.
Aplicación de 1-Nitrozo-2-Naftol en Mediciones Voltamétricas de Cobalto en Electrolito para Electrowinning de Zinc.
I Congreso Nacional de Estudiantes de Posgrado del Instituto de Ingeniería UABC. Programa de Maestría y Doctorado en Ciencias e Ingeniería. Mexicali B.C. México Nov. 2009

Anexo F

R. Zlatev, M. Stoytcheva, J-P. Magnin, M. Argüelles, J. A. Valera, B. Valdez
Application of Boron Doped Diamond (BDD) Electrode for As(III) Determination in Natural Waters
XIV Simposio en Ciencia de Materiales.
Centro de Nanociencias y Nanotecnología, UNAM, Ensenada, B.C.
México, 10-13 Feb. 2009

Anexo G

J. Valera, R. Zlatev, M. Stoytcheva, B. Valdez and M. Carrillo
Simultaneous Species Determination in Industrial Solutions by Differential Alternative Pulse Voltammetry
217th ECS Meeting in Vancouver, BC
Canada, Apr 2010.

Anexo H

Roumen Zlatev*, Margarita Stoytcheva, Benjamin Valdez and Jose Adolfo Valera

1. **On-Line Differential Pulse Polarographic Determination Of Cobalt(II) At ppb Concentrations In Zn Plant Electrolyte**
2. **In-Situ As(III) Determination In The Presence Of Pb(II) By Differential Alternative Pulses Voltammetry**

The Modern Electroanalytical Methods Conference in Prague
Czech Republic, Dec. 2009

Anexo I

R. Zlatev, M. Stoytcheva, M. Jean_Pierre, B. Valdez, M. Argüelles and J. Valera
Application of TiO2 Modified Boron Doped Diamond (BDD) Electrode for As(III) Determination in Natural Waters
215th ECS Meeting in San Francisco, CA. USA, May 2009

Anexo J

R. Zlatev, M. Stoytcheva, B. Valdez, J. A. Valera, M. Argüelles Mier
Direct As(III) Determination in Prescense of Pb(II) by Differential Alternative Pulses Voltammetry
Analytical Letters Journal, Chemistry Analytical. Published by Taylor & Francys Inc. 325 Chestnut Street, Suite 800, Philadelphia, PA 19106,
USA, Nov 2008

Anexo K
R. Zlatev, M. Stoytcheva, B. Valdez, J. A. Valera, M. Ovalle
High Resolution Voltammetric Techniques: Application for Direct Simultaneous Species Determination.
214th ECS Meeting, Honolulu, Hawai,
USA, Oct 2008

Anexo L

R. Zlatev, M. Stoytcheva, B. Valdez, J. A. Valera, M. Ovalle
High Resolution Voltammetric Techniques: Application for Direct Simultaneous Species Determination.
ESEAC 2008 in Prague
Czech Republic, May 2008

Anexo M

Constancias de Asistencia en Congresos Nacionales e Internacionales

J. A. Valera,
Aplicación de voltametría Diferencial de Pulsos alternativos (DAPV) para Determinación Simultánea de las Especies: As^{+3}, Pb^{+2} y Tl^{+1}
Congreso Nacional de Estudiantes de Posgrado del Instituto de Ingeniería UABC. Programa de Maestría y Doctorado en Ciencias e Ingeniería. Mexicali B.C.
México Nov. 2010

V Conferencia AGUA RESIDUAL Problema Social y Negocio Coyuntural
Mexicali B.C. Octubre 2009

Ocurrencia de Arsénico, Química y Especiación. Metodologias Analíticas Para su Determinación. *Instituto de Ingeniería UABC.- Mexicali B.C. Junio 2009*

XVIII Congreso Internacional de Metalurgia Extractiva: "La Metalurgia, los Material y el Medio Ambiente" *UNISON.- Hermosillo Son. Abril 2009*

ANEXO A

ECS Transactions, 29 (1) 409-419 (2010)
10.1149/1.3532337 ©The Electrochemical Society

Determination of Trace Concentrations of Co(II) in Electrolyte for Electrowinning of Zn by Differential Pulse Voltammetry

J. A. Valera, R. K. Zlatev, M. S. Stoytcheva, and B. Valdez

Instituto de Ingeniería, Universidad Autónoma de Baja California, Mexicali 21280, México

A simple and rapid *on-line* Differential Pulse Polarographic (DPP) method for direct Co^{2+} determination in Zn plant electrolyte was developed and tested in real solutions. 1-nitroso-2-naphtol was applied as Co^{2+} to Co^{3+} oxidizing and chelate forming agent in ammonia buffer (NH_4OH/HCl in 8 to 1 ratio) supporting electrolyte. The great DPP difference between Co^{3+} and Zn^{2+} peak potentials allows the complete elimination of the Zn^{2+} interference ensuring reliable results in the linear concentration range from 10 ppb to 20 ppm. Disposable mercury surface electrodes were applied as working electrodes.

Introduction

The solution used for Zn electroextraction contains about 150 g L^{-1} Zn^{2+} and a great variety of impurities, such as Cd^{2+}, Cu^{2+}, Pb^{2+}, Sb^{3+}, Co^{2+}, Fe^{2+}, Ni^{2+}, Ge^{4+} most of them in ppb levels (1, 2). The production of a high purity metal and the achievement of a high current efficiency of the electrolysis require removal of these impurities to prevent their co-deposition together with Zn^{2+} which favors the H_2 evolution due to the diminishing of the hydrogen overpotential on the Co containing cathode areas (2-12).

The purification process control requires simple, rapid and reliable *on-line* methods for impurities determination. The most applied in the industry spectral methods (absorption and emission) such as AAS and ICP can be helpful only after a preliminary sample pretreatment procedure for analyte separation. The high Zn^{2+} concentration provokes high temperature $ZnSO_4$ crystallization blocking the spectrometer nebulizer (12), thus making impossible the direct impurities determination. The application of wet laboratory methods for sample pretreatment such as analyte extraction makes the determinations complicated, long and less precise, unsuitable for *on-line* application as well.

On the other hand, the high ionic concentration of the Zn plant electrolyte favors the application of the voltammetric methods requiring conductive supporting electrolyte (1, 13). Very detailed reviews of the voltammetric monitoring of the Zn plant electrolyte impurities were presented by Bond (2) and Pilkington (1). As shown by Bond, the high Zn^{2+} concentration does not interferes the Sb^{3+}, Cd^{2+}, Ni^{2+}, Ge^{4+} and Cu^{2+} determination. For the Co^{2+} determinations however Pilkington recommends the application of some spectral methods, because of the complete overlapping of Co^{2+} peak by the huge one of Zn^{2+}.

Many authors presented their contributions to the polarographic Co^{2+} determination in Zn plant electrolyte applying a great variety of sample pretreatment procedures, quantification techniques, supporting electrolytes and electrodes. The main approaches applied are matrix exchange and chelate formation combined with Adsorptive Stripping Voltammetry. Some of the reported methods are briefly mentioned bellow.

Meites (14) reported the application of 0.1 M ethylendiamine/0.1 M KNO_3 as a chelate forming/oxidizing agent resulting in Co^{3+} formation yielding a Differential Pulse Polarography (DPP) peak at a potential of -0.5 V vs. SCE allowing its complete separation from the peak of Zn^{2+}. The Zn^{2+} chelate formation requires high ethylendiamine concentration but the LOD of 15 mg L^{-1} is not satisfactory.

Matrix exchange procedure followed by Differential Pulse Adsorptive Stripping Voltammetry (DPAdSV) was reported for Co^{2+} determination in Zn plant electrolyte employing various organic compounds (15, 16). Korolczuk et al. (17) reported the application of nioxime-cetyltrimethylammonium bromide-piperazine-N, N-bis (2-ethanesulfonic acid) in adsorptive DPAdSV step. This technique was applied for very low Co^{2+} concentrations (from 10^{-11} to 10^{-8} M) determinations (18) in Zn plant electrolyte with satisfactory results.

Mrzljak et al. (19) reported two Adsorptive Stripping Voltammetry (ADSV) methods for Co^{2+} determination in Zn plant electrolyte with detection limits of 9 ppb and 0.25 ppb based on matrix exchange procedures including filtration, acidifying with H_2SO_4, cooling, dispensing, etc. Another method for Co^{2+} determination based on the application of a carbon paste electrode modified by Dimethylglyoxime (DMG) in acetate buffer with pH 4.8 in the presence of 100-fold excess of Zn was reported by Lloyd (20).

Pilkington (1) reported the application of Differential Pulse Polarography (DPP) and Differential Pulse Anodic Stripping Voltammetry (DPASV) for Sb^{3+}, Cd^{2+}, Cu^{2+} determination in Zn plant electrolyte, but excluding the possibility for determination of Co^{2+} at all, recommending the spectral methods application.

As seen, the mentioned methods applied for Co^{2+} determination in Zn plant electrolyte are complicated and hardly applicable for direct *on-line* analysis. The main problem comes from the small $E_{½}$ difference of Co^{2+} and Zn^{2+} combined with the huge Zn^{2+} concentration causing complete overlapping of their peaks in any supporting electrolyte. It is hardly to find some sample pretreatment procedures allowing the analyte separation from the high concentration matrix able to be performed *on-line*. For example, the Zn^{2+} precipitation in alkaline media forms an amorphous $Zn(OH)_2$ having a huge surface, adsorbing the ions present in trace concentration and disturbing thus the reliability of their determination. The extraction and matrix exchange need laboratory operations made by qualified personal which precision determine the analytical results reliability. All these defined the need of searching another and simpler approach for *on-line* Co^{2+} determination in Zn plant electrolyte.

The aim of the present work is the development of a direct, simple, rapid and reliable *on-line* polarographic method and electrode for Co^{2+} determination in Zn plant electrolyte, avoiding the Zn^{2+} interference for the entire range of Zn^{2+}/Co^{2+} concentration ratio in the Zn plant electrolyte.

For this purpose a proper alkaline supporting electrolyte allowing the solution deoxygenating by Na_2SO_3 avoiding thus its purging by inert gas was chosen: NH_4OH + HCl in 8 to 1 ratio. The purpose of the NH_4OH excess is to form a soluble chelate with the Zn^{2+} preventing thus its precipitation. The next step was finding a way to shift the cobalt peak potential to more positive direction allowing it distinction from the huge Zn^{2+} peak. As it was found by Colthoff et al. and A. M. Bobtelskya et al. (21-23), the 1-nitroso-2 naphtol forms a chelate where the cobalt is trivalent allowing to register the peak of Co^{3+} at much more positive potential than Zn^{2+} (at about –500 mV). The other nitroso-naphtols (1-nitroso-2-naphtol; 2-nitroso-1-naphtol and nitroso-R-salt) also oxidize Co^{2+} to Co^{3+} making them suitable to avoid the Zn^{2+} interferences and they were tested too. The third step was choosing a simple mercury surface electrode avoiding the use of capillary which maintenance in industrial conditions is problematic. A special type of disposable mercury surface electrode was developed based on a support made by PCB technology application (24), allowing to be employed without any maintenance and easily recyclable after its use.

Various authors reported polarographic determination of Co^{2+} in the presence of 1-nitroso-2-naphtol.

Braynina (25) reported an anodic stripping voltammetric method based on electrochemical deposition of 1-nitrozo-2-naphtol Co^{3+} chelate in 0.4 M NH_4OH/0.05 M NH_4Cl on carbon electrode and its further anodic dissolution, registering the anodic peak. Co^{2+} after its oxidation to Co^{3+} forms a low soluble chelate which precipitates on the carbon electrode surface during the preconcentration step. The electrochemical reduction occurs at potential values -0.6 - -0.7 V. The small linear concentration range, the small Zn^{2+}/Co^{2+} concentration ratio (about 1000) and the complicated sample pretreatment do not allow this method to be applied for impurities determination in Zn plant electrolyte where the Zn^{2+} to Co^{2+} concentration ratio is as high as 10^6 to 1 or more (150 g L^{-1} to 50-200 μg L^{-1}).

Jugade et al. (26) reported a rapid Adsorptive Stripping Voltammetric method for Co^{2+} and Ni^{2+} determination in 0.01 M NH_4Cl solution (pH 9.5) containing 1 μM 1-nitroso-2-naphtol applied for water, food and alloy samples. A concentration ratio for various metals among which Zn^{2+} from 1 to 100 did not interfere the cobalt peak height.

Uchida et al. (27, 28) reported polarographic studies of the cobalt(III)-1-nitroso-2-naphthol chelate formation in citrate buffer (pH 5) and aqueous tartarate solutions. The cobalt(III) chelate is determined in a electrolysis solution composed of a 1/1 mixture of the extract and acetonitrile solution containing 8 mM perchloric acid and 0.2 M sodium perchlorate with a limit of determination in the range of 1-2 ppb.

Lloyd et al. (20) reported the determination of trace of cobalt and other metals in rocks using rubeanic acid and 1-nitroso-2-naphthol after sample pretreatment including precipitation and centrifugation.

Unfortunately none of the mentioned methods is applicable in Zn plant electrolyte because the interference of the huge excess of Zn^{2+}.

Geisler et al. reported a DPP method for Co^{2+} determination providing linear response from 10^{-7} to $5x10^{-6}$ M in the presence of 50,000 excess of Zn^{2+} (29).

Despite of the excellent characteristics of the mercury as electrode material, its application as mercury drop electrodes such as DME, SMDE and HMDE was restricted recently because of the mercury toxicity and its high cost. On the other hand, the maintenance of the capillary in industrial condition is complicated, requiring qualified personal. Since the electrochemical reactions occur at the electrode surface only, the deposition of a mercury film onto a conducting support material yields "mercury" electrode as well. Since the mercury forms a small droplets on the surface of Pt and the carbon materials including glassy carbon, not covering the entire surface to form a "mercury" electrode, these two materials were excluded as suitable for supports. A continuous mercury film can be achieved on amalgam forming metals only such as Ag and Au. Even ppb level of H_2S (air impurity present in the industrial areas) however forms sulfide layer on the Ag surface (30) preventing amalgam formation, that is why Ag was not tested as support material as well. Thus, Au was chosen as support material and a thick Hg film was deposited on the Au support *in-situ* just prior the determination by electrolysis in the polarographic cell. To avoid contamination of the mercury surface by the Au amalgam and the Au-Hg intermetalic compounds formed, the mercury film was produced to be thick and deposited some seconds only just before its application.

Experimental

Instrumentation

The laboratory polarographic determinations were performed by a modified Model 264A Polarographic Analyzer, coupled with Model 303A SMDE/HMDE electrode stand (EG&G PAR, USA) completely controlled by PC, running an especially created software. A PC controlled conductivity measuring module was incorporated to the Polarographic Analyzer applied for surface reproducibility correction coefficient determination. Some of the curves were recorded on paper using an X-Y recorder and scanned and digitalized after. The original reference and auxiliary electrodes mounted on the Model 303A electrode stands were employed.

Z 58 Potentiostat controlled by Z54 potentiostat software (ZENIT Lab) coupled with a Z59 electrode stand (ZENIT Lab) were employed for the *on-line* determinations. Cost effective disposable electrodes were used as working electrodes. A flow type polarographic cell with a special holder for the disposable electrodes application was used for the *on-line* industrial determination. The reference electrode was Ag/AgCl/3M KCl electrode and the counter electrode a 1mm in diameter Pt wire.

A ML-501A Hamilton Single Syringe Diluter/Dispenser was employed for the *on-line* analysis sample preparation.

Working Electrode

The disposable working electrodes supports introduced by the authors earlier (24) were produced by the application of PCB technology and covered *in-situ* by a thick

mercury film few seconds just before the application. This approach allows taking advantage from the mercury electrode surface without any risk of mercury spiel. The electrode support consisted of 5x30 mm glass fibers reinforced epoxy stick (0.5 mm thick) covered by 17 μm of Cu, a cost effective material massively used for PCB production. The working part of the electrode had the shape of a disk, 0.5 mm in diameter covered by about 0.5 μm Ni and finally by 1 μm Au. It can be stored during an unlimited time and after its application is easily recycled. A plastic band carrying about 1000 electrodes was charged in a computer controlled roll changer for electrode exchange.

Reagents

All the reagents were of analytical grade (Merck and Sigma) and the deionized water was produced by MilliQ system of Milipore. The stock solution of ammonia buffer supporting electrolyte was preliminary prepared by mixing of 8 volume parts of NH_4OH with 1 volume part of concentrated HCl, continuously cooling by running water. The NH_4OH excess allowed the formation of the soluble Zn^{2+} ammonia chelate avoiding precipitation formation. The 1-nitrozo-2-naphtol solution was preliminary prepared by dissolution of 50 mg of 1-nitrozo-2-naphtol in 50 mL of ethyl alcohol + 1 mL HCl.

Measuring Procedure

The laboratory polarographic experiments were performed in the original PAR 303A polarographic cell employing the DME mode of the mercury electrode. The Zn plant electrolyte and the supporting electrolyte containing 600 ppb solution of 1-nitroso-2-naphtol (2-nitroso-1-naphtol or nitroso-R salt for some of the experiments) were added directly into the polarographic cell in ratio 5 mL to 5 mL with the aide of the ML-501A Hamilton Single Syringe Diluter/Dispenser. The DPP polarograms was registered from -200 mV initial potential to -800 mV with a scan rate of 10 mV s^{-1} (5 mV step every 0.5 s); the pulse amplitude was -50 mV.

The *on-line* determinations of real industrial solutions were carried out in a special 10 mL flow polarographic cell. Before the determination, a thick mercury film was deposited on the electrode support by electrolysis performed in the same polarographic cell. $HgCl_2$ solution in 0.1 M HCl was added by a peristaltic pump and the electrolysis was carried out for 30 s by the Model 264A Polarographic Analyzer controlled by PC via a special interface. After rinsing the cell by a peristaltic pump, the 5 mL of the Zn plant electrolyte sample was introduced followed by 5 mL of the supporting electrolyte containing the organic reagent and the next disposable electrode was inserted. The polarograms were registered by the same way as in the laboratory conditions mentioned above and processed after by PC to calculate the Co^{2+} concentration.

Results and Discussion

Working Electrode Surface Reproducibility Determination

As mentioned above, the working electrode area was an Au disk (0.5 mm diameter) located on the lower part of a 5x30 mm plastic stick. The reproducibility of the Au disc electrode surface determined before to be covered by mercury was within 4.3 %,

determined as Relative Standard Deviation (R.S.D.) of the electroconductivity, as described by the author earlier (24).

The conductivity of the Hg^{2+} containing solution used for the mercury deposition was measured using the conductivity module incorporated in the Model 264A Polarographic Analyzer. This measurement was performed immediately after the Hg thick film deposition on the Au support by electrolysis. Since the concentration of the Hg^{2+} containing solution was kept constant, the measured conductivity was proportional to the electrode surface only at a constant temperature. The correction coefficient was calculated vs. the electrode employed for the calibration curve building as described by the author earlier (24). The reproducibility of 10^{-6} M Co^{2+} determination according to the procedure described above was determined to be within ±3.6 % determined as R.S.D., while the reproducibility determined by the DME application was found to be 1.4% R.S.D. for the same concentration. Disposable mercury surface electrodes were applied as well, the correction procedure being described in (24).

Cobalt-1-Nitrozo-2-Naphtol Chelate Formation and its Application for DPP Determination

The 1-nitrozo-2-naphtol is one of the first organic reagents applied in analytical chemistry, used for a long time for gravimetric Co^{2+} determination (21-23) because of its great specificity toward Co^{2+}, oxidizing it to Co^{3+} and forming a low soluble chelate (31).

1-nitrozo-2-naphtol, providing a good solubility in many organic solvents as acetone, ethyl alcohol, benzene, etc. is soluble in aqueous solution as well, such as acetic acid, NaOH, tartarate, etc. (27, 28, 31). The solubility of Co^{3+}(1-nitrozo-2-naphtolate) in water is about 1.5 mg L^{-1} as reported by Piatnikyi (31). A red-brown coloration of the solution appears only in the presence of ppb levels of Co^{2+}, because no chelate precipitation probably occurs. This allows the direct polarographic determinations of low Co^{2+} concentrations to be carried out applying DME without chelate preconcentration on the electrode surface.

The addition of 1-nitrozo-2-naphtol to Co^{2+} containing solution results in the appearance and the increase of a well defined DPP peak at -550 mV corresponding to the electrochemical reduction of Co^{3+} resulting from the Co^{2+} oxidation by the added organic reagent, while at the same time the height of the Co^{2+} peak situated at -1335 mV decreases respectively. This fact shows that Co^{2+} is oxidized by the organic reagent only partially and the concentration of the formed Co^{3+} and hence the sensitivity of the determinations depends on the 1-nitrozo-2-naphtol concentration (Fig. 1).

As proved by Kolthoff and other authors (21-23, 31), the composition of the formed chelate can be expressed as $Co(R)_3$, determining the optimal concentration ratio: 1-nitrozo-2-naphtol/cobalt to be 3 to 1. It can be expected that the Co^{3+} peak height will increase up to this ratio to be reached and that is why a concentration of 600 ppb was chosen as optimal one for the 1-nitrozo-2-naphtol addition, 3 times higher than the upper limit of the cobalt concentration range in the Zn plant electrolyte (from 20 to 200 ppb).

The chosen 1-nitrozo-2-naphtol concentration was tested by building of a calibration curve in coordinates: Co^{3+} peak height vs. Co^{2+} concentration which was found to be

linear at the presence of 600 ppb 1-nitrozo-2-naphtol in the Co^{2+} concentration range from 20 ppb to 500 ppb with a slope: 0.084 nA/ppb. The correlation coefficient for the higher Co^{2+} concentrations (>200 ppb) was found to be $r^2 = 0.946$, while for the lower concentrations, from 20 to 200 ppb which is the typical concentration range of the Co^{2+} impurities in Zn plant electrolyte, the correlation coefficient of the calibration curve is 0.987.

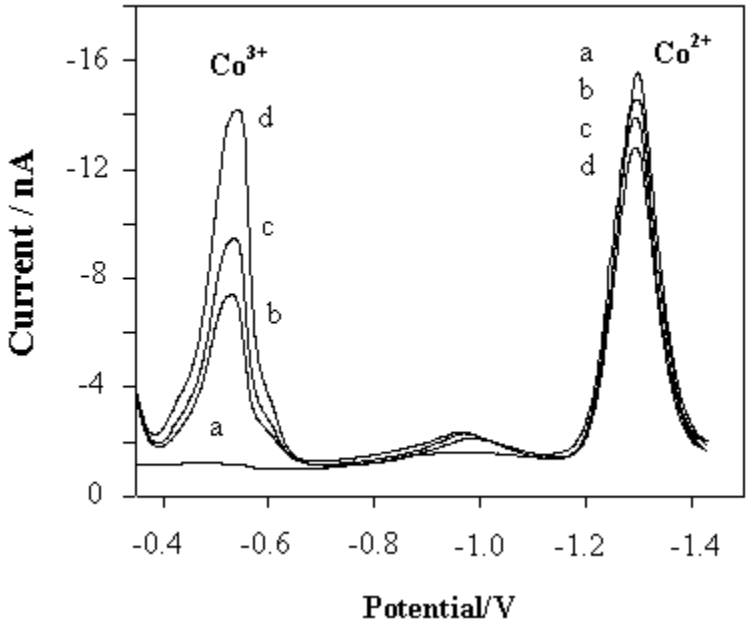

Figure 1. DPP polarograms of Co^{2+} after additions of 1-nitroso-2-naphtol. Curve a: 100 ppb Co^{2+} only in ammonia buffer; Curves b, c and d: in presence of 400, 500 and 800 ppb 1-nitroso-2-naphtol respectively.

It was found experimentally that the Co^{3+} peak height passed through a maximum with the increase of the 1-nitrozo-2-naphtol concentration and probably the decreasing part of the curve after the maximum is due to the reaching of the solubility product value of the Co-1-nitrozo-2-naphtolate resulting in chelate precipitation and lowering thus the measurable Co^{3+} concentration.

The 1-nitrozo-2-naphtol is an electrochemically active substance, yielding a DPP peak at -250 mV vs. Ag/AgCl/3M KCl in the mentioned above ammonia supporting electrolyte, which allows investigating the Co^{2+} oxidation and chelate formation. This fact permits to demonstrate the 1-nitrozo-2-naphtol consumption by increased Co^{2+} concentration, as presented in Fig. 2, where the initial 1-nitrozo-2-naphtol peak diminished with the successive additions of Co^{2+}.

The Co^{3+} peak of analytical importance is those appearing at -550 mV (Ag/AgCl/3M KCl). The peak potential difference with the Zn^{2+} peak situated at -1300 mV is 750 mV, which is sufficient to avoid any Zn^{2+} interference, as illustrated in Fig. 3. The Zn^{2+} peak in Fig. 3 corresponds to a low concentration in order to mark the peak potential only.

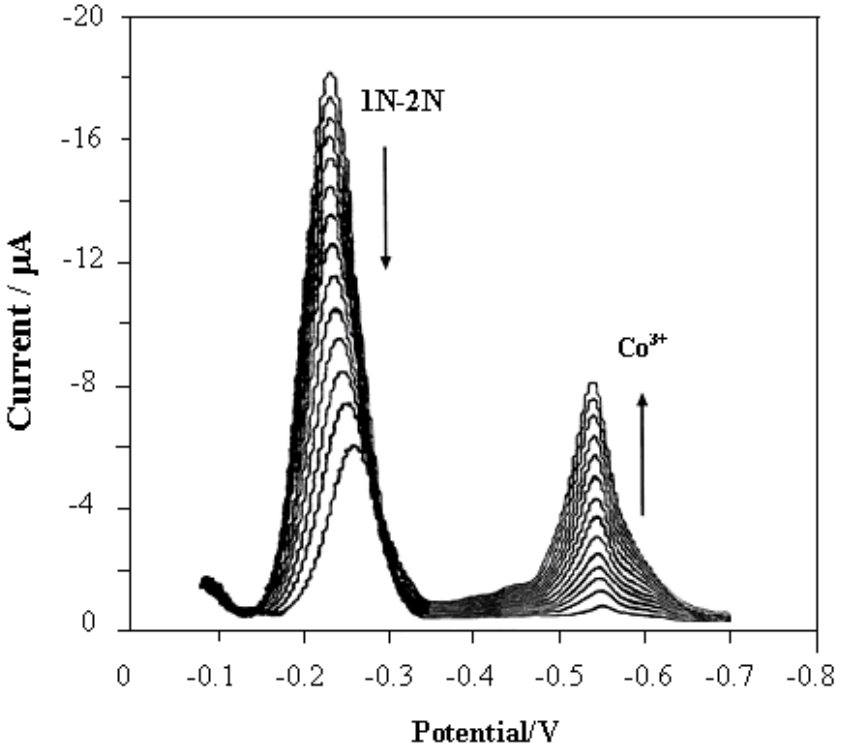

Figure 2. Decrease of the 1-nitrozo-2-naphtol (600 ppb initial concentration) DPP peak situated at -250 mV caused by successive additions of Co^{2+} in the range from 0 to 800 ppb.

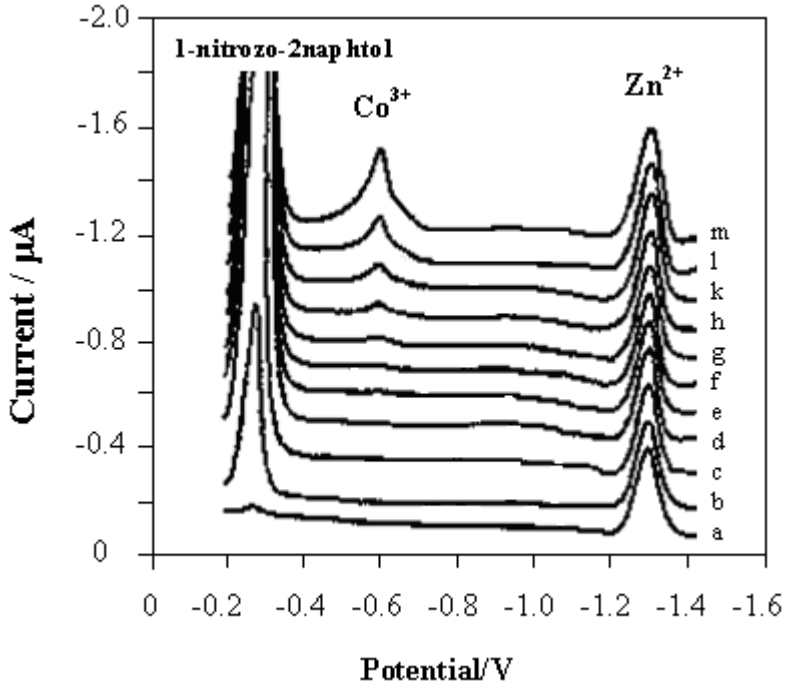

Figure 3. DPP peaks of: Co^{3+} (*E*p = -550 mV) resulted from Co^{2+} (*E*p = -1335 mV) oxidation by 1-nitrozo-2-naphtol and DPP peaks of Zn^{2+} (*E*p = -1350 mV). Curve a: Zn^{2+} only; curves b, c and d: after addition of 1-nitrozo-2-naphtol; curves from e to m: after successive additions of Co^{2+} .

The influence of Zn^{2+} concentration was evaluated by Co^{2+} increased concentration (in the range from 20 to 200 ppb) determination in a model solution containing 150 g L^{-1} Zn^{2+}. The results are shown in Table I.

Table I. Precision of Co^{2+} determination in the presence of 150 g L^{-1} Zn^{2+} by Differential Alternative Pulses Voltammetry (DAPV) application (model solutions).

Standard concentrations, ppb	Determined concentrations, ppb	Determined concentrations, ppb	Relative error, ppb	Relative error %
20	21.8	21.8	-1.8	-9.0
50	53.2	53.2	-3.2	-6.4
100	9.71	9.71	2.9	-2.9
150	148.2	148.2	-1,8	1.2
200	197.6	197.6	2.4	1.4

In spite of the higher sensitivity of the spectrophotometric determination of Co^{2+} with 2-nitrozo-1-naphtol application compared with 1-nitrozo-2-naphtol, its polarographic performance was found to be inferior. The DPP peak height of Co^{3+} in the ammonia supporting electrolyte applied in the present work is much lower and appears at much more negative potential, still far from the Zn^{2+} peak potential, as shown in Fig. 4.

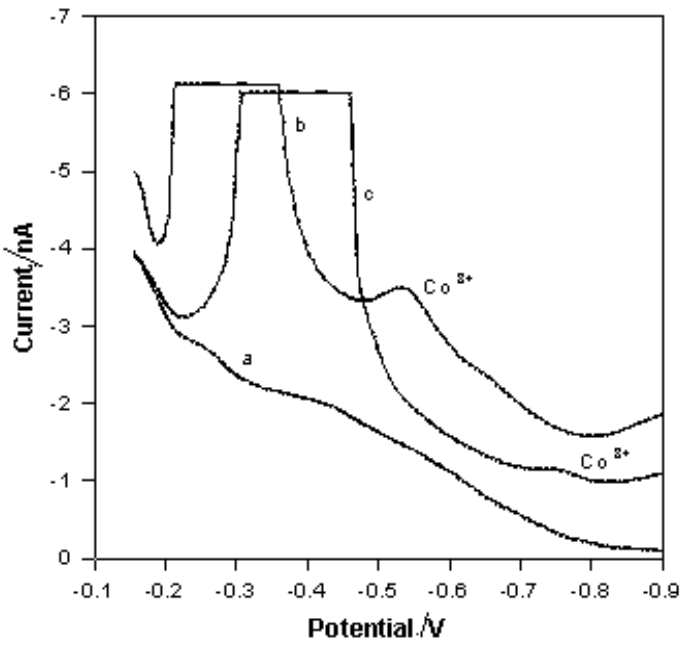

Figure 4. DPP peaks of: 1-Nitrozo-2-naphtol and Co $^{3+}$ (curve b); 2-nitrozo-1-naphtol and Co^{3+} (curve c); blank (curve a)

The third organic reagent of the nitroso-naphtol group applied in the analytical chemistry, the nitroso-R salt yielded broad Co^{3+} peaks at inferior sensitivity of the determinations compared with the 1-nitrozo-2-naphtol application.

Application for Real Samples Determinations

Typical curves of Co^{2+} containing Zn plant electrolyte registered according to the procedure described in the experimental part are shown in Fig. 5.

The peak of 600 ppb 1-nitrozo-2-naphtol appearing at -250 mV does not interfere the Co^{3+} peak, overlapping however the Ni^{2+} peak appearing at -430 mV in the employed supporting electrolyte. Since the Co^{2+} and Ni^{2+} concentrations are of the same order, the Ni^{2+} peak does not interfere with the cobalt determinations.

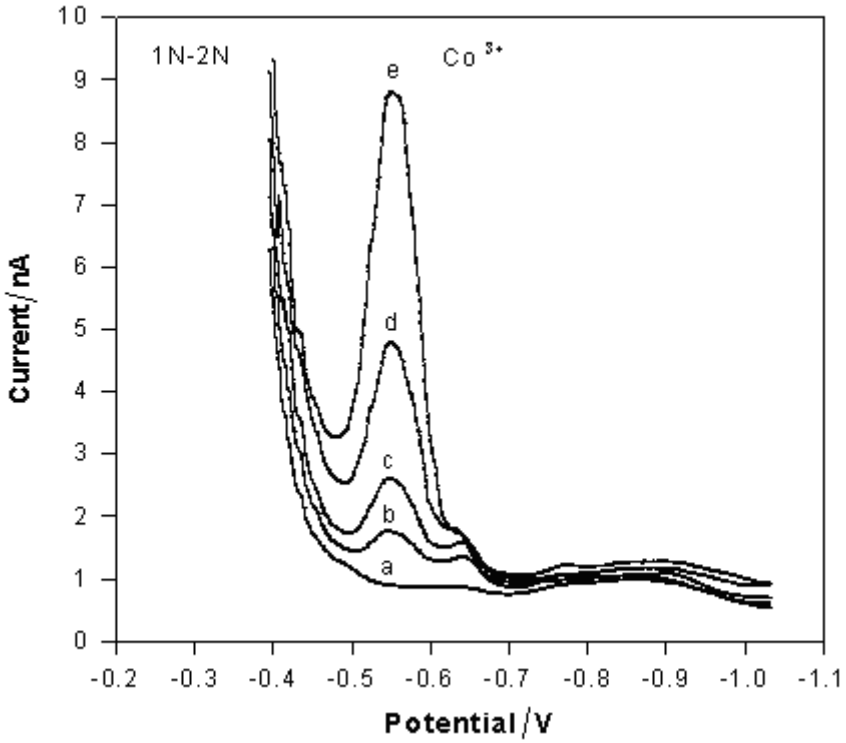

Figure 5. Co^{3+} peaks corresponding to Co^{2+} concentrations of: 20 ppb (curve b); 40 ppb (curve c); 80 ppb (curve d) and 160 ppb (curve e) in Zn plant electrolyte; blank (curve a)

The experimental results showed that the Zn^{2+} concentration does not interfere at all the Co^{2+} determination by the method subject of the present work in the entire range of the Co^{2+} concentrations present in the industrial solution.

Conclusion

1-nitroso-2-naphtol was applied as Co^{2+} to Co^{3+} oxidizing and chelate forming agent in ammonia (NH_4OH/HCl in 8 to 1 ratio) supporting electrolyte. The great DPP difference between Co^{3+} and Zn^{2+} peak potentials allows Co^{2+} concentration determination eliminating completely the Zn^{2+} interference, allowing thus obtaining reliable results in the entire concentration range of Co^{2+} (from 20 ppb to 200 ppb) in the Zn plant electrolyte. Disposable mercury surface electrodes were applied as working electrodes in the simple and rapid *on-line* Differential Pulse Polarographic (DPP) method subject of the present work developed and applied for direct Co^{2+} determination in Zn plant electrolyte.

Acknowledgments

José Adolfo Valera expresses his thanks to CONACyT, Mexico for the grant received to complete his Ph. D. thesis work (Programa de Maestría y Doctorado en Ciencias e Ingeniería, Instituto de Ingeniería, UABC).

References

1. E. Pilkington, C. Weeks and A. Bond, *Anal. Chem*., **48**, 1665 (1976).
2. D. A. Bond, *Anal. Chim. Acta,* **400**, 333 (1999).
3. G. T. Wever, *J. Metals*, **11**, 130 (1959).
4. G. C. Bratt, *Electrochem. Technol*., **2**, 323 (1964).
5. V. L. Klimenko, *Sov. J. Non-Ferrous Metals*, **12**, 18 (1971).
6. A. R. Ault, J. H. Bain, D. J. Palmer and J. B. Pullen, in *South Australia Conference*, p. 225, Australian Institute of Mining and Metallurgy, Melbourne, (1975).
7. U. F. Turoshima and V. V. Stender, *J. Appl. Chem. USSR*, **28**, 151 (1955).
8. H. H. Fukabayashi, T. J. O'Keefe and W. C. Clinton, *U. S. Bur. Mines Rep. RI 7966*, Rolla, Mo., **(**1974).
9. G. Steinvelt and H. Holtan, Jr., *J. Electrochem. Soc*., **107**, 247 (1960).
10. I. Ivanov, *Hydrometallurgy*, **72**, 73 (2004).
11. C. Bozhkov, M. Petrova and St. Rashkov, *J. Appl. Electrochem.,* **22**, 73 (1992).
12. C. L. Mantell, *Electrochemival Engineering*, p. 210, 4th Ed., McGraw-Hill, N. Y., (1960).
13. J. Wang, *Analytical Electrochemistry*, 2nd Ed., Willey, N. Y., (2000).
14. L. Meites*, Polarographic Techniques*, p. 614, 2nd Ed., Willey, N. Y, (1965).
15. E. A. Bobrowski and A. Bond, *Electroanalysis*, **16**, 1536 (2004).
16. G. R. Mrzljak, A. Bond, T. Cardwell, R. W. Cattrall, R. W. Knight, O. M. G. Newman, B. R. Champion and J. Hey, *Anal. Chim. Acta*, **281**, 281 (1993).
17. M. Korolczuk, A. Moroziewicz, M. Grabarczyk and K. Paluszek, *Talanta*, **65**, 1003 (2005).
18. M-H. Zhang and Y-Z. Liang, *J. Trace and Microprobe Techniques*, **14**, 1 (2002).
19. R. Mrzljak, A. Bond, T. Cardwell, R. Cattrall, R. Knight, M. Newman, B. Champoin, J. Hey and A. Bobrowski, *Anal. Chim. Acta*, **281**, 281 (1993).
20. S. E. Lloyd and B. A. Gatehouse, *Anal. Chem*., **27**, 901 (1955).
21. C. I. M. Kolthoff and E. Jacobsen, *J. Am. Chem. Soc.*, **79**, 3677 (1957).
22. A. M. Bobtelskya and E. Jungreis, *Anal. Chim. Acta,* **12**, 248 (1955).
23. I. M. Kolthoff and A. Langer, *J. Am. Chem. Soc.,* **62**, 3172 (1940).
24. R. Zlatev, M. Stoytcheva, B. Valdez, L. Álvarez and J. M. Cobo, *ECS Transactions*, **20**, 3 (2009).
25. Kh. Brainina, *Frez. Z. Anal. Chem*., **312**, 428 (1982).
26. R. Jugade and A. Joshi, *Ind. J. Chem., Section A*, **42**, 94 (2003).
27. T. Uchida, M. Sugawara and T. Kambara, *Fres. J. Anal. Chem*., **315**, 487 (1983).
28. T.Uchida and M.Sugawara, *Fres. J. Anal. Chem*, **322**, 470 (1985).
29. M. Geisler and R. Da Maia, *Fresenius Z. Anal. Chem*, **330**, 624 (1988).
30. L. Vargas, B. Valdez, L. Veleva, R. Zlatev, M. Schorr and J. Terrazas, *Anti-Cor. Methods and Materials*, **56**, 218 (2009).
31. I. Pjatnickyi, *Analytical Chemistry of Cobalt*, p. 54-55, Nauka Press, Moscow, **(**1965).

ANEXO B

ECS Transactions, 28 (18) 99-108 (2010)
10.1149/1.3491282 ©The Electrochemical Society

Simultaneous Species Determination in Industrial Solutions by Differential Alternative Pulse Voltammetry (DAPV)

J. A. Valera, R. Zlatev, M. Stoytcheva, B. Valdez, M. Carrillo

Engineering Institute of UABC, Blvd. Benito Juárez s/n, 21280 Mexicali, B.C., México

The Differential Alternative Pulses Voltammetry (DAPV) combining the high sensitivity of the Differential Pulse Voltammetry with the increased resolution of the second order voltammetric techniques was applied for *on-site* simultaneous determination of species as As(III), Pb(II) and Tl(I) in industrial solution without preliminary species separation. The limits of the species concentration ratios allowing simultaneous determination with preset precision of less than 10% were determined. The method was applied for determination in real industrial solutions.

Introduction

Peak overlapping makes complicated the simultaneous voltammetric determination of species at high concentration ratios and small $E_{1/2}$ difference as well. The determination of couples of ions such as: Pb(II) and Tl(I), In(III) and Cd(II), Co(II) and Ni(II), As(III) and Pb(II), etc. is problematic in all supporting electrolytes applying any of the known voltammetric techniques without some preliminary sample pretreatment for species separation.

The first order voltammetric techniques such as: Differential Pulse Voltammetry (1-5), Square Wave Voltammetry (6-13), AC voltammetry etc. are based on the nonlinearity of the I-E characteristic of the electrochemical systems. The height of peaks registered as a current response caused by a small amplitude rectangular pulse superimposition on the electrode potential is proportional to the species concentration participating in the electrochemical reactions. The peak half-width depending mainly on the reversibility of the electrochemical reaction determines the resolution power: sharper the peak higher the resolution.

The second order voltammetric techniques (14-22) such as: Radio Frequency Polarography (RFP), Differential Faradaic Rectification Polarography (DFRP) and Second Harmonic AC Polarography (SHACP) are based on the faradaic rectification effect (23-28). The shape of the registered curves: first derivative of peak, containing cathodic and anodic part allows species distinction using the peaks situated at the both sides of the zero line remained on the voltammogram after the overlapping for concentration evaluation. Unfortunately, these techniques are not widely applied; some of them required complicated equipment while others provide low sensitivity.

The Differential Alternative Pulses Voltammetry (DAPV) developed by the authors earlier (29) is a simple second order voltammetric technique providing the same sensitivity as DPV does combined with the higher resolution power of the second order ones. Two rectangular pulses with opposite polarity are superimposed on the stepping

electrode potential. Due to the nonlinearity of the I-E characteristic, the average of the faradaic currents caused by every couple opposite polarity pulses (superimposed on the same potential) deviates from the background current.

This current deviation registered against the stepped d.c. potential yields the DAPV curve shaped as the second derivative of the polarographic wave. The heights of the peaks situated on the both sides of the zero line are proportional to the analyte concentration (29). In case of overlapping one of the species can be determined using the cathodic peak, while the anodic one can be used for the other specie determination. On the other hand, the half-width of the DAPV peaks defining the resolution power of every analytical method (sharper the peaks, higher the resolution) is about 70% of that obtained by DPP, the most applied conventional voltammetric method (29). These two factors: the curve shape and the small half-width of the peaks combined with the high sensitivity of DAPV allow species determination in trace concentration and their distinction even at small $E_{1/2}$ difference or at high concentration ratio.

The aims of this work are: evaluation of the maximal concentration ratios of As(III), Pb(II) and Tl(I) allowing their simultaneous determination by DAPV application with preset relative error of less than 10% as well as *on-site* DAPV application for direct determination of any of these species in industrial solutions without preliminary species separation with the employment of a disposable Safe Mercury Multiple Drop Electrode (SMMDE) for the purpose of internal control of the plant purification process.

Experimental

Reagents

All the reagents including the standard solutions of Pb(II) and As(III) (1000 mg/L) were of analytical grade purity. The low concentrations used for calibration curves building or standard additions were prepared directly in the electrochemical cell using small volume (μL) BIOHIT automatic pipettes.

The experimental solutions were prepared using deionized water produced by Milli Q reverse osmoses installation (Millipore, USA). The supporting electrolyte for all the determinations was 1M HCl. Nitrogen gas was used for solution deoxygenating.

Electrochemical Cell, Electrodes and Instrumentation

POL 150 Trace Lab Polarographic Analyzer (Radiometer Copenhagen) controlled by TM5 software connected to EG&G PAR model 303A SMDE/HMDE electrode stand via a home made interface were employed for the laboratory DPP determination. A 10 mL glass electrochemical cell, Ag/AgCl/3M KCl reference electrode and Pt wire counter electrode, all of them parts of the Model 303A electrode stand were used in all the laboratory experiments.

A portable potentiostat Z 58 controlled by Z 54 potentiostat software (ZENIT Lab) was employed for the *on-site* DAPV determination performed by the application of Z 59 electrode stand (ZENIT Lab) employing an improved version of the disposable Safe

Mercury Multiple Drop Electrode (SMMDE) developed and described by the author earlier (30). A 30 mm long ultramicrobore PTFE tube with 0.1 mm I.D. and 0.4 mm O.D. (Cole Parmer, USA) is used as a mercury reservoir and capillary as well in SMMDE. The lower part played the role of capillary, while the upper part (20 mm long) contained about 5 μL mercury which is enough for 6 drops. A stainless steel tube 0.1 mm I.D.x0.3 mm O.D. stainless steel capillary (GL Science, Tokyo, Japan) inserted between the two parts serves as electrical contact with the mercury column. During the SMMDE storage before its usage, the mercury placed in the upper part of the PTFE tube did not have contact with the metal. To ensure a mechanical stability of the capillary end, the ultramicrobore PTFE tube was placed in 3 mm O.D. polyethylene body which upper part is half open and accessible for a roll which is a part of the electrode stand. The SMMDE construction and the drop formation based on the peristaltic pump functioning are shown in Fig. 1.

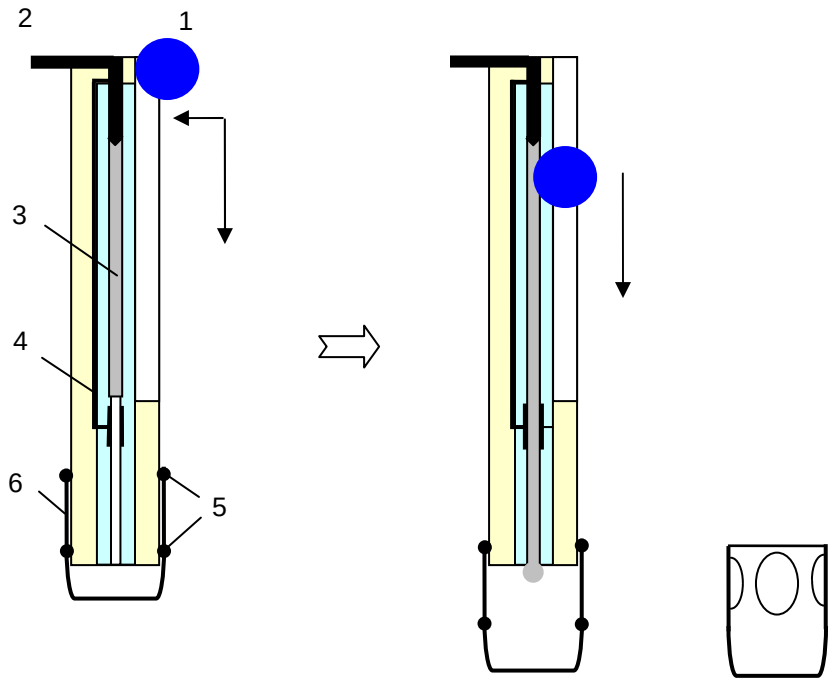

Figure 1. Principal construction of the improved SMMDE and mercury drop formation.

In "storage" mode of the SMMDE of the PVC cap [6] is closed and the O-rings [5] which are part of the cap prevents any mercury spiel. Another preventing factor is placing the mercury in the upper part of the flexible tube. In "working" mode of the SMMDE, the small plastic roll [1] which is a part of the electrode stand, presses and slides on the tube pushing the mercury out, forming thus the mercury drop, as shown in Fig. 1. In this mode the cap [6] is open and the solution enters in contact with the mercury drop through the holes in the upper part of the cap. After the determination, the cap [6] is moved up by pressing to close. Thus the dislodged mercury drops are kept in the small volume in the pseudo-conical part of the cap [6]. The exceeded solution is ejected through the caps holes during the movement.

The size of the formed mercury drop was controlled by the roll [1] displacement. Two methods: "fixed" and "controlled growth" were applied for the mercury drop formation. In the first the roll [1] passed always the same distance, pumping out the mercury and forming the drop. The influence of the flexible tube irregularities can not be avoided, so that the reproducibility of the mercury surface was less precise compared with the second approach based on the conductivity measurement. For this purpose an AC voltage with 10 mV p. p. amplitude was applied during the drop formation. The roll [1] movement was stopped in the moment when the AC current flowing through the supporting electrolyte reached the value obtained by the drop used for the calibration curve building. This procedure was described by the author earlier (31).

Model Stasar III Gilford Spectrophotometer and Model Analyst 200 Perkin Elmer were employed in referent laboratory for comparison of the results obtained with the application of the DAPV.

Analytical Procedure

The As(III), Pb(II) and Tl(I) containing model solutions were prepared by addition of small (μL) volumes of the stock solutions to the 10 mL of 1 M HCl in the polarographic cell and the solution was deoxygenated for 4 min with nitrogen before the determination. Fresh As(III) stock solution was prepared daily.

The potential scan was performed with 5 mV/s scan rate and the amplitudes of the pulses were ±25 mV for DAPV and -25 mV for DPP pulses. All the experiments were carried out at ambient temperature. The same procedure was applied for the real samples after adding of 1 mL of concentrated HCl to 9 mL water sample.

Results and discussion

Peak Potentials Determination Applying DPP

Two peaks of As(III) appear on the DPP voltammogram in 1 M HCl supporting electrolyte (Fig. 2), the first is placed at -0.43 V corresponding to the three electron reduction of As(III) to As(0) and the second at -0.78 V corresponding to the posterior reduction of As(0) to AsH_3. A very narrow third peak (a polarographic maximum) arise at about -0.7 V when the As(III) concentration is higher than 300 μg/L. (32).

Pb(II) yields a peak situated at -0.48 V while the peak of Tl(I) appears at more negative potential, at -0.52 V at same conditions and supporting electrolyte. The small potential differences result in peak overlapping occurring at any concentration ratio making thus impossible the simultaneous determination of these species applying DPP or any other voltammetric technique.

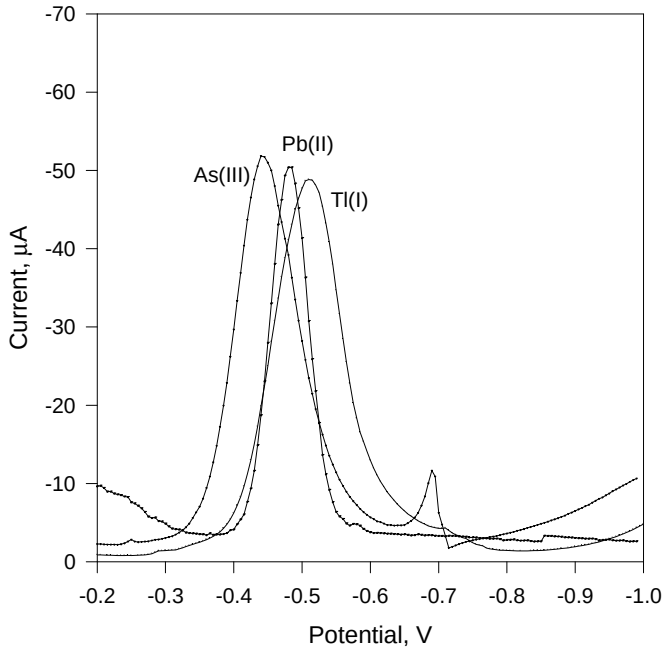

Figure 2. DPP peaks of As(III), Pb(II) and Tl(I).

DAPV Application

The main advantage of DAPV is the employment of the opposite polarity peaks remained on the voltammogram after the peak overlapping for concentrations evaluations (29). The important parameter determining the precision of the determinations is the concentration ratio of the species. For the purpose of the internal control of the plant purification process, a relative error of 10 % was considered satisfying. The maximal Pb(II) concentration allowing the As(III) determination with the preset relative error as well as the maximal As(III) concentration for Pb(II) determination were evaluated.

Simultaneous determination of Pb(II) and Tl(I) The maximal Tl(I) to Pb(II) concentration ratio allowing the Pb(II) determination with the preset relative error in excess of Tl(I) was evaluated registering DAPV voltammograms at increased Tl(I) concentrations keeping the Pb(II) concentration constant (Fig. 3). Well defined and separate anodic peak of Tl(I) and well defined cathodic peak of Pb(II) appear on the DAPV voltammogram up to concentration ratio as high as 6 to 1. At higher ratios, the Tl(I) cathodic peak increases interfering the Pb(II) one. The height measurement of the Pb(II) cathodic peak situated on the Tl(I) peak shoulder with the preset relative error was determined to be possible up to concentration ratios as high as 16 to 1. Nevertheless, distinct Pb(II) peaks are registered up to ratio as high as 20 to 1, but its analytical employment required complicated mathematical procedures application, not able to guarantee the preset precision of the determination.

The case of excess of Pb(II) is more complicated because of the larger Tl(I) peak half-width and the higher sensitivity of the voltammetric technique toward Pb(II). At this conditions Tl(I) can be determined at concentration ratios Pb(II) to Tl(I) less than 5 to 1

by the application of DAPV, while complete overlapping of the two peaks appears at ratio as small as 1 to1 as illustrated in Fig. 3 and Fig. 4.

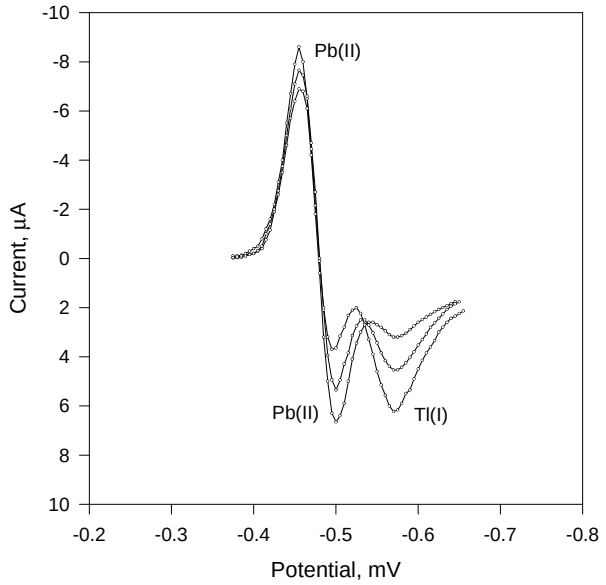

Figure 3. DAPV voltammograms of Pb(II) and Tl(I) in 1M HCl at concentration ratios 4:1 (the upper peak of Tl(I)); 2:1 (in the middle) and 1:1 (the lower peak of Tl(I)) respectively.

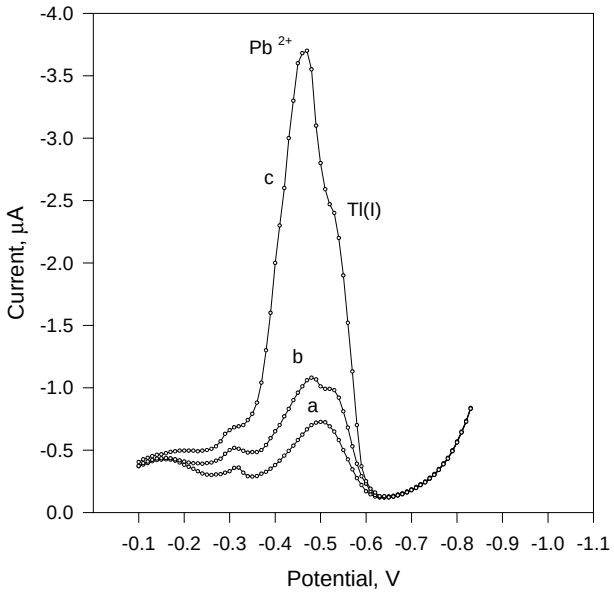

Figure 4. .DPP voltammograms of Pb(II) and Tl(I) in 1M HCl at Pb(II) excess. Concentration ratios: curve a: 0:1; curve b: 1:1; curve c: 4:1.

The results obtained by DAPV application at excess of Pb(II) were compared with the results attained by the Second Harmonic AC Voltammetry (SHACV) as well. Distinct peaks of analytical importance were registered for Pb(II) to Tl(I) concentration ratios as high as 4 to 1 by the SHACV application.

Simultaneous determination of As(III) and Pb(II) This case is similar to those presented above because of the large half-width of the As(III) peak due to the irreversible As(III) reduction and the higher sensitivity of the voltammetric technique toward the Pb(II).

A DAPV curve of 60 ppb As(III) and Pb(II) in concentration ratio 1:5 (excess of Pb(II)) is shown in Fig. 5 comparatively with a DPP one registered in 1M HCl and the same experimental conditions. While the two peaks on the DPP curve are completely undistinguishable, the DAPV curve contains well defined single anode peak for Pb(II) and well distinguished cathodic peak of As(III) as well.

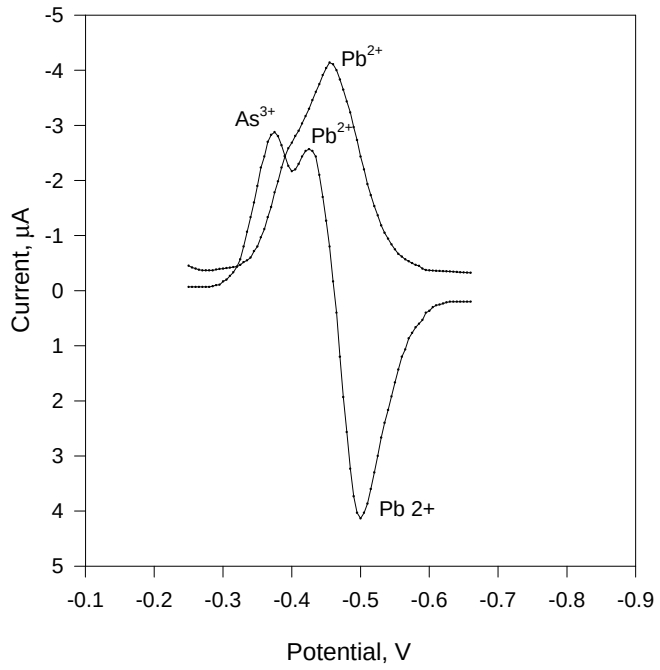

Figure 5. DAPV peaks of As(III) and Pb(II) in 1M HCl at concentration ratio 1:5.

Being placed on different sides of the zero line, the As(III) and Pb(II) peaks are completely separated up to 6-fold excess of Pb(II) allowing their direct simultaneous determination without any sample pretreatment. The studied concentration range of As(III) standard curve was found to be linear in the concentration range from 8 to 2000 µg/L for As(III). The relative standard deviation characterizing the reproducibility was inferior to 3 % in the upper part of the linear concentration range and about 10 % for the lower limit of this range. The DAPV limit of detection for As(III) determination was found to be 6.7 µg/L at 95 % confidence interval.

The calibration plot for As(III) at As(III) to Pb (II) concentration ratio from 1/ 1 to 20 / 1 (excess of As(III)) is shown in Fig. 6 while the results obtained for Pb(II) determination are shown in Table I.

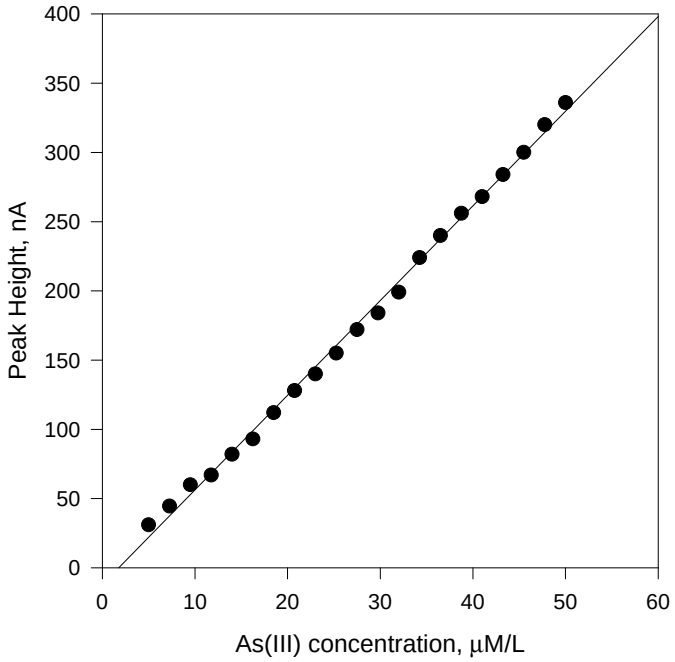

Fig. 6. Calibration curve for As(III) (from 5 µM to 50 µM) in 1 M HCl in the presence of 5 µM Pb(II).

Table I. Pb(II) determination applying different methods

Number	**DAPV**	**AAS**	**Photometry**	**DAPV**	**AAS**
	As(III), µg/L	As(III), µg/L	As(III), µg/L	Pb(II), µg/L	Pb (II), µg/L
1	47.2	42.2	49.3	106.3	98.2
2	51.0	47.7	51.4	102.4	100.7
3	49.7	46.1	53.7	98.5	101.1
4	46.3	45.2	47.3	100.7	97.2
5	48.3	50.5	50.2	98.2	99.5
Average	48.5±3.89	46.3±6.63	50.4±4.73	101.2±3.28	99.3±1.66

The results obtained applying the technique DAPV were compared with that obtained by spectral methods as AAS and Spectrophotometry (with silver diethyldithiocarbamate after sample dilution) in a referent laboratory. Real waste water sample containing As(III) and Pb(II) in concentration ratio about 1:2 were employed. Some appropriate sample pretreatment procedures were performed prior the application of the spectral methods. The DAPV determinations were performed directly, after HCl addition. No data are presented obtained by the application of DPP because of the complete overlapping of the As(III) and Pb(II) peaks even at concentration ratio 1:1. The results obtained by the three methods are presented in Table I and the comparison shows that they match well.

Simultaneous As(III), Pb(II) and Tl(I) determination. This case is much more complicated, in particular for Pb(II) determination since the Pb(II) cathodic and anodic peaks are overlapped on both sides depending on the concentration ratios As(III):Pb(II):Tl(I). The great variety of ratio values makes the simultaneous determination of the three species unpredictable and any specific case must be treated separately.

Conclusion

The limits of the species concentration ratios allowing simultaneous determination of As(III), Pb(II) and Tl(I) with preset precision of less than 10% were determined by DAPV using model solutions of 1M HCl supporting electrolyte. DAPV was applied for *on-site* determination of As(III), Pb(II) and Tl(I) in industrial samples for internal purification process control.

References

1. G. C. Barker, A. W. Gardner, *Z. Anal. Chem*., **173,** (1960) 79.
2. G. C. Barker, in: *Progress in Polarography*, P. Zuman, J. M. Kolthoff, Editor, vol. 2, p. 411, Wiley-Interscience, New York, (1962).
3. J. Osteryoung, *J. Chem. Educ.* **60** 296 (1983).
4. R. A. Osteryoung and J. Osteryoung, *Philos. Trans. Roy. Soc. London A,* **302,** 315, (1981).
5. J. Osteryoung and K. Hasebe, *Rev. Polar.,* **22**, 1 (1976).
6. G. C. Barker and I. L. Jenkins, *Analyst,* **77**, 685 (1952).
7. D. P. Whelan, J. J. O'Dea, J. Osteryoung and K. Aoki, *J. Electroanal. Chem,.* 202 (1986) 23.
8. G. C. Barker, R. L. Faircloth and A.W. Gardner, *A. E. R. E. report*, C/R 1786, Harwell (1958).
9. K. Aoki, K. Tokuda, H. Matsuda and J. Osteryoung, *J. Electroanal.Chem*., **207**, 25 (1986).
10. K. Wikiel and J. Osteryoung, *Anal. Chem*., 61, 2086 (1989).
11. S. P. Kounaves, J. J. O'Dea, P. Chandresekhar and J. Osteryoung, *Anal.Chem*., 59, 386 (1987).
12. S. P. Kounaves, J. J. O'Dea, P. Chandresekhar and J. Osteryoung, *Anal. Chem.,* **58**, 3199 (1986).
13. E. J. Zachowski, M. Wojciechowski and J. Osteryoung, *Anal. Chim. Acta,* **183**, 47 (1986).
14. K. B. Oldham, D. J. Gavaghan and A. M. Bond, *J. Phys. Chem. B*, **106**, 152 (2002).
15. G. C. Barker, *Anal. Chim. Acta,* **18**, 118 (1958).
16. G. C. Barker, A. W. Gardner and M. J. Williams, *J. Electroanal. Chem*., **42**, 21 (1973).
17. T. Kambara and Sh. Watarai, *Bull. Chem. Soc. Jpn.,* **39**, 521 (1966).
18. G. Wolff and W. H. Nurnberg, *Frezenius Z. Anal. Chem*., **224**, 332 (1967)
19. V. V. Senkevich, L. P. Chernega, V. I. Bodyu and Yu. S. Lyalikov, *Zavod. Lab.*, **34**, 1176 (1968).

20. H. P. Agarwal and M. Saxena, *Ind. J. Chem. A*, **16,** 754 (1978).
21. G. C. Barker, *Proc. Anal. Div. Chem. Soc.,* **12**, 179 (1975).
22. D. Saur, *Frezenius Z. Anal.Chem.,* **298**, 128 (1979).
23. K. S. G. Doss and H. P. Agarwal, *J. Sci. Industr. Res. India B*, **9**, 280 (1950).
24. K. S. G. Doss and H. P. Agarwal, *Proc. India Acad. Sci. A*, **34**, 263 (1951).
25. K. S. G. Doss and H. P. Agarwal, *Proc. India Acad. Sci. A*, *35*, 45 (1952).
26. K. B. Oldham, *Trans. Faraday Soc.,* **53**, 80 (1957).
27. P. Delahay, M. Senda and C. Weis, *J. Am. Chem. Soc.,* **83**, 312 (1961).
28. P. Delahay, M. Senda and C. Weis, *J. Phys. Chem.,* **64**, 960 (1960).
29. R. Zlatev, M. Stoytcheva, B. Salas, J.-P. Magnin and P. Ozil, *Electrochem. Commun.*, **8**, 1699 (2006).
30. R. Zlatev and M. Stoytcheva, *J. Univ. Chem. Technol. Metal.*, **XXXVIII**, 3 881 (2003). ISSN 1311-7629.
31. R. Zlatev, M. Stoytcheva, B. Valdez, L. Álvarez, J. Cobo, *ECS Transactions*, **20**, 3 (2009).
32. D. J. Myers, J. Osteryoung, *Anal. Chem.*, **45**, 267 (1973).

ANEXO C

ECS Transactions, 19 (32) 87-93 (2009)
10.1149/1.3268165 ©The Electrochemical Society

Application of TiO_2 Modified Boron Doped Diamond (BDD) Electrode for As(III) Determination in Natural Waters

R. Zlatev[a], M. Stoytcheva[a], J-P Magnin[b], B. Valdez[a], M. Argüelles[a] and J. A. Valera[a]

[a] Engineering Institute of UABC, Blvd. Benito Juárez s/n, 21280 Mexicali, BC, México
[b] LEPMI, ENSEEG, 1130 Rue de la Piscine, Grenoble, France

Activated by Au nanoparticles, Boron Doped Diamond (BDD) electrode was modified electrochemically by TiO_2 and applied for As(III) determination in natural ground waters. The modification with TiO_2 results in up to 49.7% sensitivity increase compared with the non modified electrode achieved at the maximum TiO_2 coverage percentage of about 73% of the BDD surface.

Introduction

As(III) is a chemically active, toxic and carcinogenic environmental pollutant affecting many regions of the planet (1-10), which determines the importance of its quantification. There are four arsenic oxidation states found in the nature: As(V), As(III), As(0) and As(-III) (1). As(III) provides the highest toxicity, about 10 times higher than As(V), the second most dominating and toxic arsenic specie (1). As(III) and As(V) affect the health mainly through the contaminated ground and underground water used for drinking.

The different toxicity, biological activity and physiological action of As(III) and As(V) require their distinct determination. EPA set the maximal concentration level for As(III) in drinking waters to 10 μg/L (11). This imposes the application of analytical techniques which must be selective and sensitive as well.

As it is known the arsenic species in water may undergo oxidation state conversion which depends on factors as pH, dissolved oxygen, presence of catalytic acting substances, etc. It is known that oxygen dissolved in water samples oxidizes As(III) to the less toxic form As(V) at low pH and in the presence of iron compounds within hours (6-10). This time is long enough to change the As(III)/As(V) ration and hence the real sample toxicity during the time of its transportation to the analytical laboratory. The HNO_3 added to the water samples to prevent hydroxides precipitation according to the sample conservation procedures favors this process. That is why the only way to obtain reliable data about the real arsenic species concentrations and the real water toxicity is their determination *"in situ"*.

Atomic Absorption Spectrometry (AAS) (2, 3), Inductively Coupled Plasma (ICP) (4) and High Performance Liquid Chromatography (HPLC) (5) require heavy, complicated and expensive laboratory equipment not applicable for *"in situ"* determination. In addition, some of the spectral methods such as AAS are not able to distinguish the arsenic species, determining "total" arsenic only. The AAS sensitivity is not satisfactory even with the application of the hydride system as well. In the case of complicated matrixes containing relatively high concentration of some impurities, AAS and ICP require preliminary laboratory As(III) separation from the matrix to prevent damaging of the equipment due to the high temperature salt crystallization.

The electroanalytical techniques such as Square Wave Anodic Stripping Voltammetry (SWASV), Differential Pulse Anodic Stripping Voltammetry (DPASV) and Differential Pulse Voltammetry (DPP), however, provide high sensitivity and resolution (12-18) allowing the direct As(III) determination even in high salt containing matrixes applying simple and portable equipment. In addition, the two main arsenic oxidation forms As(III) and As(V) can be easily distinguished since As(V) is not electrochemically active (19). Thus, after the As(III) quantification, the As(V) is reduced chemically by KI, for example, to As(III) which is determined again. As(V) concentration is found by the difference between the two As(III) quantifications (1).

The working electrodes based on mercury (mercury drop or mercury thin film) usually applied in the As(III) voltammetric determinations provide excellent electrochemical properties such as wide potential window and always clean surface. The toxicity of mercury, however, strongly limits its application as an electrode material. In an attempt to replace the toxic mercury, some solid materials such as Au, Pt, carbon (graphite, glassy carbon, carbon paste, BDD) were tested until now as working electrodes. It was found, for example, that gold has a higher hydrogen overpotential than platinum, resulting in lowering of the hydrogen evolution during the pre-deposition stage of the stripping determination.

If applied for stripping As(III) determination, the intermetallic Au-As(0) compound formed on the gold electrode surface during the electro-deposition results in higher and sharper oxidation peaks compared with a platinum working electrode (20) favoring the Au application for As(III) determination. The response of both, gold and platinum electrodes, however, is strongly depended upon the past history of the electrode surface. The surface pretreatment and oxide film formation greatly alter the electrode reaction kinetics (21). Reproducible results can be obtained only after carefully controlled electrode pretreatment or by the application of disposable electrodes (22). The main disadvantage of the gold electrodes, the “memory effect”, manifests itself as a dependence of the height and the potential of the registered peak on the electrode history.

The “memory effect” does not appear on Boron Doped Diamond Electrodes (BDD) This coupled with BDD electrodes wide potential window, high chemical and extremely high electrochemical stability make this material suitable for application in As(III) determination (23, 24). BDD’s are passive in nature and do not interact or bind to organic pollutants nor do they catalyze the oxidation of pollutants present in the determined water samples (25).

Yamada et al. (24) introduced recently the application of activated by Au nanoparticles BDD electrodes for As(III) quantification. In addition, it is known that TiO_2 exhibits adsorptive properties to As(III), and it is used in the commercial As(III) adsorbents such as Adsorbsia™ Gto™ produced by Dow Chemical for example. Manivannan et al. (26) developed a simple electrochemical technique for TiO_2 deposition on a BDD surface based on the procedure applied by Kavan et al. for TiO_2 deposition on indium tin oxide (27).

Combining the electrochemical stability and wide potential window of the BDD with the adsorption property of the TiO_2 toward As(III), a solid electrode was developed that

showed increased sensitivity toward the As(III) quantification. Its characterization in terms of sensitivity of As(III) stripping determination is the goal of the present work.

Experimental

Electrochemical cell and instrumentation

A model POL 150 Tracelab Polarographic Analyzer (Radiometer Copenhagen) controlled by a PC was employed together with an especially modified EG&G PAR model 303A electrode stand. The glass capillary was removed and replaced by the BDD electrode using a special support. The 10 mL glass electrochemical cell, the reference Ag/AgCl/3M KCl electrode and the Pt wire counter electrode were the PAR 303A stand original ones. An EG&G PAR Model 305 Stirrer was used during the deposition step of the stripping determination.

Reagents

All the reagents were of analytical grade purity. A standard solution of As(III) (1000 mg/L) was used for more diluted stock solution preparation used daily. The deionized water produced by MiliQ reverse osmoses installation (Millipore) was employed for the preparation of all the solutions. The supporting electrolyte was 0.1 M PBS (pH=5). The As(III) low concentrated solutions were prepared directly in the electrochemical cell using small volume (μL) of the diluted stock solution automatic pipettes.

BDD electrode preparation and modification with Au nanoparticles

Pieces measured 5 x 5 mm of Si(100) wafer, covered by highly boron doped diamond (BDD) providing a good electrical conductivity were fixed on acrylic stick supports. The electrical contact was made on the face side of the BDD to avoid the wafer resistance. A small drop of a silver conducting paste cured at ambient temperature was put in contact with a very small part of the BDD surface and a thin wire, the other end of which was connected to the electrode terminal. The BDD contact area was insulated by a drop of fast cured at room temperature acrylic resin. The BDD surface was used vertically to avoid the accumulation of gas bubbles produced on its surface during the electrochemical processes.

The BDD electrode activation by Au nanoparticles deposition was made as described without any modifications according to the procedure applied by Yamda (24), using very low (50 μM/L) concentration of gold salt in H_2SO_4.

Results and Discussion

BDD electrode modification with TiO_2

The procedure proposed by Kavan et al. (26) for deposition on indium tin oxide, later improved by Manivannan et al. (27) and adapted for BDD modification with TiO_2 was applied in the present work for BDD modification with TiO_2. The TiO_2 was

deposited electrochemically at constant potential from diluted (50 mM/L) aqueous solution of $TiCl_3$ at pH 2 following the Manivannan et al. procedure (27). The maximal coverage percentage of the BDD surface by TiO_2 was determined to be about 73% using SEM micrographs (Figure 1).

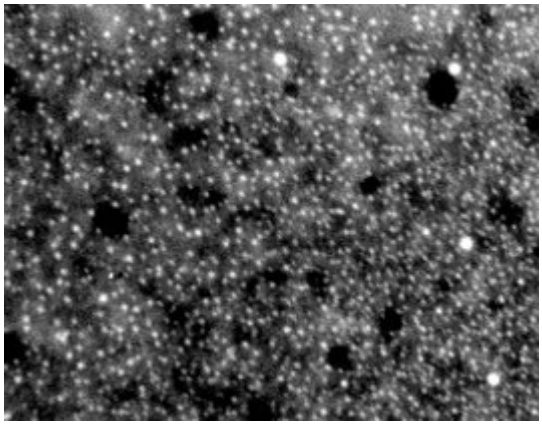

Figure 1. SEM picture of the modified BDD surface. Visible area: 4 x 3 μm

Two types of modified BDD electrodes were employed for As(III) concentration determination: (a) activated by Au nanoparticles only and (b) activated by Au nanoparticles and modified with TiO_2. The obtained results allowed evaluation of the influence of the TiO_2 adsorption properties on the sensitivity of the As(III) determination.

Six identical BDD electrodes were modified (activated) by Au nanoparticles, applying the procedure developed by Yamada mentioned above. Five of them (from number 2 to number 6 in Table I) were modified by TiO_2 as well applying five different deposition times at same conditions, obtaining thus different percentages of surface coverage. No thermal annealing at 450°C according to the procedure proposed by Kavan (26) was applied.

Voltammetric measurements

The Square Wave Anodic Stripping Voltammetry (SWASV) was used as the As(III) quantification technique in all the experiments. During the deposition step performed at a potential value of –400 mV, a reduction of As(III) to As(0) occurred. During the dissolution step, the deposited on the electrode surface As(0) monolayer is oxidized back to As(III) at a potential value near to 0.00 V (Ag/3M AgCl).

Because of the negligible conductivity of the deposited As(0) due to its semiconductor properties, a monolayer film only can be formed on the BDD electrode surface during the electrolysis, making complicated the application of all type of solid electrodes in As(III) stripping determination. The long electrochemical deposition, applied at high As(III) concentrations and small electrode areas leads to a complete covering of the entire electrode surface by As(0) monolayer; the small electrical conductivity prevented further development of the process. As a result, the dissolution step yields peaks having equal heights not dependent on As(III) concentration, corresponding to the deposited As(0) monolayer, thus limiting the quantification linear

response range. To avoid this problem a preliminary determination to adjust the deposition time according to the As(III) concentration and electrode area must be performed.

The presence of TiO_2 affects the deposition step of the stripping determination only resulting in an increase of the local As(III) concentration on the BDD electrode surface (X=0), due to the TiO_2 adsorptive properties towards As(III). As a result, the quantity of the deposited As(0) increase compared with the activated with Au only BDD electrode at same conditions. As a result the height of the registered peak increases.

A family of SWASV curves for As(III) in the concentration range from 0 to 50 ppb in phosphate buffer solution with pH=5 supporting electrolyte registered with the Au/TiO_2 modified BDD electrode of 25 mm^2 and 73 % of coverage are presented in Figure 2. The stripping parameters were the following: deposition potential, E_{dep}= -0.4 V, deposition time, T_{dep}=60 s.

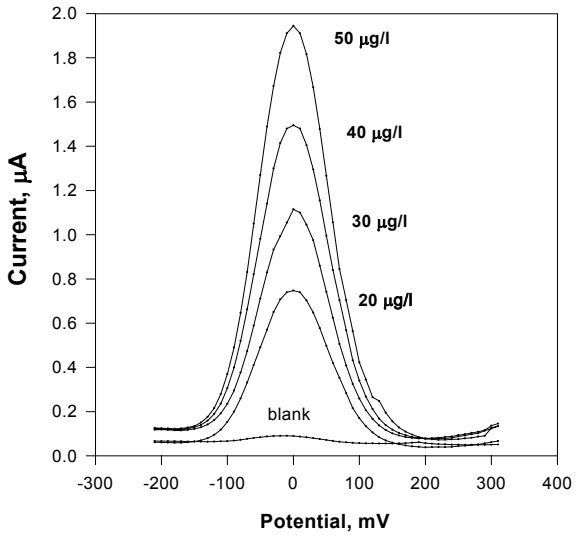

Figure 2. Family of SWASV curves for As(III) in the concentration range from 0 to 50 ppb in PBS (pH=5) with Au/TiO_2 modified BDD electrode with 73 % TiO_2 coverage

Influence of TiO_2 coverage percentage (deposition time) on As(III) SWASV peak height

As shown in Table I the increased coverage percentage of the BDD surface by TiO_2 controlled by deposition time results in increase of the registered by SWASV As(III) peaks. This effect however appears for the highest (>45%) coverage percentages only.

Table I. Dependence of the peak height on TiO_2 coverage percentage of activated BDD

Number of electrode	*Percentage of coverage by TiO_2, %*	*Peak Height Increase, %*
1	0	0
2	22	0
3	31	0
4	45	3.4
5	58	22.1
6	73	49.7

This fact can be explained by the random (chaotic) distribution of the TiO_2 and Au nanoparticles on the BDD surface. Since the Au nanoparticles serve as active zones of As(0) depositions during the first step of the stripping analysis, the TiO_2 nanoparticles must be located in close proximity to the Au nanoparticles to see the effect of the As(III) adsorption by TiO_2. That is why the higher TiO_2 coverage of the BDD surface increases the probability of TiO_2 nanoparticles deposition near the Au ones, thus increasing the adsorption effect of the TiO_2 toward As(III).

Curve B in Figure 3 presents the calibration plot based on the measurement series partly shown in Figure 2, performed with Au-73 % TiO_2 modified electrode, while the curve A corresponds to the same As(III) concentrations at same conditions but registered with the application of Au activated onlv BDD electrode.

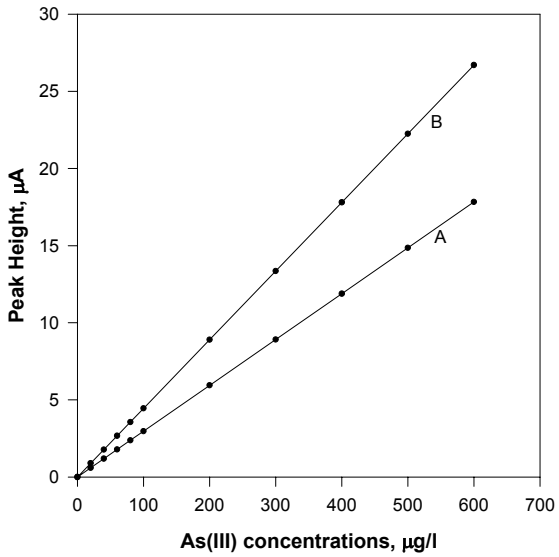

Figure 3. Calibration curves for 0 to 500 ppb As(III) in PBS, pH=5. Curve A: Au only modified BDD electrode; curve B: Au/TiO_2 modified BDD electrode, 73 % coverage.

Conclusion

Highly Boron Doped Diamond electrodes (BDD) activated by Au nanoparticles were modified electrochemically by TiO_2 and applied for As(III) determination. The adsorption properties of TiO_2 deposited on the BDD electrode surface results in sensitivity increase of the As(III) SWASV determinations with 49.7% at maximum surface coverage by TiO_2 of 73 % compared with the non modified BDD electrode. The small coverage percentages (< 45 %) do not affect the sensitivity of quantification due to the random (chaotic) distribution of the Au and TiO_2 nanoparticles.

Acknowledgement

This work was supported by research grants: 91241/SNI 1, 2008 of CONACYT Mexico and 2409 of the “13 Convocatoria de Proyectos de Investigación” of the UABC, Mexicali, Mexico.

References

1. D. Hung, O. Nekrassova and R. Compton, *Talanta*, **64,** 269 (2004).
2. M. Sager, *Fuel*, **72**, 1327 (1993).
3. Pei Liang and Rui Liu, *Anal. Chim. Acta,* **602**, 32 (2007).
4. K. Jitmanee, O. Mitsuko and M. Shoji, *Talanta,* **66**, 529 (2005).
5. O. Shuvaeva, O. Koscheeva and N. Beisel, *Anal. Sci.,* **17**, 179 (2001).
6. S. Hug, L. Canonica, M. Wegelin, D. Gechter and U. Von Gunten, *Environ. Sci. Technol*., **35**, 2114 (2001).
7. A. Voegelin and S. Hug, *Environ. Sci. Technol*., **37**, 972 (2003).
8. O. Leupin and S. Hug, J. *Water Res.,* **39**, 1729 (2005).
9. S. Hug, O. Leupin *Environ Sci Technol* **37,** 2734 (2003).
10. Kim Myoung-Jin and J. Nriagu, *Sci. Total Environ.,* **247**, 71 (2000).
11. B. K. Mandal and K. T. Suzuki, *Talanta,* **58** 201 (2002).
12. M. Leandro, P. Nascimento and D. Bohrer, *Quim. Nova,* **27**, 261 (2004).
13. Y. He, Y. Zheng, M. Ramnaraine and D. Locke, *Anal. Chim. Acta,* **511**, 55 (2004).
14. M. Esteban, C. Arino, I. Ruisanchez, M. Larrechi and F. Rius, *Anal. Chim. Acta*, **285**, 193 (1994).
15. G. Henze, W. Wagner and S. Sander, *Fr. J. Anal. Chem.,* **358**, 741 (1997).
16. E. X. Dai and R. G. Compton, *Electroanalysis,* **17,** 1325 (2005).
17. E. X. Dai, O. Nekrasova, M. Hyde and R. G. Compton, *Anal. Chem.,* **76,** 5924 (2004).
18. C. Prado, S. J. Wilkins, F. Marken and R. G. Compton, *Electroanalysis,* **14,** 262 (2002).
19. D. Myers and J. Osterioung, *Anal. Chem.*, **45,** 267 (1973).
20. G. Forsberg, J. O'Laughl, R. Megargle and S. Koirtyohann, *Anal. Chem.*, **47**, 1586 (1975).
21. D. G. Davis, *Talanta*, **3,** 335 (1960).
22. S. Laschi, G. Bagni, I. Palchetti and M. Mascini, *Anal Letters*, **40**, 3002 (2007).
23. Y. Song and G. M. Swain, *Anal. Chem.*, **79,** 2412 (2007).
24. D. Yamada, T. A. Ivandini, M. Komatsu, A. Fujishima and Y. Einada, *J. Elecroanal. Chem.,* **615,** 145 (2008).
25. D. Gandini, P.A. Michaud, I. Duo, E. Mahé, W. Hänni and A. Perret, *New Diamond and Frontier Carbon Technology*, Ed. MYU, Tokyo, JP, **9/5** 303 (1999).
26. L. Kavan, B. O'Regan, A. Kay and M. Grätzel, *J. Electroanal. Chem.,* **346,** 291 (1993).
27. A. Manivannan, N. Spataru, K. Arihara and A. Fujishima, *Electrochem. Solid-State Lett.*, **8,** C138 (2005).

ANEXO D

Sociedad Mexicana de Electroquímica

Congreso de la Sociedad Mexicana de Electroquímica

UNIDAD ACADÉMICA DE CIENCIAS QUÍMICAS

Estimados Colegas:

Por este conducto el Comité Científico del XXV CSMEQ tiene el agrado de comunicarles que el trabajo titulado:

DETERMINATION OF TRACE CONCENTRATIONS OF COBALT (II) IN ELECTROLYTE FOR ELECTROWINNING OF Zn BY DIFFERENTIAL PULSE VOLTAMMETRY

presentado por:

J. Adolfo Valera, R. Zlatev, M. Stoytcheva, B. Valdez

ha sido ***aceptado*** para su presentación en el marco del **XXV** Congreso de la SMEQ y el 3rd Meeting of The Mexican Section of the Electrochemical Society, a celebrarse en la Cd. de Zacatecas del 31 de mayo al 4 de junio del año en curso. El trabajo quedo registrado dentro de la temática de ***Electroquímica Analítica*** con la clave **EA262.**

.

Le recordamos que para la publicación del mismo en las Memorias del Congreso se requiere que al menos uno de los autores esté inscrito antes del 15 de mayo.

Agradecemos su participación y aprovechamos la ocasión para enviarle un afectuoso saludo.

Zacatecas, Zac., 1 de Marzo de 2010

ATENTAMENTE

Comité Organizador del XXV Congreso de la SMEQ y el
3rd Meeting of The Mexican Section of the Electrochemical Society

DETERMINATION OF TRACE CONCENTRATIONS OF COBALT (II) IN ELECTROLYTE FOR ELECTROWINNING OF Zn BY DIFFERENTIAL PULSE VOLTAMMETRY

J. Adolfo Valera, R. Zlatev*, M. Stoytcheva, B. Valdez

UABC-Mexicali, Instituto de Ingeniería, Blvd. B. Juárez s/n, C. P. 21280, México
*Tel/Fax 01(52-696)566-4150; roumen@iing.mxl.uabc.mx

RESUMEN

Se desarrolló y probó un método sencillo y rápido basado en la polarografía diferencial de pulsos (DPP), para la determinación directa y en línea de Co^{2+} en soluciones reales de electrólitos industriales para el electroextracción de Zn. El 1-nitroso-2-naftol se utilizó para la oxidación del Co^{2+} a Co^{3+} y para la formación de quelato en una solución amortiguadora de amoníaco (NH_4OH/HCl en proporción 8:1) usada como electrólito soporte. La gran diferencia entre los potenciales de los picos del Co^{3+} y del Zn^{2+}, obtenidos por DPP preemitió la eliminación completa de la interferencia debida al Zn^{2+}, asegurando resultados confiables en el rango lineal de concentraciones a partir de 10 ppb hasta 20 ppm. Como electrodos de trabajo se aplicaron electrodos desechables con superficie de mercurio.

Palabras Clave: DPP, Determinación de Co(II) en electrolito de Zn(II)

ABSTRACT

A simple and rapid *on-line* Differential Pulse Polarographic (DPP) method for direct Co^{2+} determination in Zn plant electrolyte was developed and tested in real solutions. 1-nitroso-2-naphtol was applied as Co^{2+} to Co^{3+} oxidizing and chelate forming agent in ammonia buffer (NH_4OH/HCl in 8 to 1 ratio) supporting electrolyte. The great DPP difference between Co^{3+} and Zn^{2+} peak potentials allows the complete elimination of the Zn^{2+} interference ensuring reliable results in the linear concentration range from 10 ppb to 20 ppm. Disposable mercury surface electrodes were applied as working electrodes.

Keywords: DPP, Co(II) determination, Zn(II) electrolyte.

1. INTRODUCTION

The solution used for Zn electroextraction contains about 150 g L^{-1} Zn^{2+} and a great variety of impurities, such as Cd^{2+}, Cu^{2+}, Pb^{2+}, Sb^{3+}, Co^{2+}, Fe^{2+}, Ni^{2+}, Ge^{4+} most of them in ppb levels [1,2]. The production of a high purity metal and the achievement of a high current efficiency of the electrolysis require removal of these impurities to prevent their co-deposition together with Zn^{2+} which favors the H_2 evolution due to the diminishing of the hydrogen overpotential on the Co containing cathode areas [2-12].

The purification process control requires simple, rapid and reliable *on-line* methods for impurities determination. The most applied in the industry spectral methods (absorption and emission) such as AAS and ICP can be helpful only after a preliminary sample pretreatment procedure for analyte separation. The high Zn^{2+} concentration provokes high temperature $ZnSO_4$ crystallization blocking the spectrometer nebulizer [12], thus making impossible the direct impurities determination. The application of wet laboratory methods for sample pretreatment such as analyte extraction makes the determinations complicated, long and less precise, unsuitable for *on-line* application as well.

On the other hand, the high ionic concentration of the Zn plant electrolyte favors the application of the voltammetric methods requiring conductive supporting electrolyte [1,13]. Very detailed reviews of the voltammetric monitoring of the Zn plant electrolyte impurities were presented by Bond [2] and Pilkington [1]. As shown by Bond, the high Zn^{2+} concentration does not interferes the Sb^{3+}, Cd^{2+}, Ni^{2+}, Ge^{4+} and Cu^{2+} determination. For the Co^{2+} determinations however Pilkington recommends the application of some spectral methods, because of the complete overlapping of Co^{2+} peak by the huge one of Zn^{2+}.

Many authors presented their contributions to the polarographic Co^{2+} determination in Zn plant electrolyte applying a great variety of sample pretreatment procedures, quantification techniques, supporting electrolytes and electrodes. The main approaches applied are matrix exchange and chelate formation combined with Adsorptive Stripping Voltammetry. Some of the reported methods are briefly mentioned bellow.

Meites [14] reported the application of 0.1 M ethylendiamine/0.1 M KNO_3 as a chelate forming/oxidizing agent resulting in Co^{3+} formation yielding a DPP peak at a potential of -0.5 V vs. SCE allowing its complete separation from the peak of Zn^{2+}. The Zn^{2+} chelate formation requires high ethylendiamine concentration but the LOD of 15 mg L^{-1} is not satisfactory.

Matrix exchange procedure followed by Differential Pulse Adsorptive Stripping Voltammetry (DPAdSV) was reported for Co^{2+} determination in Zn plant electrolyte employing various organic compounds [15,16]. Korolczuk et al. [17] reported the application of nioxime-cetyltrimethylammonium bromide-piperazine-N, N-bis(2-ethanesulfonic acid) in adsorptive DPAdSV step. This technique was applied for very low Co^{2+} concentrations (from 10^{-11} to 10^{-8} M) determinations [18] in Zn plant electrolyte with satisfactory results.

Mrzljak et al. [19] reported two ADSV methods for Co^{2+} determination in Zn plant electrolyte with detection limits of 9 ppb and 0.25 ppb based on matrix exchange procedures including filtration, acidifying with H_2SO_4, cooling, dispensing, etc. Another method for Co^{2+} determination based on the application of a carbon paste electrode modified by DMG in acetate buffer with pH 4.8 in the presence of 100-fold excess of Zn was reported by Lloyd [20].

Pilkington [1] reported the application of DPP and DPASV for Sb^{3+}, Cd^{2+}, Cu^{2+} determination in Zn plant electrolyte, but excluding the possibility for determination of Co^{2+} at all, recommending the spectral methods application.

As seen, the mentioned methods applied for Co^{2+} determination in Zn plant electrolyte are complicated and hardly applicable for direct *on-line* analysis. The main problem comes from the small $E_{½}$ difference of Co^{2+} and Zn^{2+} combined with the huge Zn^{2+} concentration causing complete overlapping of their peaks in any supporting electrolyte. It is hardly to find some sample pretreatment procedures allowing the analyte separation from the high concentration matrix able to be performed *on-line*. For example, the Zn^{2+} precipitation in alkaline media forms an amorphous $Zn(OH)_2$ having a huge surface, adsorbing the ions present in trace concentration and disturbing thus the reliability of their determination. The extraction and matrix exchange need laboratory operations made by qualified personal which precision determine the analytical results reliability. All these defined the need of searching another and simpler approach for *on-line* Co^{2+} determination in Zn plant electrolyte.

The aim of the present work is the development of a direct, simple, rapid and reliable *on-line* polarographic method and electrode for Co^{2+} determination in Zn plant electrolyte, avoiding the Zn^{2+} interference for the entire range of Zn^{2+}/Co^{2+} concentration ratio in the Zn plant electrolyte.

For this purpose a proper alkaline supporting electrolyte allowing the solution deoxygenating by Na_2SO_3 avoiding thus its purging by inert gas was chosen: NH_4OH + HCl in 8

to 1 ratio. The purpose of the NH_4OH excess is to form a soluble chelate with the Zn^{2+} preventing thus its precipitation. The next step was finding a way to shift the cobalt peak potential to more positive direction allowing it distinction from the huge Zn^{2+} peak. As it was found by Colthoff et al. and A. M. Bobtelskya et al. [21-23] the 1-nitroso-2 naphtol forms a chelate where the cobalt is trivalent allowing to register the peak of Co^{3+} at much more positive potential than Zn^{2+} (at about –500 mV). The other nitroso-naphtols (1-nitroso-2-naphtol; 2-nitroso-1-naphtol and nitroso-R-salt) also oxidize Co^{2+} to Co^{3+} making them suitable to avoid the Zn^{2+} interferences and they were tested too. The third step was choosing a simple mercury surface electrode avoiding the use of capillary which maintenance in industrial conditions is problematic. A special type of disposable mercury surface electrode was developed based on a support made by PCB technology application [24], allowing to be employed without any maintenance and easily recyclable after its use.

Various authors reported polarographic determination of Co^{2+} in the presence of 1-nitroso-2-naphtol:

Braynina [25] reported an anodic stripping voltammetric method based on electrochemical deposition of 1-nitrozo-2-naphtol Co^{3+} chelate in 0.4 M NH_4OH/0.05 M NH_4Cl on carbon electrode and its further anodic dissolution, registering the anodic peak. Co^{2+} after its oxidation to Co^{3+} forms a low soluble chelate which precipitates on the carbon electrode surface during the preconcentration step. The electrochemical reduction occurs at potential values -0.6 - -0.7 V. The small linear concentration range, the small Zn^{2+}/Co^{2+} concentration ratio (about 1000) and the complicated sample pretreatment do not allow this method to be applied for impurities determination in Zn plant electrolyte where the Zn^{2+} to Co^{2+} concentration ratio is as high as 10^6 to 1 or more (150 g L^{-1} to 50-200 μg L^{-1}).

Jugade et al. [26] reported a rapid Adsorptive Stripping Voltammetric method for Co^{2+} and Ni^{2+} determination in 0.01 M NH_4Cl solution (pH 9.5) containing 1 μM 1-nitroso-2-naphtol applied for water, food and alloy samples. A concentration ratio for various metals among which Zn^{2+} from 1 to 100 not interfered the cobalt peak height. Uchida et al. [27,28] reported polarographic studies of the cobalt(III)-1-nitroso-2-naphthol chelate formation in citrate buffer (pH 5) and aqueous tartarate solutions. The cobalt(III) chelate is determined in a electrolysis solution composed of a 1/1 mixture of the extract and acetonitrile solution containing 8 mM perchloric acid and 0.2 M sodium perchlorate with a limit of determination is in the range of 1-2

ppb. Lloyd et al. [20] reported the determination of trace of cobalt and other metals in rocks using rubeanic acid and 1-nitroso-2-naphthol after sample pretreatment including precipitation and centrifugation. Unfortunately none of the mentioned methods is applicable in Zn plant electrolyte because the interference of the huge excess of Zn^{2+}. Geisler et al. reported a DPP method for Co^{2+} determination providing liner response from 10^{-7} to $5x10^{-6}$ M in the presence of 50,000 excess of Zn^{2+} [29].

Despite of the excellent characteristics of the mercury as electrode material, its application as mercury drop electrodes such as DME, SMDE and HMDE was restricted recently because of the mercury toxicity and its high cost. On the other hand, the maintenance of the capillary in industrial condition is complicated, requiring qualified personal. Since the electrochemical reactions occur at the electrode surface only, the deposition of a mercury film onto a conducting support material yields "mercury" electrode as well. Since the mercury forms a small droplets on the surface of Pt and the carbon materials including glassy carbon, not covering the entire surface to form a "mercury" electrode, these two materials were excluded as suitable for supports. A continuous mercury film can be achieved on amalgam forming metals only such as Ag and Au. Even ppb level of H_2S (air impurity present in the industrial areas) however forms sulphide layer on the Ag surface [30] preventing amalgam formation, that is why Ag was not tested as support material as well. Thus, Au was chosen as support material and a thick Hg film was deposited on the Au support *in-situ* just prior the determination by electrolysis in the polarographic cell. To avoid contamination of the mercury surface by the Au amalgam and the Au-Hg intermetalic compounds formed, the mercury film was produced to be thick and deposited some seconds only just before its application.

2. EXPERIMENTAL

2.1. Instrumentation

The laboratory polarographic determinations were performed by a modified Model 264A Polarographic Analyzer, coupled with Model 303A SMDE/HMDE electrode stand (EG&G PAR, USA) completely controlled by PC, running an especially created software. A PC controlled conductivity measuring module was incorporated to the Polarographic Analyzer applied for surface reproducibility correction coefficient determination. Some of the curves were recorded on

paper using an X-Y recorder and scanned and digitalized after. The original reference and auxiliary electrodes mounted on the Model 303A electrode stands were employed.

Z 58 Potentiostat controlled by Z54 potentiostat software (ZENIT Lab) coupled with a Z59 electrode stand (ZENIT Lab) were employed for the *on-line* determinations. Cost effective disposable electrodes were used as working electrodes. A flow type polarographic cell with a special holder for the disposable electrodes application was used for the *on-line* industrial determination. The reference electrode was Ag/AgCl/3M KCl electrode and the counter electrode a 1mm in diameter Pt wire.

A ML-501A Hamilton Single Syringe Diluter/Dispenser was employed for the *on-line* analysis sample preparation.

2.2. Working Electrode

The disposable working electrodes supports introduced by the authors earlier [24] were produced by the application of PCB technology and covered *in-situ* by a thick mercury film few seconds just before the application. This approach allows taking advantage from the mercury electrode surface without any risk of mercury spiel. The electrode support consisted of 5x30 mm glass fibers reinforced epoxy stick (0.5 mm thick) covered by 17 μm of Cu, a cost effective material massively used for PCB production. The working part of the electrode had the shape of a disk, 0.5 mm in diameter covered by about 0.5 μm Ni and finally by 1 μm Au. It can be stored during an unlimited time and after its application is easily recycled. A plastic band carrying about 1000 electrodes was charged in a computer controlled roll changer for electrode exchange.

2.3. Reagents

All the reagents were of analytical grade (Merck and Sigma) and the deionized water was produced by MiliQ system of Milipore. The stock solution of ammonia buffer supporting electrolyte was preliminary prepared by mixing of 8 volume parts of NH_4OH with 1 volume part of concentrated HCl, continuously cooling by running water. The NH_4OH excess allowed the formation of the soluble Zn^{2+} ammonia chelate avoiding precipitation formation. The 1-nitrozo-2-

naphtol solution was preliminary prepared by dissolution of 50 mg of 1-nitrozo-2-naphtol in 50 mL of ethyl alcohol + 1 mL HCl.

2.4. Measuring Procedure

The laboratory polarographic experiments were performed in the original PAR 303A polarographic cell employing the DME mode of the mercury electrode. The Zn plant electrolyte and the supporting electrolyte containing 600 ppb solution of 1-nitroso-2-naphtol (2-nitroso-1-naphtol or nitroso-R salt for some of the experiments) were added directly into the polarographic cell in ratio 5 mL to 5 mL with the aide of the ML-501A Hamilton Single Syringe Diluter/Dispenser. The DPP polarograms was registered from -200 mV initial potential to -800 mV with a scan rate of 10 mV s^{-1} (5 mV step every 0.5 s); the pulse amplitude was -50 mV.

The *on-line* determinations of real industrial solutions were carried out in a special 10 mL flow polarographic cell. Before the determination, a thick mercury film was deposited on the electrode support by electrolysis performed in the same polarographic cell. $HgCl_2$ solution in 0.1 M HCl was added by a peristaltic pump and the electrolysis was carried out for 30 s by the Model 264A Polarographic Analyzer controlled by PC via a special interface. After rinsing the cell by a peristaltic pump, the 5 mL of the Zn plant electrolyte sample was introduced followed by 5 mL of the supporting electrolyte containing the organic reagent and the next disposable electrode was inserted. The polarograms were registered by the same way as in the laboratory conditions mentioned above and processed after by PC to calculate the Co^{2+} concentration.

3. RESULTS AND DISCUSSION

3.1. Working Electrode Surface Reproducibility Determination

As mentioned above, the working electrode area was a Au disk (0.5 mm diameter) located on the lower part of a 5x30 mm plastic stick. The reproducibility of the Au disc electrode surface determined before to be covered by mercury was within 4.3 %, determined as R.S.D. of the electroconductivity, as described by the author earlier [24].

The conductivity of the Hg^{2+} containing solution used for the mercury deposition was measured using the conductivity module incorporated in the Model 264A Polarographic Analyzer.

This measurement was performed immediately after the Hg thick film deposition on the Au support by electrolysis. Since the concentration of the Hg^{2+} containing solution was kept constant, the measured conductivity was proportional to the electrode surface only at a constant temperature. The correction coefficient was calculated vs. the electrode employed for the calibration curve building as described by the author earlier [24]. The reproducibility of 10^{-6} M Co^{2+} determination according to the procedure described above was determined to be within +/- 3.6 % determined as R.S.D., while the reproducibility determined by the DME application was found to be 1.4% R.S.D. for the same concentration. Disposable mercury surface electrodes were applied as well, the correction procedure being described in [24].

3.2. Cobalt - 1-nitrozo-2-naphtol chelate Formation and its Application for DPP Determination

The 1-nitrozo-2-naphtol is one of the first organic reagents applied in analytical chemistry, used for a long time for gravimetric Co^{2+} determination [21-23] because of its great specificity toward Co^{2+}, oxidizing it to Co^{3+} and forming a low soluble chelate [31].

1-nitrozo-2-naphtol, providing a good solubility in many organic solvents as acetone, ethyl alcohol, benzene, etc. is soluble in aqueous solution as well, such as acetic acid, NaOH, tartarate ,etc. [27,28,31]. The solubility of Co^{3+}(1-nitrozo-2-naphtolate) in water is about 1.5 mg L^{-1} as reported by Piatnikyi [31]. A red-brown coloration of the solution appears only in the presence of ppb levels of Co^{2+}, because no chelate precipitation probably occurs. This allows the direct polarographic determinations of low Co^{2+} concentrations to be carried out applying DME without chelate preconcentration on the electrode surface.

The addition of 1-nitrozo-2-naphtol to Co^{2+} containing solution results in the appearance and the increase of a well defined DPP peak at –550 mV corresponding to the electrochemical reduction of Co^{3+} resulting from the Co^{2+} oxidation by the added organic reagent, while at the same time the height of the Co^{2+} peak situated at -1335 mV decreases respectively. This fact shows that Co^{2+} is oxidized by the organic reagent only partially and the concentration of the formed Co^{3+} and hence the sensitivity of the determinations depends on the 1-nitrozo-2-naphtol concentration (Fig. 1).

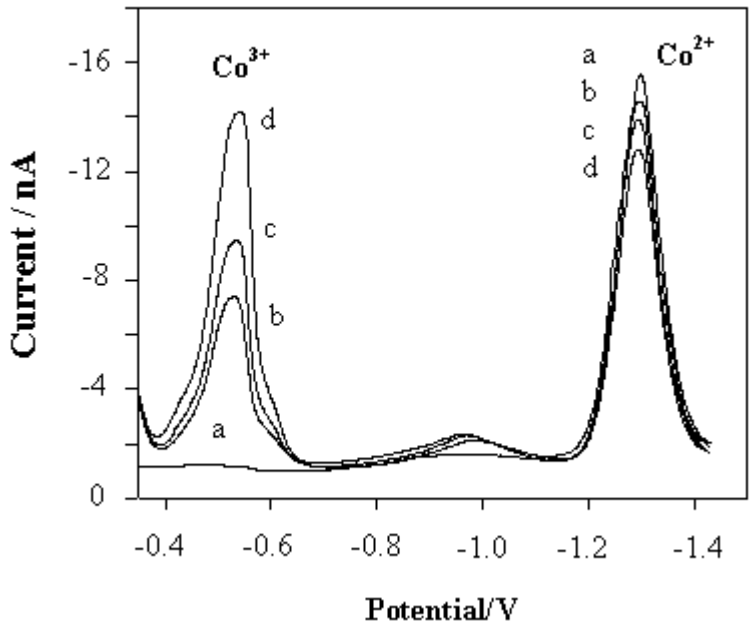

Figure 1. DPP polarograms of Co^{2+} after additions of 1-nitroso-2-naphtol. Curve a: 100 ppb Co^{2+} only; Curve b, c and d: after additions of 400, 500 and 800 ppb 1-nitroso-2-naphtol, respectively.

As proved by Kolthoff and other authors [21-23,31], the composition of the formed chelate can be expressed as $Co(R)_3$, determining the optimal concentration ratio: 1-nitrozo-2-naphtol/cobalt to be 3 to 1. It can be expected that the Co^{3+} peak height will increase up to this ratio to be reached and that is why a concentration of 600 ppb was chosen as optimal one for the 1-nitrozo-2-naphtol addition, 3 times higher than the upper limit of the cobalt concentration range in the Zn plant electrolyte (from 20 to 200 ppb).

The chosen 1-nitrozo-2-naphtol concentration was tested by building of a calibration curve in coordinates: Co^{3+} peak height vs. Co^{2+} concentration which was found to be linear at the presence of 600 ppb 1-nitrozo-2-naphtol in the Co^{2+} concentration range from 20 ppb to 500 ppb with a correlation coefficient $r^2 = 0.946$, while for a smaller concentration range (from 20 to 200 ppb which is the typical concentration range for the Co^{2+} impurities in Zn plant electrolyte), the correlation coefficient is higher (0.987).

It was found experimentally that the Co^{3+} peak height passed through a maximum with the increase of the 1-nitrozo-2-naphtol concentration and probably the decreasing part of the curve after the maximum is due to the reaching of the solubility product value of the Co-1-nitrozo-2-naphtolate resulting in chelate precipitation and lowering thus the measurable Co^{3+} concentration.

The 1-nitrozo-2-naphtol is an electrochemically active substance, yielding a DPP peak at -250 mV vs. Ag/AgCl/3M KCl in the mentioned above ammonia supporting electrolyte, which allows investigating the Co^{2+} oxidation and chelate formation. This fact permits to demonstrate the 1-nitrozo-2-naphtol consumption by increased Co^{2+} concentration as presented in Fig. 2, where the initial 1-nitrozo-2-naphtol peak diminished with the successive additions of Co^{2+}.

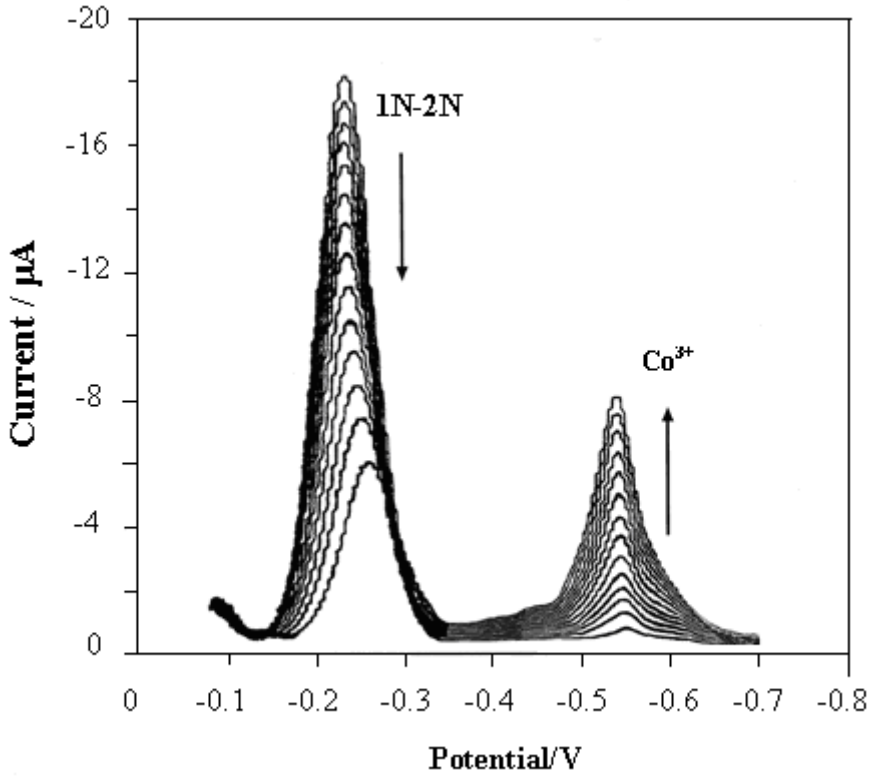

Figure 2. Decrease of the 1-nitrozo-2-naphtol (600 ppb initial concentration) DPP peak situated at -250 mV caused by successive additions of Co^{2+} in the range from 0 to 800 ppb.

The Co^{3+} peak of analytical importance is those appearing at -550 mV (Ag/AgCl/3M KCl). The peak potential difference with the Zn^{2+} peak situated at -1300 mV is 750 mV, which is sufficient to avoid any Zn^{2+} interference, as illustrated in Fig. 3. The Zn^{2+} peak in Fig. 3 corresponds to a low concentration in order to mark the peak potential only.

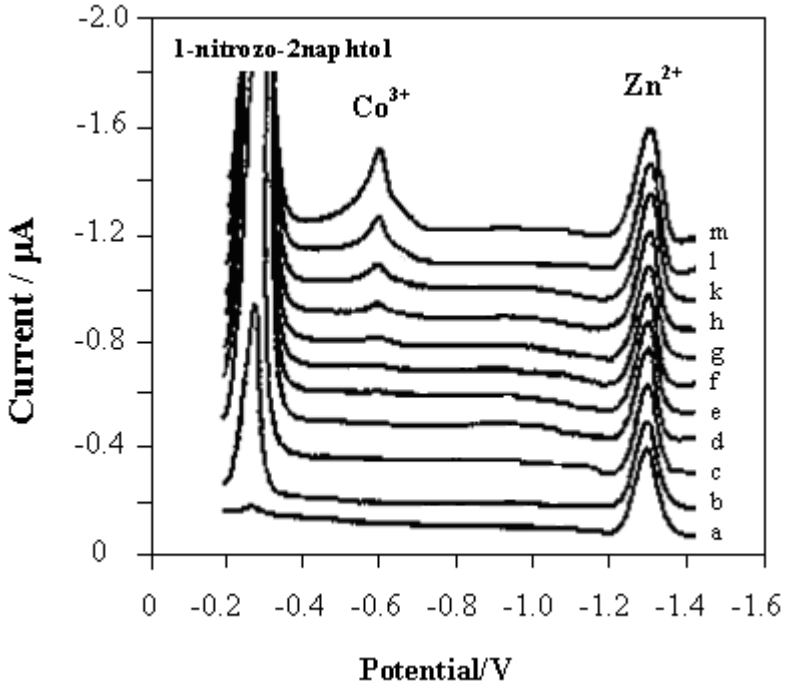

Figure 3. DPP peaks of: Co^{3+} (*E*p = -550 mV) resulted from Co $^{2+}$ (*E*p = -1335 mV) oxidation by 1-nitrozo-2-naphtol and DPP peaks of Zn $^{2+}$ (*E*p = - 1350 mV). Curve a: Zn $^{2+}$ only; curves b, c and d: after addition of 1-nitrozo-2-naphtol; curves from e to m after successive additions of Co^{2+}.

The influence of Zn^{2+} concentration was evaluated by Co^{2+} increased concentration (in the range from 20 to 200 ppb) determination in a model solution containing 150 g L^{-1} Zn^{2+}. The results are shown in Table I.

Table I. Precision of Co^{2+} determination in the presence of 150 g L^{-1} Zn^{2+} by DAPV application (model solutions).

Standard concentrations, ppb	Determined concentrations, ppb	Determined concentrations, ppb	Relative error, ppb	Relative error %
20	21.8	21.8	-1.8	-9.0
50	53.2	53.2	-3.2	-6.4
100	9.71	9.71	2.9	-2.9
150	148.2	148.2	-1,8	1.2
200	197.6	197.6	2.4	1.4

In spite of the higher sensitivity of the spectrophotometric determination of Co^{2+} with 2-nitrozo-1-naphtol application compared with 1-nitrozo-2-naphtol, its polarographic performance was found to be inferior. The DPP peak height of Co^{3+} in the ammonia supporting electrolyte

applied in the present work is much lower and appears at much more negative potential, still far from the Zn^{2+} peak potential, as shown in Fig. 4.

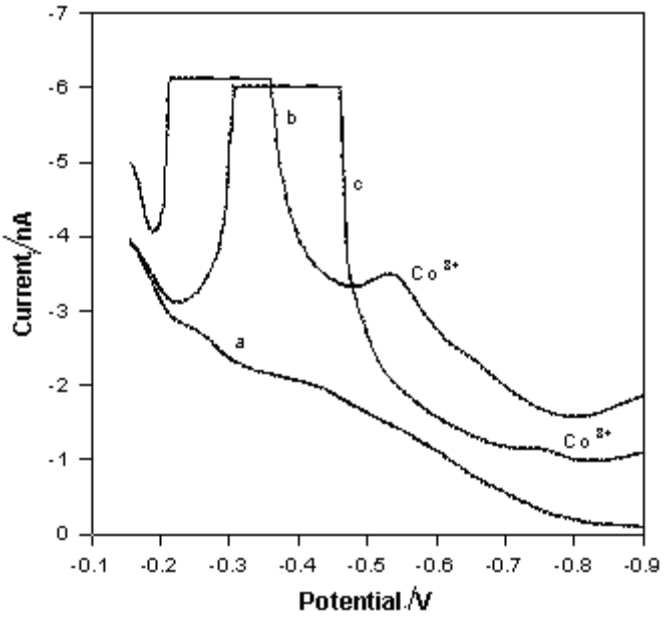

Figure 4. DPP peaks of: 1-Nitrozo-2-naphtol and Co^{3+} (curve b); 2-nitrozo-1-naphtol and Co^{3+} (curve c); blank (curve a)

The third organic reagent of the nitroso-naphtol group applied in the analytical chemistry, the nitroso-R salt yielded broad Co^{3+} peaks at inferior sensitivity of the determinations compared with the 1-nitrozo-2-naphtol application.

3.3. Application for real samples determinations

Typical curves of Co^{2+} containing Zn plant electrolyte registered according to the procedure described in the experimental part are shown in Fig. 5.

The peak of 600 ppb 1-nitrozo-2-naphtol appearing at -250 mV does not interfere the Co^{3+} peak, overlapping however the Ni^{2+} peak appearing at -430 mV in the employed supporting electrolyte. Since the Co^{2+} and Ni^{2+} concentrations are of the same order, the Ni^{2+} peak does not interfere with the cobalt determinations.

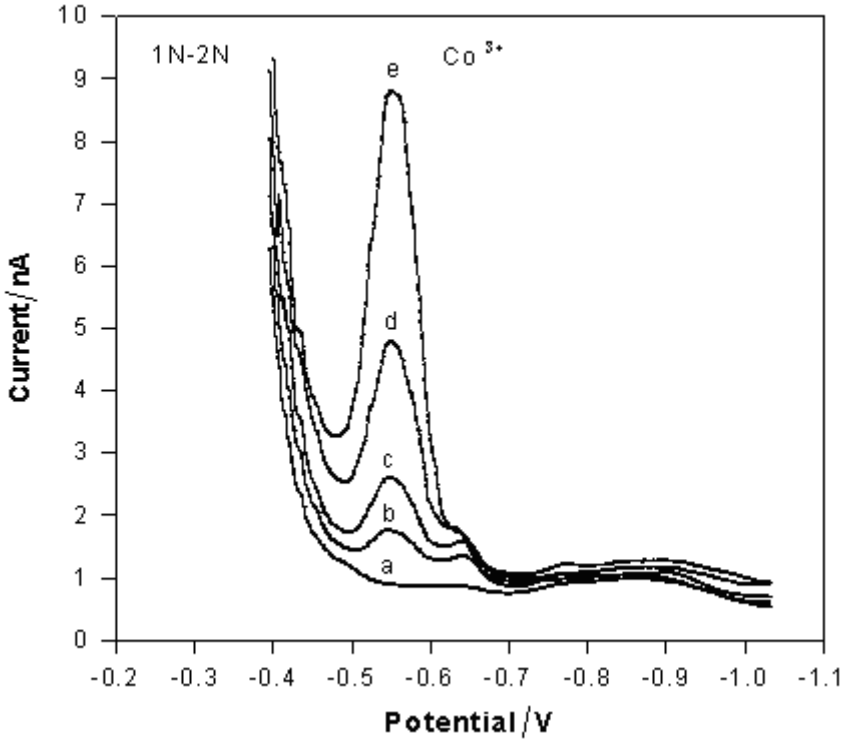

Figure 5. Co^{3+} peaks corresponding to Co^{2+} concentrations of: 20 ppb (curve b); 40 ppb (curve c); 80 ppb (curve d) and 160 ppb (curve e); blank (curve a)

The experimental results showed that the Zn^{2+} concentration does not interfere at all the Co^{2+} determination by the method subject of the present work in the entire range of the Co^{2+} concentrations present in the industrial solution.

4. CONCLUSIONS

1-nitroso-2-naphtol was applied as Co^{2+} to Co^{3+} oxidizing and chelate forming agent in ammonia (NH_4OH/HCl in 8 to 1 ratio) supporting electrolyte. The great DPP difference between Co^{3+} and Zn^{2+} peak potentials allows Co $^{2+}$ concentration determination eliminating completely the Zn^{2+} interference, allowing thus obyaining reliable results in the entire concentration range of Co^{2+} (from 20 ppb to 200 ppb) in the Zn plant electrolyte. Disposable mercury surface electrodes were applied as working electrodes in the simple and rapid *on-line* Differential Pulse Polarographic (DPP) method subject of the present work developed and applied for direct Co^{2+} determination in Zn plant electrolyte.

5. ACKNOWLEDGEMENTS

José Adolfo Valera externa su gratitud al CONACYT por el apoyo otorgado para la culminación de su trabajo doctoral.

6. REFERENCES

[1] E. Pilkington, C. Weeks, and A. Bond, *Anal. Chem*., **48**, 1665 (1976).

[2] D. A. Bond, *Anal. Chim. Acta,* **400**, 333 (1999).

[3] G. T. Wever, *J. Metals*, **11**, 130 (1959).

[4] G. C. Bratt, *Electrochem. Technol*., **2**, 323 (1964).

[5] V. L. Klimenko, *Sov. J. Non-Ferrous Metals*, **12**, 18 (1971).

[6] A. R. Ault, J. H. Bain, D. J. Palmer and J. B. Pullen, in *South Australia Conference*, p. 225, Australian Institute of Mining and Metallurgy, Melbourne, (1975).

[7] U. F. Turoshima and V. V. Stender, *J. Appl. Chem. USSR*, **28**, 151 (1955).

[8] H. H. Fukabayashi, T. J. O'Keefe and W. C. Clinton, *U. S. Bur. Mines Rep. RI 7966*, Rolla, Mo., **(**1974).

[9] G. Steinvelt and H. Holtan, Jr., *J. Electrochem. Soc*., **107**, 247 (1960).

[10] I. Ivanov, *Hydrometallurgy*, **72**, 73 (2004).

[11] C. Bozhkov, M. Petrova and St. Rashkov, *J. Appl. Electrochem.,* **22**, 73 (1992).

[12] C. L. Mantell, *Electrochemival Engineering*, p. 210, 4th Ed., McGraw-Hill, N. Y., (1960).

[13] J. Wang, *Analytical Electrochemistry*, 2nd Ed., Willey, N. Y., (2000).

[14] L. Meites, *Polarographic Techniques*, p. 614, 2nd Ed., Willey, N. Y, (1965).

[15] E. A. Bobrowski and A. Bond, *Electroanalysis*, **16**, 1536 (2004).

[16] G. R. Mrzljak, A. Bond, T. Cardwell, R. W. Cattrall, R. W. Knight, O. M. G. Newman, B. R. Champion and J. Hey, *Anal. Chim. Acta*, **281**, 281 (1993).

[17] M. Korolczuk, A. Moroziewicz, M. Grabarczyk and K. Paluszek, *Talanta*, **65**, 1003 (2005).

[18] M-H. Zhang and Y-Z. Liang, *J. Trace and Microprobe Techniques*, **14**, 1 (2002).

[19] R. Mrzljak, A. Bond, T. Cardwell, R. Cattrall, R. Knight, M. Newman, B. Champoin, J. Hey and A. Bobrowski, *Anal. Chim. Acta*, **281**, 281 (1993).

[20] S. E. Lloyd and B. A. Gatehouse, *Anal. Chem*., **27**, 901 (1955).

[21]. C. I. M. Kolthoff and E. Jacobsen, *J. Am. Chem. Soc*., **79**, 3677 (1957).

[22]. A. M. Bobtelskya and E. Jungreis, *Anal. Chim. Acta,* **12**, 248 (1955).

[23]. I. M. Kolthoff and A. Langer, *J. Am. Chem. Soc.,* **62**, 3172 (1940).

[24]. R. Zlatev, M. Stoytcheva, B. Valdez, L. Álvarez and J. M. Cobo, *ECS Transactions*, **20**, 3 (2009).

[25]. Kh. Brainina, *Frez. Z. Anal. Chem*., **312**, 428 (1982).

[26] R. Jugade and A. Joshi, *Ind. J. Chem., Section A*, **42**, 94 (2003).

[27]. T. Uchida, M. Sugawara and T. Kambara, *Fres. J. Anal. Chem*., **315**, 487 (1983).

[28] T.Uchida and M.Sugawara, *Fres. J. Anal. Chem*, **322**, 470 (1985).

[29] M. Geisler and R. Da Maia, *Fresenius Z. Anal. Chem*, **330**, 624 (1988).

[30]. O. L. Vargas, S. B. Valdez, M. L. Veleva, K. R. Zlatev, M. Schorr and G. J. Terrazas, *Anti-Cor. Methods and Materials*, **56**, 218 (2009).

[31]. I. Pjatnickyi, *Analytical Chemistry of Cobalt*, p. 54-55, Nauka Press, Moscow, **(**1965).

ANEXO E

Aplicación de 1-Nitrozo-2-Naphtol en Mediciones Voltamétricas de Cobalto en Electrolito para Electrowining de Zinc

J. A. Valera, R. Zlatev, M. Stoytcheva

Engineering Institute, UABC, Blvd. Benito Juarez S/N, 21280 Mexicali, Baja California, Mexico

RESUMEN

Co2+ es una de las impurezas de los niveles de rastro del electrólito de la planta del producción de Zn que incluye durante el electroextraction del Zn en el metal producido, así bajando su pureza y también favorece la evaluación H_2 en el cátodo del Zn que aumenta la energía perdida. La cristalización da alta temperatura $ZnSO_4$ en el nebulizador debido a la alta concentración de Zn^{2+} (cerca de 150 g/l) hace Co^{2+} imposible la determinación en línea por la espectroscopia de absorción atómica (AAS) y el plasma inductivo juntada (ICP) durante el proceso de la purificación.

Un simple y rápido método aplicando la Polarográfia Diferencial del Pulsos (DPP) para la determinación directa de Co^{2+} en el electrólito de la planta del Zn conveniente para el uso en línea fue desarrollado y probado con las soluciones verdaderas de la planta del Zn. El método se basa en el uso de 1-Nitrozo-2-Naphtol en el electrólito favorable del almacenador intermediario del amoníaco donde Co^{2+} se oxida a Co^{3+}. La gran diferencia potencial máxima de DPP entre Co^{3+} y Zn^{2+} en estas condiciones permite la eliminación completa de la interferencia de Zn^{2+}.

ABSTRACT

Co^{2+} is one of the trace levels impurities of the Zn plant electrolyte including during the Zn electroextraction in the produced metal, thus lowering its purity and also favors the H_2 evaluation on the Zn cathode increasing the energy lost. The high temperature $ZnSO_4$ crystallization on the nebulizer due to the high Zn^{2+} concentration (about 150 g/l) makes impossible Co^{2+} on-line determination by Atomic Absorption Spectrometry (AAS) and Inductively Coupled Plasma (ICP) during the purification process.

A simple and rapid Differential Pulse Polarographic (DPP) method for direct Co^{2+} determination in Zn plant electrolyte suitable for on-line application was developed and tested with real Zn plant solutions. The method is based on the application of 1-Nitrozo-2-Naphtol in ammonia buffer supporting electrolyte where Co^{2+} is oxidized to Co^{3+}. The great DPP peak potential difference between Co^{3+} and Zn^{2+} at these conditions allows the complete elimination of the Zn^{2+} interference.

1. INTRODUCTION

The solution used for Zn electroextraction contains about 150 g/l Zn^{2+} and a great variety of impurities, such as Cd^{2+}, Cu^{2+}, Pb^{2+}, Sb^{3+}, Co^{2+}, Ni^{2+} , Ge^{4+} most of them in ppb levels. The production of a high purity metal and the achievement of a high current efficiency of the electrolysis require their removal in order to prevent the co-deposition together with the Zn^{2+} and H_2 evaluation in parallel during the electrolysis, as well. The control of the purification process requires simple, rapid and reliable methods for impurities determination. The spectral methods (absorption and emission) such as AAS and ICP can be applied only after a preliminary sample pretreatment procedure for analyte separation. The high Zn^{2+}

concentration provoke blocking of the spectrometer nebulizer because of $ZnSO_4$ crystallization due to the high temperature applied during the determination [1], thus making impossible the direct impurities determination. Their separation from the high concentrated matrix applying laboratory chemical methods makes in total the spectroscopic determinations complicated, long and less precise.

On the other hand the high ionic concentrations favor the application of the voltammetric methods [2-4]. The most detailed review of the voltammetric monitoring of the Zn plant electrolyte impurities was presented by Bond [1] together with detailed description of the technological and purification processes. As shown by Bond the high Zn^{2+} concentration does not interferes the Sb^{3+}, Cd^{2+}, Ni^{2+}, Ge^{4+} and Cu^{2+} determination but the direct Co^{2+} and Ni^{2+} voltammetric determinations however are mentioned as impossible because of the complete overlapping of their peak by the huge peak of Zn^{2+}.

Matrix exchange procedure followed by Differential Pulse Adsorptive Stripping Voltammetry (DPAdSV) was reported to yield good results for Co^{2+} determination in Zn plant electrolyte employing various organic compounds [1]. Korolczuk et al. [2] reported the application of nioxime-cetyltrimethylammonium bromide-piperazine-N,N_-bis(2-ethanesulfonic acid) in adsorptive DPAdSV step. This method can be applied for very low Co concentration (10^{-11} – 10^{-9} M/l) determinations in PIPES and HEPES buffer [2], in ammonia buffer, dimethylglyoxime (DMG), and $NaNO_2$. The concentration ratio Co^{2+}/Zn^{2+} reported is $1/10^3$.

Mrzljak et al [5] reported two ADSV methods for Co^{2+} determination in Zn plant electrolyte with detection limits of 9 ppb and 0.25 ppb based on matrix exchange procedures including many steps such as filtration, acidifying with H_2SO_4, cooling, dispensing etc. Other methods for Co^{2+} determination [7] are based on the application of a carbon paste electrode modified by DMG in 4.8 acetate buffer in presence of 100-fold excess of Zn. Pilkington [12] reported the application of DPP and DPASV for Sb^{3+}, Cd^{2+}, Cu^{2+} determination in Zn plant electrolyte, excluding the possibility for determination of Co^{2+} by the direct use of reduction step.

Braynina [6] reported a DPAdSV method based on the application of 1Nitrozo-2 Naphtol modified carbon electrode. The determined Co^{2+} form a low soluble complex with 1Nitrozo-2 Naphtol on the electrode surface during the preconcentration step. The electrochemical reduction occurs at potential values -0,6 - -0,7 V, while the $E_{1/2}$ of Zn^{2+} is more negative than -1V. The small linear concentration range, the small Zn^{2+}/Co^{2+} concentration ratio (about 1000) and the complicated sample pretreatment are the drawbacks of this approach.

Uchida [7] reported a differential pulse-polarographic method for determination of cobalt in the ppb-region after extraction of cobalt(III)-1-nitroso-2-naphthol chelate from citrate buffer solution (pH 5) into benzene. The cobalt(III) chelate is determined in a electrolysis solution composed of a 1:1 mixture of the extract and acetonitrile solution containing 8 mmol/l perchloric acid and 0.2 mol/l sodium perchlorate with a limit of determination is in the range of 1-2 ppb.

The aim of the present work is the development of a direct, simple, rapid and reliable on-line voltammetric method for Co^{2+} determination in Zn plant electrolyte based on the application of 1Nitrozo-2 Naphtol allowing the achievement of practically unlimited Zn^{2+}/Co^{2+} concentration ratio. Unlike the method proposed by Braynina [6] the proposed method subject of the present work is direct, no preliminary accumulation of substance occurs on the electrode surface; moreover a renewable mercury surface electrode is used. No extraction or other complicated laboratory sample pretreatment procedures are applied as it was proposed by Uchida [7]. The cobalt determination is direct and rapid and the great Zn^{2+} concentration does not interfere at all.

2. EXPERIMENTAL

Instrumentation

The laboratory voltammetric determinations were performed by the application of POL 150 Trace Analyzer coupled with a EG&G PAR Model 303A Polarographic Stand connected to a computer running Trace Master 5 software (Tacussel, France). For the on-line determinations a properly modified Model 264A Polarographic Analyzer, coupled with the Model 303A electrode stand connected to a PC running a especially created software were employed. The original reference and auxiliary electrodes mounted on the electrode stands were employed. Especially designed exchangeable solid electrodes described bellow were used in on-line determinations performed in special voltammetric cell.
Automatic pipettes were employed for the sample preparation

Reagents

All the reagents were of analytical grade purchased from Merck and Sigma. The deionized water was produced by MiliQ system produced by Milipore. The ammonia buffer supporting electrolyte was preliminary prepared by adding of 8 volume parts of NH_4OH to 1 volume part of concentrated HCl continuously cooling by running water. The NH_4OH excess allowed the formation of soluble Zn^{2+} ammonia complex after the precipitation due to the high pH value.
The 1-nitrozo-2-naphtol solution was preliminary prepared by dissolution of 50 mg of 1-nitrozo-2-naphtol in 50 ml of ethyl alcohol.

3. RESULTADOS Y DISCUSSIONES

Working electrode

In spite of the excellent characteristics of the mercury as electrode material its application in mercury drop electrodes such as DME, SMDE and HMDE is already limited because of mercury toxicity and its high cost as well. Since the electrochemical reactions occur at the electrode surface, the deposition of a thin mercury layer onto a conducting support material yields “mercury” electrode. The mercury inside the mercury drop plays no positive role, just the opposite: it decreases the surface/volume ratio decreasing thus the sensitivity of the stripping analysis because of the diffusion for example.

For the purpose of the present work thin Ag and Au were tested as support materials. The Hg film was deposited in-situ just prior the determination. Both, Au and Ag amalgam forming metals lowering thus the Hg evaporation during the electrode storage before the recycling were chosen preliminary as Hg supports. Taking in consideration however that even ppb level of H_2S concentrations form sulphide layer on the Ag surface [Gustavo, Lidia] thus making problematic the Hg deposition on it, Ag was abandoned. The Pt was not tested at all because it does not form amalgam but separate Hg drops on its surface not satisfying thus the requirements mentioned above.

In-situ electrolysis performed at -1V (SCE) and stirring conditions just prior the determination was used for the Hg layer formation. The electrode itself plays also the role of the stirrer tip turning with 500 rpm by the aim of a small motor.
The PCB technology was used for electrode preparation on 0.6 mm epoxy support metalized by 38 μm copper, and covert by 1 μm Au without Ni intermediate layer formation between

them. The solid state diffusion is very slow process as well as Cu atoms on the electrode surface will represent negligibly small percentage of the entire surface. On the other hand Cu is able to form amalgam as well and small numbers of the Cu atoms will not interfere the electrode surface characteristics. Some experiments were performed with covered by gold disk electrodes stored two ears. No difference was found compared with less time stored electrodes.

The active working electrode area is a disk with 1 mm diameter placed on the lower part of a 5 x 30 mm stick, connected by an epoxy insulated thin route with the contact placed on the upper part of the stick (Fig. 1). The contact area is used also to stick the electrode to the rotating support. The reproducibility of the golden electrode surface produced applying the PCB technology was within 4.3 %, determined as RSD of electro conductivity determination of 1 mg/l NaCl solution at 25 ^{o}C. After the conductivity measurements every electrode was marked on his back behind the contact by a special optically readable code representing the correction coefficient for precise concentration calculations. The incretion of the stick makes the apparatus to read the code determining thus the correction of the measured current response according to the preliminary built calibration curve with the application of another electrode. The reproducibility of the results determined by multiple measurements of 10^{-6} M/L Co^{2+} applying new single use electrodes for every measurement and the corrections mentioned above was within +/- 3.6 % determined as R.S.D.

Determinations with HMDE application was performed as well for results comparison. The obtained results presented bellow in Table 1 shoed that HMDE can be completely replaced by the amalgamed golden disk stick electrode.

Sample preparing and analytical procedure

5 ml of Zn plant electrolyte, 5 ml of the ammonia buffer (8/1) and 5 ml of deionized water were added into the polarographic cell at ambient temperature, followed by addition of 200 µl of the 1-nitrozo-2-naphtol solution. No precipitation appear because of the high solubility of the Zn(NH4OH) formed chelate. After 2 minutes of purging with nitrogen the DPP curve was registered in the potential range: – 150 mV to -400 mV (SCE). The well defined cobalt peak appears at -260 mV.

Application of 1-Nitrozo-2-Naphtol

The 1-nitrozo-2-naphtol is a very specific reagent for Co^{2+} [XYZ] capable to oxidizing the Co^{2+} to Co^{3+} with a low dissolubility complex formation [7]. This fact is used in the analytical practice for gravimetric determination of high cobalt concentration as well as for Zn plant electrolyte purification in the Zn hydrometallurgy.

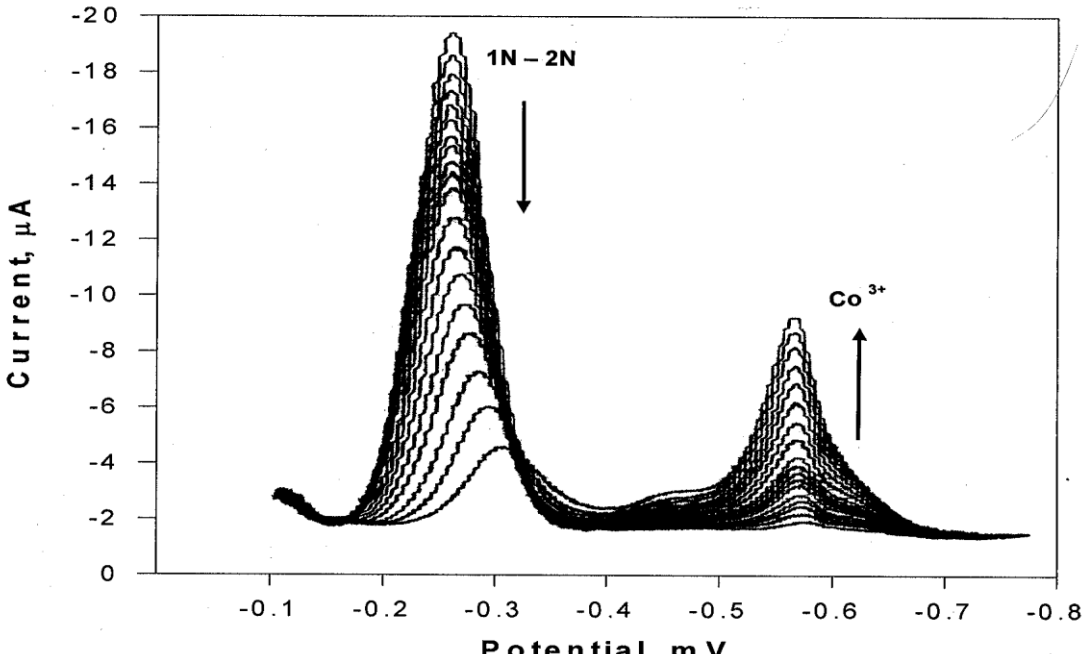

Figure 1. DPP peaks of 1Nitroso-2 Naphtol and Co $^{3+}$

The solubility of the 1-nitrozo-2-naphtolate of Co^{3+} in water is 1.5 mg/l that is why no precipitation occurs for cobalt concentration less than this value, but red-brown coloration of the solution occurs only. This fact represents the base of the voltammetric method subject of the present work.

1-nitrozo – 2-naphtol is soluble in many organic solvents such as acetone, ethyl alcohol benzene etc. as well in acetic acid [7]. It is electrochemically active substance as well, yielding a DPP reduction peak in ammonia buffer (pH = 9.5) at - 280 mV (SCE) as shown on Fig. 1. Although the 1-nitrozo – 2-naphtol peak potential is close to that of Co^{3+} no interference occurs at any concentration values due to the small half-width of the two peaks.

The Co^{3+} / 1-nitrozo – 2-naphtol interaction with chelate formation was proved registering the 1-nitrozo – 2-naphtol peak at presence of Co^{2+} increased concentration obtained by Co^{2+} additions. The successive Co^{2+} additions results in lowering of the 1-nitrozo – 2-naphtol peak and corresponding increasing of the peak situated at - 490 mV (SCE) as shown on Fig. 1. The height of the latter increases with the addition of Co^{3+} as well (produced by Co^{2+} oxidation by H_2O_2), thus proving that it belong to Co^{3+}. This fact shoed, that the Co^{2+} is oxidized by 1-nitrozo – 2-naphtol in ammonia buffer with Co^{3+} formation, yielding a reduction peak at -570 mV. As it can be seen on Fig. 1 the 1-nitrozo – 2-naphtol peak height decreases with Co^{2+} addition due to the consumption of the 1-nitrozo – 2-naphtol because of Co^{3+} chelate formation.

As shown on Figure 2 the peak of the Co $^{3+}$ is much more positive compared with the peak of the Zn $^{2+}$ allowing the determination of trace (ppb level) of Co $^{3+}$ in presence of 150 g/l Zn $^{2+}$

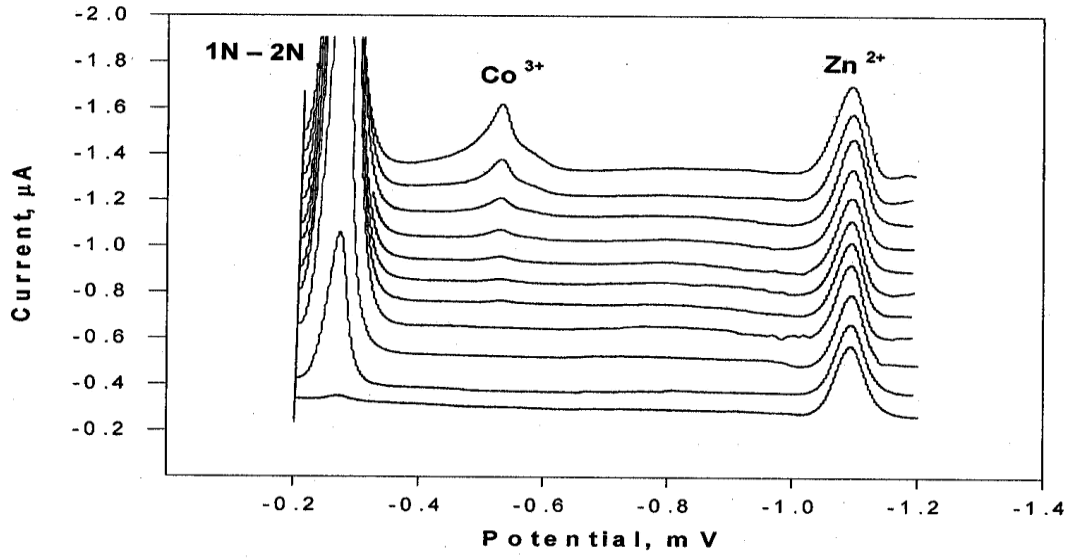

Figure 2. Determination of Co $^{3+}$ 1Nitroso-2Naphtol chelate in presence of Zn $^{2+}$

The Co^{3+} peak height as a function of the Co^{2+} to 1-nitrozo – 2-naphtol concentration ratio was studied as well and a calibration curve: Peak Height – Co $^{2+}$ concentration was build

for an exceeded 1-nitrozo – 2-naphtol concentration using a real Zn plant solution in ammonia buffer with pH = 9.

The limit of detection (LOD) was found to be 8.9 ppb and the linear concentration range: up to 28 mg/l for exceeded 1-nitrozo – 2-naphtol concentration. This analytical characteristics of the method due to the application of the 1-nitrozo – 2-naphtol allowed its on-line application in the industry

4. CONCLUSIONES

A direct DPP method for trace Co^{2+} concentrations determination in Zn plant electrolyte based on the application of water-ethanol solution of 1Nitrozo-2 Naphtol used in ammonia buffer as a supporting electrolyte. The 1Nitrozo-2 Naphtol oxidize the Co^{2+} to Co^{3+} which peak potential is much more positive compared with that of Co^{2+} and Zn^{2+}. The great $E_{1/2}$ difference permits the achievement of practically unlimited concentration ratio in determination of Co^{2+} in presence of Zn^{2+}.

REFERENCIAS

[1] A. Bond, *Anal. Chim. Acta*, 400 (1999) 333-379

[2] M. Korolczuk, A. Moroziewicz, M. Grabarczyk, K. Paluszek, *Talanta*, 65 (2005) 1003–1007

[3] A. Bobrowski, Alan M. Bond, *Electroanalysis*, vol. 4(10) (2004) 975 - 979

[4] R. Mrzljak, A. Bond, T. Cardwell., R. Cattrall, R. Knight, M. Newman, B. Champoin, J. Hey, A. Bobrowski, *Anallytica Chimica Acta,* vol. 281(2) (1993) 281-290

[5] Z-Q. Zhang, H. Liu, H. Zhang, Y-F. Li, *Analytica Chimica Acta* 333 (1996) 119-124

[6] Kh. Brainina. *Frezenius Z. Anal. Chem* 312 (1982) 428-437

[7] T. Uchida, M. Sugawara and T. Kambara, *Fresenius Journal of Analytical Chemistry,* vol. 322(5) (1985) 470-473

Congreso Nacional de Estudiantes de Posgrado del Instituto de Ingeniería, UABC
Mexicali B.C, 25,26 y 27 de Noviembre 2009
Programa de Maestría y doctorado en Ingeniería

Aplicación de 1-Nitrozo-2-Naphtol en Mediciones Voltamétricas de Cobalto en Electrolito para Electrowinning de Zinc

J. A. Valera, R. Zlatev, M. Stoytcheva

Engineering Institute, UABC, Blvd. Benito Juares S/N, 21280 Mexicali, Baja California, Mexico

RESUMEN

Co2+ es una de las impurezas de los niveles de rastro del electrólito de la planta del producción de Zn que incluye durante el electroextraction del Zn en el metal producido, así bajando su pureza y también favorece la evaluación H_2 en el cátodo del Zn que aumenta la energía perdida. La cristalización da alta temperatura $ZnSO_4$ en el nebulizador debido a la alta concentración de Zn^{2+} (cerca de 150 g/l) hace Co^{2+} imposible la determinación en línea por la espectroscopia de absorción atómica (AAS) y el plasma inductivo juntada (ICP) durante el proceso de la purificación.

Un simple y rápido método aplicando la Polarográfia Diferencial del Pulsos (DPP) para la determinación directa de Co^{2+} en el electrólito de la planta del Zn conveniente para el uso en línea fue desarrollado y probado con las soluciones verdaderas de la planta del Zn. El método se basa en el uso de 1-Nitrozo-2-Naphtol en el electrólito favorable del almacenador intermediario del amoníaco donde Co^{2+} se oxida a Co^{3+}. La gran diferencia potencial máxima de DPP entre Co^{3+} y Zn^{2+} en estas condiciones permite la eliminación completa de la interferencia de Zn^{2+}.

ABSTRACT

Co^{2+} is one of the trace levels impurities of the Zn plant electrolyte including during the Zn electroextraction in the produced metal, thus lowering its purity and also favors the H_2 evaluation on the Zn cathode increasing the energy lost. The high temperature $ZnSO_4$ crystallization on the nebulizer due to the high Zn^{2+} concentration (about 150 g/l) makes impossible Co^{2+} on-line determination by Atomic Absorption Spectrometry (AAS) and Inductively Coupled Plasma (ICP) during the purification process.

A simple and rapid Differential Pulse Polarographic (DPP) method for direct Co^{2+} determination in Zn plant electrolyte suitable for on-line application was developed and tested with real Zn plant solutions. The method is based on the application of 1-Nitrozo-2-Naphtol in ammonia buffer supporting electrolyte where Co^{2+} is oxidized to Co^{3+}. The great DPP peak potential difference between Co^{3+} and Zn^{2+} at these conditions allows the complete elimination of the Zn^{2+} interference.

1. INTRODUCTION

The solution used for Zn electroextraction contains about 150 g/l Zn^{2+} and a great variety of impurities, such as Cd^{2+}, Cu^{2+}, Pb^{2+}, Sb^{3+}, Co^{2+}, Ni^{2+} , Ge^{4+} most of them in ppb levels. The production of a high purity metal and the achievement of a high current efficiency of the electrolysis require their removal in order to prevent the co-deposition together with the Zn^{2+} and H_2 evaluation in parallel during the electrolysis, as well. The control of the purification process requires simple, rapid and reliable methods for impurities determination. The spectral methods (absorption and emission) such as AAS and ICP can be applied only after a preliminary sample pretreatment procedure for analyte separation.

The high Zn^{2+} concentration provoke blocking of the spectrometer nebulizer because of $ZnSO_4$ crystallization due to the high temperature applied during the determination [1], thus making impossible the direct impurities determination. Their separation from the high concentrated matrix applying laboratory chemical methods makes in total the spectroscopic determinations complicated, long and less precise.

On the other hand the high ionic concentrations favor the application of the voltammetric methods [2-4]. The most detailed review of the voltammetric monitoring of the Zn plant electrolyte impurities was presented by Bond [1] together with detailed description of the technological and purification processes. As shown by Bond the high Zn^{2+} concentration does not interferes the Sb^{3+}, Cd^{2+}, Ni^{2+}, Ge^{4+} and Cu^{2+} determination but the direct Co^{2+} and Ni^{2+} voltammetric determinations however are mentioned as impossible because of the complete overlapping of their peak by the huge peak of Zn^{2+}.

Matrix exchange procedure followed by Differential Pulse Adsorptive Stripping Voltammetry (DPAdSV) was reported to yield good results for Co^{2+} determination in Zn plant electrolyte employing various organic compounds [1]. Korolczuk et al. [2] reported the application of nioxime-cetyltrimethylammonium bromide-piperazine-N,N_-bis(2-ethanesulfonic acid) in adsorptive DPAdSV step. This method can be applied for very low Co concentration (10^{-11} – 10^{-9} M/l) determinations in PIPES and HEPES buffer [2], in ammonia buffer, dimethylglyoxime (DMG), and $NaNO_2$. The concentration ratio Co^{2+}/Zn^{2+} reported is $1/10^3$.

Mrzljak et al [5] reported two ADSV methods for Co $^{2+}$ determination in Zn plant electrolyte with detection limits of 9 ppb and 0.25 ppb based on matrix exchange procedures including many steps such as filtration, acidifying with H_2SO_4, cooling, dispensing etc. Other methods for Co^{2+} determination [7] are based on the application of a carbon paste electrode modified by DMG in 4.8 acetate buffer in presence of 100-fold excess of Zn. Pilkington [12] reported the application of DPP and DPASV for Sb^{3+}, Cd^{2+}, Cu^{2+} determination in Zn plant electrolyte, excluding the possibility for determination of Co $^{2+}$ by the direct use of reduction step.

Braynina [6] reported a DPAdSV method based on the application of 1Nitrozo-2 Naphtol modified carbon electrode. The determined Co^{2+} form a low soluble complex with 1Nitrozo-2 Naphtol on the electrode surface during the preconcentration step. The electrochemical reduction occurs at potential values -0,6 - -0,7 V, while the $E_{1/2}$ of Zn^{2+} is more negative than -1V. The small linear concentration range, the small Zn^{2+}/Co^{2+} concentration ratio (about 1000) and the complicated sample pretreatment are the drawbacks of this approach.

Uchida [7] reported a differential pulse-polarographic method for determination of cobalt in the ppb-region after extraction of cobalt(III)-1-nitroso-2-naphthol chelate from citrate buffer solution (pH 5) into benzene. The cobalt(III) chelate is determined in a electrolysis solution composed of a 1:1 mixture of the extract and acetonitrile solution containing 8 mmol/l perchloric acid and 0.2 mol/l sodium perchlorate with a limit of determination is in the range of 1-2 ppb.

The aim of the present work is the development of a direct, simple, rapid and reliable on-line voltammetric method for Co^{2+} determination in Zn plant electrolyte based on the application of 1Nitrozo-2 Naphtol allowing the achievement of practically unlimited Zn^{2+} /Co^{2+} concentration ratio. Unlike the method proposed by Braynina [6] the proposed method subject of the present work is direct, no preliminary accumulation of substance occurs on the electrode surface; moreover a renewable mercury surface electrode is used. No extraction or other complicated laboratory sample pretreatment procedures are applied as it was proposed by Uchida [7]. The cobalt determination is direct and rapid and the great Zn^{2+} concentration does not interfere at all.

2. EXPERIMENTAL

Instrumentation

The laboratory voltammetric determinations were performed by the application of POL 150 Trace Analyzer coupled with a EG&G PAR Model 303A Polarographic Stand connected to a computer running Trace Master 5 software (Tacussel, France). For the on-line determinations a properly modified Model 264A Polarographic Analyzer, coupled with the Model 303A electrode stand connected to a PC running a especially created software were employed. The original reference and auxiliary electrodes mounted on the electrode stands were employed. Especially designed exchangeable solid electrodes described bellow were used in on-line determinations performed in special voltammetric cell.
Automatic pipettes were employed for the sample preparation

Reagents

All the reagents were of analytical grade purchased from Merck and Sigma. The deionized water was produced by MiliQ system produced by Milipore. The ammonia buffer supporting electrolyte was preliminary prepared by adding of 8 volume parts of NH_4OH to 1 volume part of concentrated HCl continuously cooling by running water. The NH_4OH excess allowed the formation of soluble Zn^{2+} ammonia complex after the precipitation due to the high pH value.
The 1-nitrozo-2-naphtol solution was preliminary prepared by dissolution of 50 mg of 1-nitrozo-2-naphtol in 50 ml of ethyl alcohol.

3. RESULTADOS Y DISCUSSIONES

Working electrode

In spite of the excellent characteristics of the mercury as electrode material its application in mercury drop electrodes such as DME, SMDE and HMDE is already limited because of mercury toxicity and its high cost as well. Since the electrochemical reactions occur at the electrode surface, the deposition of a thin mercury layer onto a conducting support material yields “mercury” electrode. The mercury inside the mercury drop plays no positive role, just the opposite: it decreases the surface/volume ratio decreasing thus the sensitivity of the stripping analysis because of the diffusion for example.

For the purpose of the present work thin Ag and Au were tested as support materials. The Hg film was deposited in-situ just prior the determination. Both, Au and Ag amalgam forming metals lowering thus the Hg evaporation during the electrode storage before the recycling were chosen preliminary as Hg supports. Taking in consideration however that even ppb level of H_2S concentrations form sulphide layer on the Ag surface [Gustavo, Lidia] thus making problematic the Hg deposition on it, Ag was abandoned. The Pt was not tested at all because it does not form amalgam but separate Hg drops on its surface not satisfying thus the requirements mentioned above.

In-situ electrolysis performed at -1V (SCE) and stirring conditions just prior the determination was used for the Hg layer formation. The electrode itself plays also the role of the stirrer tip turning with 500 rpm by the aim of a small motor. The PCB technology was used for electrode preparation on 0.6 mm epoxy support metalized by 38 μm copper, and covert by 1 μm Au without Ni intermediate layer formation between them.

The solid state diffusion is very slow process as well as Cu atoms on the electrode surface will represent negligibly small percentage of the entire surface. On the other hand Cu is able to form amalgam as well and small numbers of the Cu atoms will not interfere the electrode surface characteristics. Some experiments were performed with covered by gold disk electrodes stored two ears. No difference was found compared with less time stored electrodes.

The active working electrode area is a disk with 1 mm diameter placed on the lower part of a 5 x 30 mm stick, connected by an epoxy insulated thin route with the contact placed on the upper part of the stick (Fig. 1). The contact area is used also to stick the electrode to the rotating support. The reproducibility of the golden electrode s 3 produced applying the PCB technology was within 4.3 %, determined as RSD of electro conductivity determination of 1 mg/l NaCl solution at 25 ^{o}C. After the conductivity measurements every electrode was marked on his back behind the contact by a special optically readable code representing the correction coefficient for precise concentration calculations. The incretion of the stick makes the apparatus to read the code determining thus the correction of the measured current response according to the preliminary built calibration curve with the application of another electrode. The reproducibility of the results determined by multiple measurements of 10^{-6} M/L Co^{2+} applying new single use electrodes for every measurement and the corrections mentioned above was within +/- 3.6 % determined as R.S.D.

Determinations with HMDE application was performed as well for results comparison. The obtained results presented bellow in Table 1 shoed that HMDE can be completely replaced by the amalgamed golden disk stick electrode.

Sample preparing and analytical procedure

5 ml of Zn plant electrolyte, 5 ml of the ammonia buffer (8/1) and 5 ml of deionized water were added into the polarographic cell at ambient temperature, followed by addition of 200 µl of the 1-nitrozo-2-naphtol solution. No precipitation appear because of the high solubility of the Zn(NH4OH) formed chelate. After 2 minutes of purging with nitrogen the DPP curve was registered in the potential range: – 150 mV to -400 mV (SCE). The well defined cobalt peak appears at -260 mV.

Application of 1-Nitrozo-2-Naphtol

The 1-nitrozo-2-naphtol is a very specific reagent for Co^{2+} [XYZ] capable to oxidizing the Co^{2+} to Co^{3+} with a low dissolubility complex formation [7]. This fact is used in the analytical practice for gravimetric determination of high cobalt concentration as well as for Zn plant electrolyte purification in the Zn hydrometallurgy.

The solubility of the 1-nitrozo-2-naphtolate of Co^{3+} in water is 1.5 mg/l that is why no precipitation occurs for cobalt concentration less than this value, but red-brown coloration of the solution occurs only. This fact represents the base of the voltammetric method subject of the present work.

1-nitrozo – 2-naphtol is soluble in many organic solvents such as acetone, ethyl alcohol benzene etc. as well in acetic acid [7]. It is electrochemically active substance as well, yielding a DPP reduction peak in ammonia buffer (pH = 9.5) at - 280 mV (SCE) as shown on Fig. 1. Although the 1-nitrozo – 2-naphtol peak potential is close to that of Co^{3+} no interference occurs at any concentration values due to the small half-width of the two peaks.

The Co^{3+} / 1-nitrozo – 2-naphtol interaction with chelate formation was proved registering the 1-nitrozo – 2-naphtol peak at presence of Co^{2+} increased concentration obtained by Co^{2+}

additions. The successive Co^{2+} additions results in lowering of the 1-nitrozo – 2-naphtol peak and corresponding increasing of the peak situated at - 490 mV (SCE) as shown on Fig. 1. The height of the latter increases with the addition of Co^{3+} as well (produced by Co^{2+} oxidation by H_2O_2), thus proving that it belong to Co^{3+}. This fact shoed, that the Co^{2+} is oxidized by 1-nitrozo – 2-naphtol in ammonia buffer with Co^{3+} formation, yielding a reduction peak at -570 mV. As it can be seen on Fig. 1 the 1-nitrozo – 2-naphtol peak height decreases with Co^{2+} addition due to the consumption of the 1-nitrozo – 2-naphtol because of Co^{3+} chelate formation.

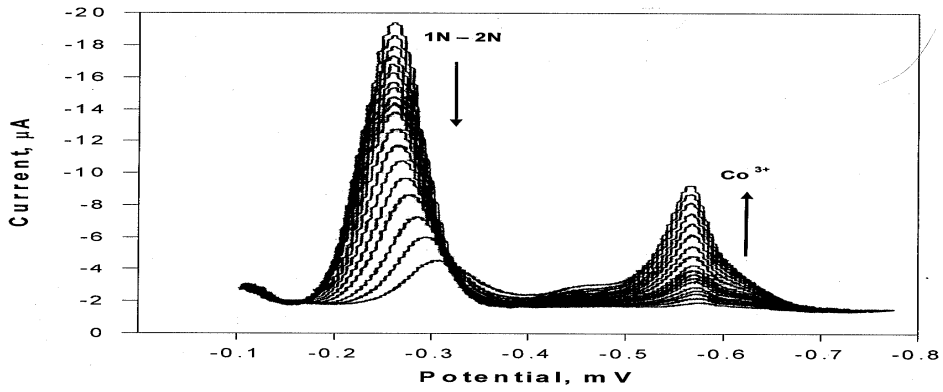

Figure 1. DPP peaks of 1Nitroso-2 Naphtol and Co $^{3+}$

As shown on Figure 2 the peak of the Co $^{3+}$ is much more positive compared with the peak of the Zn $^{2+}$ allowing the determination of trace (ppb level) of Co $^{3+}$ in presence of 150 g/l Zn $^{2+}$

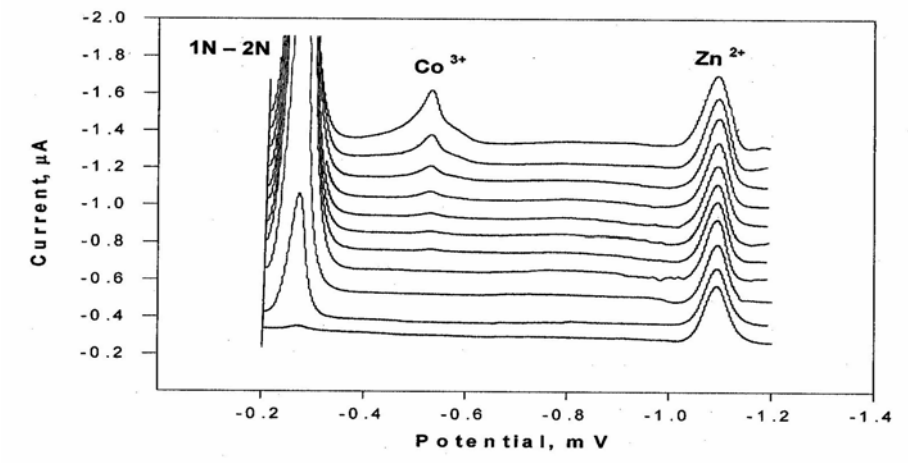

Figure 2. Determination of Co $^{3+}$ 1Nitroso-2Naphtol chelate in presence of Zn $^{2+}$

The Co^{3+} peak height as a function of the Co^{2+} to 1-nitrozo – 2-naphtol concentration ratio was studied as well and a calibration curve: Peak Height – Co^{2+} concentration was build for an exceeded 1-nitrozo – 2-naphtol concentration using a real Zn plant solution in ammonia buffer with pH = 9.

The limit of detection (LOD) was found to be 8.9 ppb and the linear concentration range: up to 28 mg/l for exceeded 1-nitrozo – 2-naphtol concentration. This analytical characteristics of the method due to the application of the 1-nitrozo – 2-naphtol allowed its on-line application in the industry

4. CONCLUSIONES

A direct DPP method for trace Co^{2+} concentrations determination in Zn plant electrolyte based on the application of water-ethanol solution of 1Nitrozo-2 Naphtol used in ammonia buffer as a supporting electrolyte. The 1Nitrozo-2 Naphtol oxidize the Co^{2+} to Co^{3+} which peak potential is much more positive compared with that of Co^{2+} and Zn^{2+}. The great $E_{1/2}$ difference permits the achievement of practically unlimited concentration ratio in determination of Co^{2+} in presence of Zn^{2+}.

REFERENCIAS

[1] A. Bond, *Anal. Chim. Acta*, 400 (1999) 333-379
[2] M. Korolczuk, A. Moroziewicz, M. Grabarczyk, K. Paluszek, *Talanta*, 65 (2005) 1003–1007
[3] A. Bobrowski, Alan M. Bond, *Electroanalysis*, vol. 4(10) (2004) 975 - 979
[4] R. Mrzljak, A. Bond, T. Cardwell., R. Cattrall, R. Knight, M. Newman, B. Champoin, J. Hey, A. Bobrowski, *Anallytica Chimica Acta,* vol. 281(2) (1993) 281-290
[5] Z-Q. Zhang, H. Liu, H. Zhang, Y-F. Li, *Analytica Chimica Acta* 333 (1996) 119-124
[6] Kh. Brainina. *Frezenius Z. Anal. Chem* 312 (1982) 428-437
[7] T. Uchida, M. Sugawara and T. Kambara, *Fresenius Journal of Analytical Chemistry,* vol. 322(5) (1985) 470-473

Universidad Autónoma de Baja California
Instituto de Ingeniería

Otorga la Presente

CONSTANCIA

José A. Valera, Roumen Zlatev, Margarita Stoytcheva

COMO AUTORES DE LA PONENCIA TITULADA

"Aplicación de 1-nitrozo-2-naphtol en mediciones voltamétricas de cobalto en electrolito para electrowining de zinc"

En el Congreso Nacional de Estudiantes de Posgrado del Instituto de Ingeniería, UABC

Mexicali, Baja California, 25 al 27 de Noviembre de 2009

" POR LA REALIZACIÓN PLENA DEL HOMBRE"

DR. BENJAMIN VALDEZ SALAS
DIRECTOR

ANEXO F

Centro de Nanociencias y Nanotecnología
Km. 107 carret. Tijuana-Ensenada, Ensenada, B.C.
Tel. (646) 174-4602, Fax (646) 174-4603

R. Zlatev,
Instituto de Ingenieria
UABC, Mexicali
valenzue@cnyn.unam.mx

Estimado participante:

En nombre del Comité Organizador del XIV Simposio en Ciencia de Materiales, nos es grato informarle que su trabajo titulado:

"APPLICATION OF BORON DOPED DIAMOND (BDD) ELECTRODE FOR AS(III) DETERMINATION IN NATURAL WATERS**"** por R. Zlatev, M. Stoytcheva, J.-P. Magnin, A. Arguelles, J. A. Valera, B. Valdez.

ha sido aceptado para presentación en la Sesión de Carteles No. II del día jueves 12 de febrero de 2009.

Agradecemos su participación.

A t e n t a m e n t e,
"POR MI RAZA HABLARÁ EL ESPÍRITU"
Ensenada, B.C., a 13 de enero de 2009.

Dra. Amelia Olivas Sarabia
simposio@cnyn.unam.mx

XIV Simposio en Ciencia de Materiales
10 al 13 de Febrero de 2009, Ensenada, B.C., México

APPLICATION OF BORON DOPED DIAMOND (BDD) ELECTRODE FOR AS(III) DETERMINATION IN NATURAL WATERS

R. Zlatev*, M. Stoytcheva, J-P. Magnin[1], M. Argüelles, J. A. Valera, B. Valdez

Instituto de Ingeniería, Universidad Autónoma de Baja California,
Blvd. Benito Juarez s/n, 21280 Mexicali, Baja California, México
[1]Laboratoire d'Electrochimie et de Physico-Chimie des Matériaux et Interfaces (LEPMI), UMR 5631, CNRS-UJF-INPG, BP75, 38402 St. Martin d'Hères, France

Abstrac

An important advantage of the *BDD electrodes* [1] is the wide window of potentials allowing species oxidation at high electrode potentials in aqueous electrolytes. BDD electrodes are passive in nature and do not interact or bind to ions nor do they catalyze the oxidation of species. BDD are chemically stable and exhibit extreme electrochemical stability. As(III) is known as a toxic and carcinogenic pollutant of the natural water even in ppb range concentration. The dissolved oxygen easily oxidized the highly toxic As(III) to much less toxic As(V). These facts define the importance of "in-situ" determination of As(III) and its distinction from As(V).

The wide potential window of BDD electrode was employed for direct As(III) determination in natural waters employing 0.1 M HCl as a supporting electrolyte. The Differential Alternative Pulses Voltammetry [2] was applied and voltamograms of the oxidation of As(III) to As(V) were registers. This approach allows prevention of the interferences occurring if electrochemical reduction of As(III) is applied. Reduction of species as Pb^{2+}, Tl^{+}, Bi^{3+} usually presenting together with As(III) and having near $E_{1/2}$ occurs, causing overlapping of the registered peaks. These species however do not participates in electrochemical oxidation and can not interfere the As(III) determination.

The analytical characteristics of the method are presented and discussed.

Agradecimientos.
CONACYT – proyecto 91245, Área II, Apoyo Complementario (SNI1) 2008
UABC – proyecto con código programático 2409 del 13ª Convocatoria de Apoyo a Proyectos de Investigación

Referencias

1. D. Gandini, P.A. Michaud, I. Duo, E. Mahé, W. Hänni, A. Perret, "New Diamond and Frontier Carbon Technology", Ed. MYU, Tokyo, JP, 9/5 (1999) 303
2. R. Zlatev, M. Stoytcheva, B. Valdez, J-P. Magnin, P. Ozil, Electrochemistry Communications, 8 (2006), 1699-1706

* roumen@iing.mxl.uabc.mx

ANEXO G

January 13, 2010

Roumen Zlatev
Universidad Autonoma de Baja California, Mexicali, 21280 Mexico

Dear Roumen Zlatev:

We are pleased to inform you that the following submission has been accepted for presentation at the 217th ECS Meeting in Vancouver, BC, Canada:

Abstract Number/Title:	# 1715: "Simultaneous Species Determination in Industrial Solutions by Differential Alternative Pulse Voltammetry" by J. Valera, R. Zlatev, M. Stoytcheva, B. Valdez and M. Carrillo
Presentation Type:	Poster
Date/Time/Location:	Tuesday, April 27, 2010 at 18:00h in Exhibit and Poster Hall, Conference Floor, Fairmont
Symposium:	I1 - Physical and Analytical Electrochemistry General Session

The entire technical program for the Meeting, including the abstracts, is currently available on the ECS website (http://www.electrochem.org). Please keep the following guidelines in mind as you make your arrangements.

MEETING REGISTRATION: All authors attending the Meeting, including invited speakers, must pay the registration fee in order to present their paper. Online registration is now open. The deadline for advance meeting registration is March 26, 2010. Register online: (http://www.electrochem.org/meetings/biannual/217/217.htm

HOTEL RESERVATIONS: The meeting will be held at both the Fairmont Hotel Vancouver and the Hyatt Regency Vancouver where special rates have been reserved. Please make your reservations by March 26, 2010 using the online reservation system.

We encourage you to make your reservations as soon as possible since we expect the hotels to fill up quickly.

POSTER INFORMATION: Poster presentations must be displayed in English, on a 4' high x 8' wide (1.22m x 2.45m poster board, and correspond to the abstract number and day of presentation as detailed in the final program. Posters may be mounted starting at 13:00h on Monday for the Student Poster Session, which begins at 18:00h (judging begins at 15:00h) and 13:00h on Tuesday for the ECS General Poster Session, which begins at 18:00h. ORAL PRESENTATIONS: Oral presentations must be in English. Only LCD projectors will be provided as standard equipment for all oral presentations. **Authors are required to provide their own laptop computers for LCD presentations.** Speakers requiring special equipment must email their request to meetings@electrochem.org, by April 12, 2010 and appropriate arrangements will be made at the expense of the author. VISA INFORMATION: An original copy of this letter (frequently used by foreign travelers to obtain a visa) will be mailed to all presenting authors with non-Candian or non-U.S. addresses only. To request that a "letter of invitation" on ECS letterhead be faxed or emailed to you, please complete the electronic form located at https://www.electrochem.org/meetings/mtg_app/visa_mtg_form.asp and your letter will be sent to you within two business days. If you are a meeting participant traveling to Canada with financial assistance from your own organization, this should also be stated in the letter of invitation you will be using to obtain a visa. To facilitate this disclosure in a custom letter, please note this to ECS in the Special Instructions section of the online letter request form when asking for a "letter of invitation" from ECS.

If you require a visa to enter Canada, we strongly encourage you to start the visa application process immediately.

Your paper represents an important contribution to the success of the 217th ECS Meeting and we appreciate your participation.

Sincerely,

Paul J. Urso, Jr.

Associate Director of Technical Programming

abstracts@electrochem.org

Physical and Analytical Electrochemistry **217th ECS Meeting**, 2010

Simultaneous Species Determination in IndustrialSolutions by Differential Alternative Pulse Voltammetry (DAPV)

Jose Adolfo Valera, Roumen Zlatev*, Margarita Stoytcheva, Benjamin Valdez, Monica Carrillo
Engineering Institute of UABC, Blvd. Benito Juárez s/n,
21280 Mexicali, B.C., México
*e-mail: roumen@iing.mxl.uabc.mx

The direct voltammetric determinations of species inmulticomponent industrial solutions are complicated because of the peaks overlapping due to small E1/2 difference or high concentration ratio. The galvanic industry electrolytes for example contain a great concentration of the main component and trace but variable concentrations of the impurities, which must be controlled on-line. At these conditions the application of spectral methods such as AAS [1] or ICP [2] is impossible because of high temperature crystallization occurring on the nebulizers. The high ionic strength of the industrial electrolytes however favors the application of the voltammetric methods. The second order ones such as RFP [3], DFRP [4] and Second Harmonic AC Voltammetry [5] yields peaks situated on both side of the zero line. Distinct peaks appear on the second order voltammetric technique curves (Fig. 1 right) even in case of complete peaks overlapping on the first order voltammetric techniques curves (Fig. 1 left) In spite of their obvious advantages, the second order techniques however did not find a wide application because of the complicated equipment needed or low sensitivity of some of them or problems caused by the high frequency applied.

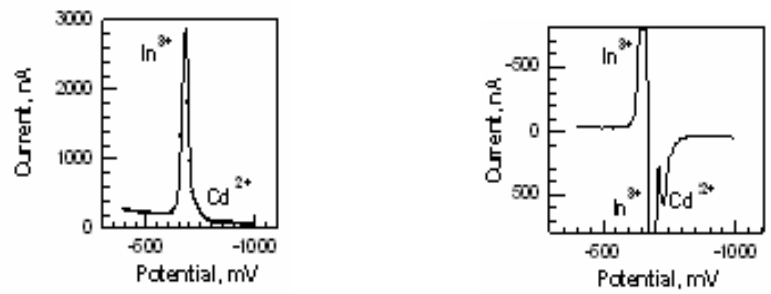

Fig. 1. DPP (left) and DAPV (right) voltammograms of In3+ and Cd2+ (_E1/2 = 38 mV) at concentration ratio 52:1

The Differential Alternative Pulse Volatammetry (DAPV) introduced by the authors recently [6] employing couples of rectangular alternative polarity pulses combined with an appropriate signal processing provides higher resolution compared not only with the conventional first order techniques such as DPP (Fig. 1 right) but even compared with some of the other second order techniques, providing the same sensitivity as DPP. The applications of DAPV for multicomponent industrial electrolytes analysis without preliminary sample pretreatment allowing on-line applications are the subject of the present work. Results obtained with couples of species with small E1/2 difference such as In(III)/Cd(II) and Pb(II)/Tl(I) Co(II)/Ni(II)/Zn(II) at a wide range of concentration ratios are presented.

REFERENCES

1. Pei Liang and Rui Liu, *Anal. Chim. Acta,* 602 (2007) 32
2. K. Jitmanee, O. Mitsuko and M. Shoji, *Talanta, 66,(2005) 529*
3. Barker G., *Proc. Anal. Div. Chem. Soc.* 12 (1975) 179
4. Saur D., *Frezenius Z. Anal.Chem.* 298 (1979) 128
5. Blutstein H., *Bond A.: Anal. Chem.* 46 (1974) 1531
6. Zlatev et al, *J.Electrochem. Comm.* 8 (2006) 1699

ANEXO H

CHARLES UNIVERSITY IN PRAGUE
Faculty of Science
Department of Analytical Chemistry
Organizing Committee of the Modern Electroanalytical Methods 2009 Conference
Albertov 6, 128 43 Prague 2, Czech Republic

ATTESTATION

Prague, 6th December 2009

I, the undersigned, Dr. Karel Nesmerak, the head of the organization committee of the international conference Modern Electroanalytical Methods 2009, certify that abstracts entitled:

1. *"On line differential pulse polarographic determination of cobalt(II) at ppb concentrations in Zn plant electrolyte",*
   by R. Zlatev, M. Stoytcheva, B. Valdez and J. A. Valera

2. *"In situ As(III) determination in the presence of Pb(II) by differential alternative pulses voltammetry",*
   by R. Zlatev, M. Stoytcheva, B. Valdez and J. A. Valera

presented by **Mr Jose Adolfo Valera** (Autonomus University of Baja California, Mexico) have been accepted for poster presentation during above-mentioned conference in Prague, Czech Republic, on 9–13 December 2009.

Karel Nesmerak, PhD.
Chairman of the Organizing committee
e-mail: nesmerak@natur.cuni.cz
http://www.natur.cuni.cz/heyrovsky/

ON-LINE DIFFERENTIAL PULSE POLAROGRAPHIC DETERMINATION OF COBALT(II) AT PPB CONCENTRATIONS IN ZN PLANT ELECTROLYTE

ROUMEN ZLATEV*, MARGARITA STOYTCHEVA, BENJAMIN VALDEZ and JOSE ADOLFO VALERA

Engineering Institute of UABC Blvd. Benito Juárez s/n, 21280 Mexicali, B.C. México
e-mail: roumen@iing.mxl.uabc.mx

The on-line determination of the impurities in the industrial $ZnSO_4$ solution used for metal Zn electroextraction is of a great importance for the Zn electrolyte purification which prevents both, the metal Zn purity and the current efficiency degradation. The purification process control requires simple, rapid and reliable methods for trace (ppb) concentrations of: Cd^{2+}, Cu^{2+}, Pb^{2+}, Sb^{3+}, Co^{2+}, Ni^{2+} , Ge^{4+} determination in presence of about 150 g/l $ZnSO_4$. The high Zn^{2+} concentration makes the application of the AAS and ICP long and less precise, requiring preliminary laboratory analyte separation.

The high ionic concentrations of the Zn plant electrolyte however favors the application of the voltammetric methods for the determination of almost all the impurities except Co^{2+} and Ni^{2+} defined by Bond as impossible[4] because of the complete peak overlapping with the huge peak of Zn^{2+}.

A simple and rapid Differential Pulse Polarographic (DPP) method for direct on-line Co^{2+} determination in Zn plant electrolyte with DME was developed and tested with real industrial solutions. The method is based on the Co^{2+} to Co^{3+} oxidation by 1-Nitrozo-2-Naphtol (1N-2N) in pH 9 ammonia buffer used as supporting electrolyte where directly on-line is added the sample. The DPP Co^{3+} peak appear at -550 mV (SCE) and the great E½ potential difference completely eliminates the Zn^{2+} interference as shown in Figure 1.

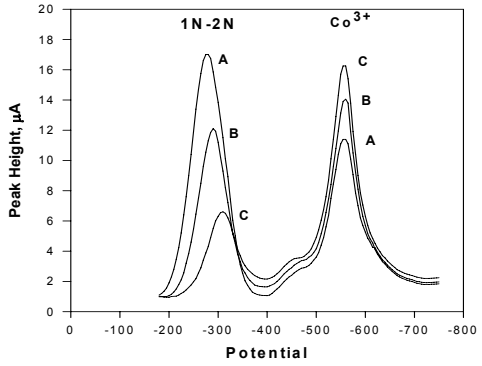

Figure 1. DPP curves of 4 (curve A), 5 (curve B) and 6 (curve C) ppb Co^{2+} in presence of 1N-2N (ammonia buffer, pH 9)

Unlike the stripping method of Braynina[2] based on electrochemical deposition of 1-Nitrozo-2-Naphtol chelate layer of Co^{3+} on a graphite electrode followed by DC anodic dissolution, the proposed DPP determination is direct and rapid. The high precision of the results (4.2% rel. at 20 ppb) and the wide linear concentration range covering entire range of Co^{2+} concentrations in Zn plant electrolyte (from 1 to about 500 ppb) make it suitable for on-line application.

REFERENCES

1. Bond A.: Anal. Chim. Acta 400, 333 (1999)
2. Brainina K.: Fresenius' J. Anal. Chem. 312, 428 (1982).

IN-SITU AS(III) DETERMINATION IN THE PRESENCE OF PB(II) BY DIFFERENTIAL ALTERNATIVE PULSES VOLTAMMETRY

ROUMEN ZLATEV*, MARGARITA STOYTCHEVA, BENJAMIN VALDEZ and JOSE ADOLFO VALERA

Engineering Institute of UABCBlvd. Benito Juárez s/n, 21280 Mexicali, B.C. México
e-mail: roumen@iing.mxl.uabc.mx

The Differential Alternative Pulses Voltammetry (DAPV) introduced by the author earlier[1] combines the high sensitivity of the Differential Pulse Polarography (DPP) and the high resolution power of the second order polarographic techniques. The small peaks half-width and the shape of the DAPV curve, as second derivative of the polarographic wave allow direct simultaneous determination of species having very small E½ difference as well as at high concentration ratios using the peaks situated at both side of the zero line (Figure 1)

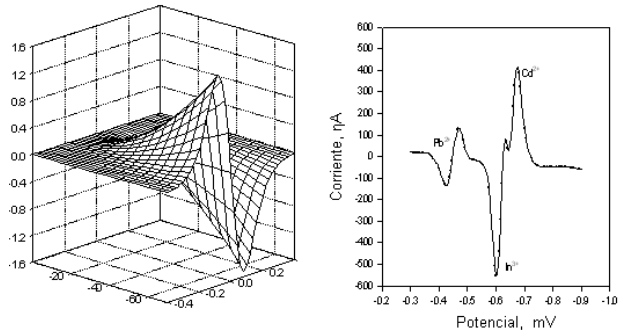

Figure 1. Theoretical DAPV curves (left); Pb(II) and As(III) at 0.5:1 ratio DPP and DAPV polarograms in HCl (right)

DAPV was applied for direct determination of As(III) in ground water containing also Pb(II) using HCl as supporting electrolyte where the As(III)/Pb(II) E½ difference is about 40 mV. No chemical pretreatment procedure was applied for analyte separation. Complete peak overlapping occurs at 0.5:1 Pb(II) to As(III) concentration ratio applying DPP, while the DAPV application yields distinct peaks registration up to ratio as high as 12:1. The DAPV allows reliable, rapid, simple and precise *in-situ* As(III) determination preventing thus its oxidation to electrochemically inactive As(V) by the oxygen during the sample transportation to the analytical laboratory.

This work was supported by research grants: # 91241 (SNI 1), 2008 from CONACYT, Mexico and # 2409 (13 Convocatoria de Proyectos de Investigacion) from UABC, Mexicali, Mexico.

REFERENCES

1. Zlatev R., Stoytcheva M, Valdez B., Magnin J-P., Ozil P.: Electrochem. Comm, 8, 1699,(2006)

ANEXO I

January 27, 2009

Roumen zlatev
Engineering Institute Mexicali, 21280 Mexico.

Dear Roumen zlatev:

We are pleased to inform you that the following submission has been accepted for presentation at the 215th ECS Meeting:

Abstract Number/Title:	# 1362: "Application of TiO2 Modified Boron Doped Diamond (BDD) Electrode for As(III) Determination in Natural Waters" by R. zlatev, M. Stoytcheva, M. Jean_Pierre, B. Valdez, M. Argüelles and **J. Valera**
Presentation Type:	Poster
Date/Time/Location:	Tuesday, May 26, 2009 at 18:00h in Grand Ballroom, Building 2
Symposium:	I1 - Physical and Analytical Electrochemistry General Session

The entire technical program for the Meeting, including the abstracts, registration form and hotel reservation information will be available on the ECS website (http://www.electrochem.org). Please keep the following guidelines in mind as you make your arrangements.

MEETING REGISTRATION: All authors attending the Meeting, *including invited speakers*, must pay the registration fee in order to present their paper. Online registration will be available in mid February on the ECS website. The deadline for advance registration is April 24, 2009.

HOTEL RESERVATIONS: The Meeting will be held at the Hilton San Francisco (333 O'Farrell Street, San Francisco, CA 94102) from May 24 - May 29, 2009. Please make your reservations by April 24, 2009 using the online reservations system: http://www.hilton.com/en/hi/groups/personalized/SFOFHHH-ECS-20090524/index.jhtml.

We encourage you to make your reservations as soon as possible since we expect the hotel to fill up quickly.

POSTER PRESENTATIONS: Poster presentations must be displayed in English, on a 4' high x 8' wide (1.22m x 2.45m) poster board, and correspond to the abstract number and

day of presentation as detailed in the final program. Posters may be mounted starting at 13:00h on Monday for the Student Poster Session, which begins at 18:00h (judging begins at 15:00h) and 13:00h on Tuesday for the General Poster Session, which begins at 18:00h.

ORAL PRESENTATIONS: Oral presentations must be in English. Only LCD projectors will be provided as standard equipment for all oral presentations. Authors are required to provide their own laptop computers for LCD presentations. Speakers requiring special equipment must email their request to meetings@electrochem.org, by May 8, 2009 and appropriate arrangements will be made at the expense of the author.

OBTAINING A VISA: An original copy of this letter, that is frequently used by foreign travelers to obtain a U.S. visa, will be mailed to all presenting authors with non-U.S. addresses only. If you would like to receive a copy of this letter in PDF format so that you may begin the visa application process as early as possible,please fill out the electronic form here https://www.electrochem.org/meetings/mtg_app/visa_mtg_form.asp and one will be emailed to you within 2 business days. **If you require a visa to enter the United States, we strongly encourage you to start the visa application process immediately**. If you have any questions, please contact Paul Urso, Meetings and Program Coordinator, at paul.urso@electrochem.org or 1-609-737-1902 (extension 107), for assistance.

Your paper represents an important contribution to the success of the 215th ECS Meeting and we appreciate your participation.

Sincerely,

Stephanie Plassa,

Director of Meetings and Exhibits

abstracts@electrochem.org

Application of TiO2 Modified Boron Doped Diamond (BDD) Electrode for As(III) Determination in Natural Waters

R. Zlatev a, M. Stoytcheva a, J-P Magnin b, B. Valdez a, M. Argüelles a, J. A. Valera a
a Engineering Institute of UABC, 21280 Blvd. Benito Juárez, Mexicali s/n, BC, México
b LEPMI, ENSEEG, 1130 Rue de la Piscine, Grenoble, France

One of the major advantages of BDD electrodes is their wide window of potentials allowing species oxidation in aqueous electrolytes at high anodic electrode potentials. BDD electrodes exhibit also high chemical and extremely high electrochemical stability. They are passive in nature and do not interact or bind to organic pollutants nor do they catalyze the oxidation of pollutants presenting in the determined water samples [1].

As(III) is known as a highly toxic and carcinogenic pollutant of the natural water even in ppb range of concentration. The oxidation of the As(III) turning it to less toxic As(V) by the oxygen dissolved in the water samples prior its laboratory determination yields analytical results not adequate to the real water toxicity. This fact defines the need of "in-situ" determination of the highly toxic As(III) and its distinction from As(V).

The "in-situ" application of the spectral methods such as AAS and ICP is impossible because of the complicity of the employed equipment. On the other hand the AAS sensitivity to arsenic determination is not satisfying and the two oxidation arsenic forms can not be distinguished as well. Since, however only As(III) is electrochemically active the application of some of the voltammetric methods could solve the problem.
A great variety of methods were developed for voltammetric As(III) determination most of them in acid media employing: direct cathodic reduction to As(0) [2]; direct oxidation to As(V); reduction-oxidation [3] or reduction only after adsorptive accumulation realized as anodic or cathodic stripping voltammetry respectively allowing the achievement of very low LOD in the ppt range [3].

A great variety of modified electrodes were reported as well applied for As(III) determination. In the present work the Anodic Stripping Differential Alternative Pulses Voltammetry [4, 5] reported by the authors earlier providing high resolution was applied as an analytical method preventing the influence of interfering species having E1/2 closed to that of As(III).

The oxidation of the deposited arsenic on the electrode surface requires application of an electrode material providing excellent electrochemical resistance and wide anodic potential window. The mercury and silver are not suitable because the arsenic oxidation peak appears on the shoulder of their anodic oxidation and on the other hand the mercury is toxic. Au exhibit better characteristics than Pt in respect to the hydrogen overpotential but some pretreatment procedure must be applied to keep the electrode surface free of oxide films greatly altering the kinetics of the electrode reaction [6].

The BDD electrode characteristics however satisfies all the requirements for its application in As(III) determination. BDD electrode modified by gold was already successfully applied for anodic stripping determination of arsenic [7]. In order to prevent the oxide films formation on the gold surface requiring complicated cleaning procedures application, the application of TiO2 modified BDD for As(III) determination was investigated.

BDD electrode modified by TiO2 usually employed as photocatalyst [8] provides an additional advantage due to the adsorption properties of TiO2 toward the As(III) allowing the sensitivity of the determination increasing. The results obtained with the application of modified and non modified BDD electrode at different experimental conditions for "in-situ" As(III) determination in arsenic contaminated natural waters are presented and discussed.

References

1. D. Gandini, P.A. Michaud, I. Duo, E. Mahé, W. Hänni,A. Perret, New Diamond and Frontier carbon Technology, Ed. MYU, Tokyo, JP, 9/5 (1999) 303.
2. D. Myers, J. Osterioung, Anal. Chem. 45 No 2 (1973) 267.
3. G. Forsberg, J. O'Laughl, R. Megargle, S. Koirtyohann, Anal. Chem, 47, No 9, (1975) 1586.
4. R Zlatev, M Stoytcheva, B Valdez, J-P Magnin, P.Ozil, Electrochemistry Communications, 8(2006), 1699
5. R. Zlatev, M. Stoytcheva, B. Valdez, J-P Magnin, Z. Velkova, ECS Transactions, 13 (15) (2008) 57-63
6. D. G. Davis, Talanta, 3 (1960) 335-345.
7. D. Yamada, T. Ivandini, M. Komatsu, A. Fujishima, Y. Einada, J. Electroanal. Chem. 615 (2008) 145
8.R. Hoffman, S. Martin, W. Choi, D. Bahnemann, Chem. Rev., 95 (1995) 69

R. Zlatev *
M. Stoytcheva
J-P Magnin
B. Valdez
M. Argüelles
J. A. Valera

roumen@iing.mxl.uabc.mx

UNIVERSIDAD AUTONOMA DE BAJA CALIFORNIA
Instituto de Ingeniería

Blvd. Benito Juárez y Calle a la Normal s/n,
Col. Insurgentes Este, 21280. Mexicali, Mexico

Application of TiO_2 Modified Boron Doped Diamond (BDD) Electrode for As(III) Determination in Natural Waters

1. INTRODUCTION and OBJECTIVE

As(III) is chemically active, toxic and carcinogenic elements, important environmental pollutants requiring concentration control. The EPA standards allow less than 10 µg/l As(III) in drinking waters. The two species As(III) and As(V) have different toxicity [As(III) >> As(V)], biological activity and physiological action, which determine the need of distinguishing of the two species.

The spectral methods recently used for As(III) determination determine the "total" arsenic only, no As(III) / As(V) distinction available as well as Preliminary sample pretreatment must be applied for As(III) separation from the high salt containing matrixes. The Differential Pulse Anodic Stripping Voltammetry (DPASV) and Differential Pulse Voltammetry (DPP) however allow the direct As(III) determination in high salt containing matrixes and its distinction from non electrochemically active As(V) [*Myers et al*].

Gold is widely used as a solid working electrode for this purpose because of its higher hydrogen overpotential than platinum lowering the hydrogen simultaneous evolution during the arsenic deposition and the higher and sharper oxidation peaks than platinum as well [*Forsberg et al*]. The response of both, gold and platinum electrodes however is very strongly depended upon the past history, of the surface pretreatment and the oxide film formation greatly altered the electrode reaction kinetics. Reproducible results can be obtained only after carefully controlled electrode pretreatment or the application of disposable electrodes [*Laschi et al*].

These problems has been overcame by the application of Boron Doped Diamond Electrode (BDDE) modified with TiO_2 known with its photoelectrochemical properties but also with its sorption affinity toward the arsenic, allowing thus the increase of the sensitivity of the determinations

2. RESULTS AND DISCUSSION

Highly boron–doped polycrystalline diamond film drown on Si(100) wafer by microwave plasma-assisted chemical vapor deposition was used. The Ti(IV) oxide was deposited electrochemically at constant potential from 50 mM/L aqueous solution of $TiCl_3$, at pH = 2 according to the method of Kavan [*Kavan et al*]. The percentage of the surface coverage by TiO_2 depends on the deposition time, reaching values up to about 79% determined by the cathodic peak height current ratio. The cyclic voltammograms showed typical behavior of n-type semiconductor.

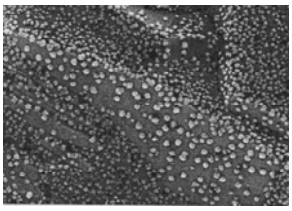

10 X 6 µm SEM picture of TiO2 modified BDD

The stripping parameters were optimized: for E_{dep} = - 0.4 V the peak height has a maximal value, the deposition time was in the range 1 – 10 minutes, the supporting electrolyte was phosphate buffer with pH 5.
When E_{dep} is applied the As(III) is reduced to As(0). During the dissolution step As(0) is oxidized back to As(III) at potential value near 0 V (Ag/AgCl).
The presence of TiO2 increase the local surface concentration of the As(III) at the electrode surface, increasing thus the sensitivity of the determinations

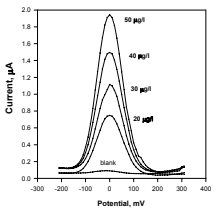

DP Stripping Voltammograms of As(III) in 0.1 phosphate buffer, pH5
E_{dep} = - 0.4V (Ag/AgCl)/ 5 min. TiO_2 modifier BDD electrode

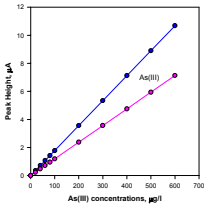

Standard curves of As(III) obtained with modified BDD electrode (blue) and no modified electrode (red)

3. CONCLUSIONS

1. The Highly Boron Doped Diamond Electrode (BDD) modified electrochemically by $Ti0_2$ applied for As(III) determination, overcomes the "memory" effect appearing with gold and platinum application as working electrodes.
2.The sensitivity of the As(III) determinations obtained with the modified electrode application was found to be 57% higher compared with the no modified BDD electrode

4. REFERENCES

***S. Laschi** et al. , Analytical Letters, 2007, 40, (16) 3002-3013*
***G. Forsberg** et al, Anal. Chem, 1975, 47 (9) 1586-1592*
***Myers** et al., Anal. Chem, 45 (2), 1973, 267-271*
***Kavan** et al, J. Electroanal. Chem, (1993) 346, 291-299*

ANEXO J

Submission Confirmation

Thank you for submitting your manuscript to *Analytical Letters*.

Manuscript ID:	LANL-2008-7194
Title:	Direct As(III) Determination in Presence of Pb(II) by Differential Alternative Pulses Voltammetry
Authors:	Zlatev, Roumen Stoytcheva, Margarita Valdez, Benjamin Valera, Jose-Adolfo Argüelles, Mafalda
Date Submitted:	10-Nov-2008

Journal Details

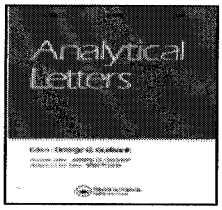

Analytical Letters

Published By: Taylor & Francis
Volume Number: 42
Frequency: 18 issues per year
Print ISSN: 0003-2719
Online ISSN: 1532-236X

Aims & Scope

2007 Impact Factor: 1.362
Ranking: 45/70 (Chemistry, Analytical)

Analytical Letters Taylor & Francis 2008

Direct As(III) Determination in Prescense of Pb(II) by Differential Alternative Pulses Voltammetry

R. Zlatev, M. Stoytcheva, B. Valdez, J. A. Valera, M. Argüelles Mier

Instituto de Ingeniería, Universidad Autónoma de Baja California,
Blvd. Benito Juárez y calle de la Normal s/n, 21280 Mexicali, México

Abstract

The Differential Alternative Pulses Voltammetry (DAPV) introduced by the authors earlier combines the high sensitivity of the Differential Pulse Voltammetry with the high resolution of the second order voltammetric techniques, allowing the direct simultaneous determination of trace levels of species in presence of higher concentrations of interfering ions without preliminary separation. DAPV was applied for determination of species having small $E_{1/2}$ difference, such as As(III) and Pb(II) in natural and industrial waste waters and the results are reported and discussed. In spite of the small $E_{1/2}$ difference of As(III) and Pb(II) (about 50 mV) a concentration ratio as high as 1:14 was achieved, while the DPV peaks are completely overlapped at the same conditions.

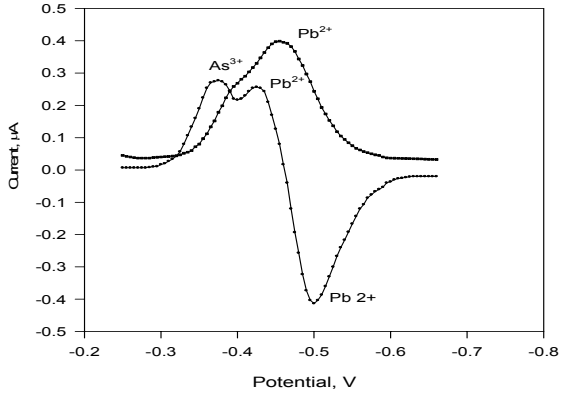

References

1. Barker, G., 1958. *Anal. Chim. Acta*, 18, 118
2. Barker, G., Gardner, A., Williams, 1973. M., *Electroanal. Chem*., 42, 21.
3. Barker G., Gardner A., Williams M., *J. Electroanal. Chem*. 42 (1973) App. 21.
4. Saur, D., 1979. Fresenius Z. *Anal. Chem*., 298, 128
5. Zlatev, R.et al. *Electrochemistry Communications*, 8 (2006), 1699-1706,
6. Zlatev, R., 1990, 41-st ISE Meeting, Prague, Czechoslovakia, p. TU-172
7. Moore, J., Ramamoorthy, S., 1984. *Heavy Metals in Natural Waters, Springer-Verlag*, N.Y.
8. Roy R., Anupama Saha A., *Current Science*, vol. 82, 1, 10, January 2002
9. R. E. Clement, P. W. Yang, C. J. Koester, *Analytical Chemistry*, 73:12 (2001) 2761.
10. Stoytcheva, M., Sharkova, V., Panayotova, M., 1998. *Anal. Chim. Acta, 364*, 195-201.
11. Reed, M., Stolzberg, R., 1987. *Anal. Chem., 59, 3,* 393.
12. Tam, K., 1974. *Environmental Sci. Technol., 8*, 734.

ANEXO K

Meet. Abstr. - Electrochem. Soc. / MA2008-02 / I1 - Physical, Analytical, and Spectro-Electrochemistry General Session

High Resolution Voltammetric Techniques: Application for Direct Simultaneous Species Determination

Abstract 2781

214th ECS Meeting

MA2008-02, October 12 - October 17, 2008 , Honolulu, HI

I1 - Physical, Analytical, and Spectro-Electrochemistry General Session

Organizer(s): P. Trulove, K. Shimazu, S. Sun, E. Wang

ABSTRACT

Roumen Zlatev, Margarita S. Stoytcheva, Benjamin Valdez, Jose Adolfo Valera, and Marcela M. Ovalle

Universidad Autonoma de Baja California

PUBLICATION INFORMATION

ISSN:

1091-8213 (print) 2151-2043 (online)

Publisher:

ECS

High Resolution Voltammetric Techniques: Application for Direct Simultaneous Species Determination – case of As (III) and Pb (II)

R. Zlatev, M.Stoytcheva, B.Valdez, J.A.Valera, M. Ovalle
Engineering Institute, UABC, Blvd. Benito Juárez s/n, 21280 Mexicali BC, México

A voltammetric method for direct As(III) and Pb(II) simultaneous determination was developed based on the Differential Alternative Pulses Voltammetry (DAPV) introduced by the authors recently (1). It combines the high sensitivity of the differential pulse voltammetry with the great resolution of the second order voltammetric methods allowing the direct simultaneous determination of low concentrations of arsenic without sample pretreatment, as well as the distinction of As(III) and As(V) in presence of excess of Pb(II). The method was applied for As(III) and Pb(II) simultaneous determination in industrial waste waters and the results are reported.

The peak overlapping occurring at high concentration ratios, also at small $E_{1/2}$ difference makes the simultaneous voltammetric species determination complicated even if the Differential Pulse Voltammetry (DPV) is applied (2). The second order voltammetric techniques such as: Radio Frequency Polarography (RFP), developed by Barker (3) Differential Faradaic Rectification Polarography (DFRP), developed by Saur (4), Second Harmonic AC Polarography (SHACP) provide high resolution due to the shape of the registered curves and the small half-width of the peaks. In case of overlapping, the peaks situated on both sides of the zero line are emplyed for concentration evaluation. In spite of their advantages in terms of resolution these voltammetric techniques are not widely applied. Some of them need complicated equipment which does not exist commercially; others provide low sensitivity of the determinations.

The $E_{1/2}$ differences of some ion couples such as Pb(II) and Tl(I), As(III) and Pb(II), In(III) and Cd(II), Co(II) and Ni(II), etc. are too small in all the supporting electrolytes and on many of the working electrode materials, causing peak overlapping. Some preliminary sample pretreatment procedure like analyte extraction for example must be applied for their simultaneous determination, thus making the analyses complicated, time consuming, less precise and impossible for automation. The simpler way is the application of some high resolution voltammetric technique.

The Differential Alternative Pulses Voltammetry (DAPV) introduced recently by the authors (1), is a simple second order voltammetric technique providing the same sensitivity as Differential Pulse Voltammetry does (4), and superior resolution power compared even with the other second order techniques (1). The aim of this work is the application of the DAPV for As(III) and Pb(II) simultaneous determination in real water samples without any sample pretreatment and the comparison of the results with those obtained by DPV and some spectral methods.

References

1. Zlatev, R.et al. *Electrochemistry Communications*, 8 (2006), 1699-1706,
2. Barker, G., 1958. *Anal. Chim. Acta*, 18, 118
3. Barker, G., Gardner, A., Williams, 1973. M., *Electroanal. Chem*., 42, 21.
4. Saur, D., 1979. Fresenius Z. *Anal. Chem*., 298, 128
5. Moore, J., Ramamoorthy, S., 1984. *Heavy Metals in Natural Waters, Springer-Verlag*, N.Y.
7. Reed, M., Stolzberg, R., 1987. *Anal. Chem., 59, 3,* 393.
6. Stoytcheva, M., Sharkova, V., Panayotova, M., 1998. *Anal. Chim. Acta, 364*, 195-201.

ANEXO L

----- Original Message -----

From: <nesmerak@natur.cuni.cz>

To: <margarita@iing.mxl.uabc.mx>

Sent: Thursday, March 20, 2008 1:19 PM

Subject: ESEAC

>

>

> Dear colleague,

>

> I have the pleasure to inform you that your poster presentation entitled:

>

> HIGH RESOLUTION VOLTAMMETRIC TECHNIQUES: APPLICATION FOR DIRECT

> SIMULTANEOUS SPECIES DETERMINATION

>

> was accepted for ESEAC 2008 in Prague.

>

> Please, keep in mind that no abstracts will be printed in the

> conference proceedings unless the registration fee is paid before May

> 10, 2008.

>

> On behalf of organizing committee,

>

> Karel Nesmerak

> Department of Analytical Chemistry

> Charles University, Faculty of Science

>

>

HIGH RESOLUTION VOLTAMMETRIC TECHNIQUES: APPLICATION FOR DIRECT SIMULTANEOUS SPECIES DETERMINATION

***Abstract of 12th International Conference on Electroanalysis, ESEAC* June 16-19, 2008**

ROUMEN ZLATEV*, MARGARITA STOYTCHEVA, BENJAMIN VALDEZ, JOSE ADOLFO VALERA and JEAN-PIERRE MAGNIN
Engineering Institute, UABC, Blvd. Benito Juárez s/n, 21280 Mexicali BC, México
roumen_zlatev@yahoo.com

The peak overlapping due to the small $E_{1/2}$ difference or high concentration ratio or both makes the direct multicomponent trace level voltammetric determinations complicated without preliminary analyte extraction. Employing of some of the second order voltammetric techniques such as RFP[1], DFRP[2], Second Harmonic AC[3] yields distinguished peaks placed on the both side of the zero line even if complete peaks overlapping occurs on the first order voltammetric techniques curves. In spite of their obvious advantages the second order techniques however did not find a wide application because of the complicated equipment needed and problems caused by the high frequency used.

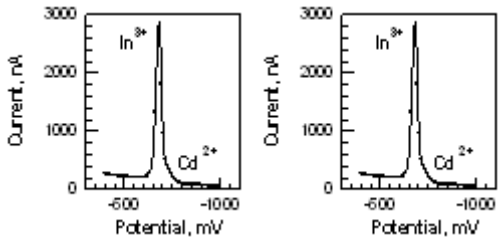

Fig. 1. DPP (left) and DAPV (right) voltammograms of In^{3+} and Cd^{2+} at concentration ratio 40:1 ($\Delta E_{1/2}$ = 38 mV)

A simple approach applied by the authors recently[4] employing single couples of rectangular alternative polarity pulses combined with an appropriate signal processing yields a true second order voltammetric technique DAPV, providing higher resolution than the conventional first order techniques such as DPP (Fig. 1) and even than the other second order techniques, providing the same sensitivity as DPP.
The applications of this approach to various potential-time waveforms and the comparison of their resolution power and sensitivity is the subject of the present work. Results obtained with couples of species with small $E_{1/2}$ difference such as In(III)/Cd(II) and Pb(II)/Tl(I) at a wide range of concentration ratios will be presented.

REFERENCES

1. Barker G.: Proc. Anal. Div. Chem. Soc. *12*, 179 (1975).
2. Saur D.: Frezenius Z. Anal.Chem. *298*, 128 (1979).
3. Blutstein H., Bond A.: Anal. Chem. *46,* 1531 (1974).
4. Zlatev et al: J.Electrochem. Comm. *8*, 1699 (2006).

ANEXO M

Aplicación de voltametría diferencial de pulsos alternativos (DAPV) para la determinación simultánea de las especies: As^{+3}, Pb^{+2}, Tl^{+1}

José Adolfo Valera González* (Estudiante), Roumen Zlatev (Director de Tesis)
*E-mail: jose.valerag@uvmnet.edu

Abstract

The Differential Alternative Pulse Voltammetry (DAPV) combining the high sensitivity of the Differential Pulse Voltammetry with the increased resolution of the second order voltammetric techniques was applied for on-site simultaneous determination of species as As^{+3}, Pb^{+2} and Tl^{+1}in industrial solution without preliminary species separation. The limits of the species concentration ratios allowing simultaneous determination with preset precision of less than 10% were determined. The method was applied for determination in real industrial solutions.

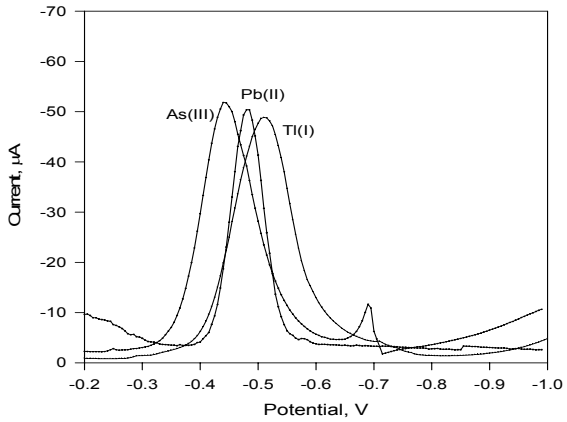

Resumen

El método electroanalítico (DAPV) combina la "alta sensibilidad" de la voltametría diferencial de pulsos (DPV) con la "alta resolución" de las técnicas de voltametría de segundo orden: voltametría de radiofrecuencia, voltametría AC de segunda armónica y voltametría diferencial de rectificación farádica.

Esto permitió realizar la determinación simultánea de especies tales como As^{+3}, Pb^{+2} y Tl^{+1} cuyo potenciales de pico muy similares (cercanos entre sí), son -0.43, -0.47 y -0.51 volts respectivamente. La cercanía entre esos potenciales de pico provoca un traslape de sus picos al momento de utilizar la técnica de voltametría más comúnmente aplicada, DPV.

El propósito principal de utilizar DAPV es el poder determinar la relación de concentraciones entre las especies, de tal manera que sea posible medir cada una de sus concentraciones de forma clara y precisa, es decir sin que se presenten los traslapes de picos.

Universidad Autónoma de Baja California
Instituto de Ingeniería

Otorga la presente

CONSTANCIA

a: *José Adolfo Valera González*

Por su excelente presentación de la conferencia:

"Aplicación de Voltametría Diferencial de Pulsos Alternativos (DAPV) para Determinación Simultánea de las Especies: As^{+3}, Pb^{+2} y Tl^{+1}"

Durante el 2do. Congreso de Estudiantes de Posgrado
del Instituto de Ingeniería de la UABC

"POR LA REALIZACION PLENA DEL HOMBRE"
Mexicali, Baja California, 23 a 25 de Noviembre de 2010

Dr. Benjamín Valdez Salas
DIRECTOR

Dra. Mónica Carrillo Beltrán
Coordinadora MYDCI

Suavisal

Otorga la presente:

C O N S T A N C I A

A: *Jose Adolfo Valera Gonzalez*

Por haber participado en la V Conferencia:
AGUA RESIDUAL
Problema Social y Negocio Coyuntural

José de Jesús Cervantes Miranda

CESPM

Ing. Jorge Mestas Arthur

Suavisal

Mexicali, Baja California a 22 de Octubre del 2009

Universidad Autónoma de Baja California
Instituto de Ingeniería

Otorga la presente

CONSTANCIA

A: *Jose Adolfo Valera González*

Por su participación como ASISTENTE durante la presentación del tema:
"Ocurrencia de arsénico, química y especiación. Metodologías analíticas para su determinación "

dirigido a profesores y estudiantes del programa Maestría y Doctorado en Ciencias e Ingeniería, realizado en las instalaciondes del Instituto de Ingeniería

POR LA REALIZACIÓN PLENA DEL HOMBRE
Mexicali, Baja California, 17 de Junio de 2009

Dr. Benjamín Valdez Salas
DIRECTOR

UNIVERSIDAD DE SONORA

DIVISIÓN DE INGENIERÍA

DEPARTAMENTO DE INGENIERÍA QUÍMICA Y METALURGIA

Otorga la presente

CONSTANCIA

a:

José Adolfo Valera González

Por su participación como ASISTENTE

En el XVIII Congreso Internacional de Metalurgia Extractiva

" La Metalurgia, los Materiales y el Medio Ambiente"

En honor a: "Jorge Ornelas Tabares"

a realizarse los días del 22 al 24 de Abril de 2009 en Hermosillo, Sonora, Mexico

M.C. Ma. de los Angeles Navarrete H.
DIRECTORA DE DIVISIÓN DE INGENIERÍA

Dr. Jesús L. Valenzuela G.
JEFE DEL DEPARTAMENTO DE INGENIERÍA QUÍMICA Y METALURGIA

Dr. Luis Alonso Almazán Holguín
COMITÉ ORGANIZADOR